

Computational biology, 2023

Teachers Kristian Gustafsson, Bernhard Mehlig, Ludvig Storm
(problem sessions)

Canvas course page <https://chalmers.instructure.com/courses/22434>

Literature and references

Lecture notes will be made available.

Course book ‘Mathematical Biology I’, by J. D. Murray (at Cremona)

Selected chapters from

- ‘Nonlinear Dynamics and Chaos’, by Strogatz
- ‘Diffusion and Ecological Problems’, by Okubo and Levin
- ‘Calculating the Secrets of Life’, by Lander and Waterman
- ‘Mathematical Biology II’, by Murray

Examination

Three sets of hand-in problems + exam on campus (you must sign up before Feb. 26). To pass the course a pass grade on both the problem sets and the exam are required (see course page).

Piazza discussion forum

Forum for questions about homework or lectures. Questions should be asked here rather than in emails to the teachers. This allows other students to answer questions and to see answers to the questions.

Contents of the course This course introduces mathematical modeling of complex biological systems, such as

- Population growth
- Interacting species and reaction kinetics
- Spreading of diseases (epidemiology: influenza, AIDS, etc.)
- Population genetics
- Morphogenesis (pattern formation, animal coating)
- Synchronization

Some of the methods we use to model and analyze the systems are

- Discrete and continuous dynamical systems
- Stochastic approaches
- Reaction-diffusion equations
- Time-series analysis

1 Population dynamics (Murray Ch. 1,2)

1.1 Introduction

The dynamics of biological populations (anything from microbes to humans) is in general a complicated problem influenced by many factors such as

- | | |
|--|--|
| <ul style="list-style-type: none">• population size• reproduction pattern• geographical distribution | <ul style="list-style-type: none">• mutation• migration• natural selection |
|--|--|

It is very difficult to analyze the combined effect of these (and more) factors on the evolution of a population. In practice it is therefore necessary to set up a model that only includes a small number of essential factors that influence the population. There are several types of models:

- **Experimental models** For example a lab experiment with cultures of bacteria isolated from their surroundings (Petri dish).
- **Computer models** For example simulating the dynamics of a population given a set of numerical rules. One example could be agent-based modelling to simulate interactions between individuals in a population.
- **Mathematical models** Defined by a set of hypotheses that specifies relations between observables and parameters. For example equations of motion in Physics or the growth equations in the following sections.

There are several ways in which Mathematical models may be useful:

- They may reveal which parameters or mechanisms are most significant and may thus suggest critical experiments (experiment that determines whether a hypothesis is superior to all other accepted hypotheses in a scientific community)
- They may serve as guide to collection, organization, and interpretation of data
- They make quantitative predictions of the behaviour of a system that can be confirmed in experiments.

Computer models are often useful in situations where a number of elementary rules appear reasonable, but at the same time the behaviour of the system appears too complicated (or chaotic, or irregular), in other words too complex to cast in terms of a few elementary mathematical relations between observables.

Some obvious requirements for a model to be meaningful are:

- it must be possible to test the validity of the model by comparison with empirical data
- it must be simple (if it is not simpler than the real situation, it is not a model)
- it must be manageable mathematically or on a computer
- it should ideally include all essential features of the modelled system and exclude non-essential ones.

1.2 Cont. VS discrete growth models (M1.1,2.1)

Growth model: mathematical model for the time evolution of a single species with $N(t)$ individuals at time t . Negative values of $N(t)$ are not allowed, the species become extinct if $N(t) < 1$ at any time. As a starting point, neglect spatial dependence, all interaction and competition for resources with other species, and external influences (most suitable for laboratory conditions, but can also give qualitative information about real-world species). To model how N changes with t we must consider whether generations overlap or not. Many species have little or no overlap between successive generations:

- A natural time for a new generation to appear is often one year.
- Some insects have new generations on the time scale of days.
- The time for cells can be hours.
- Bacteria and viruses can have shorter time between generations.

If there is a large overlap between generations or if the time between generations is small compared to all other time scales in the system, $N(t)$ changes smoothly in time and it is suitable to model its time evolution using a continuous model.

If the overlap is not large, it may be more suitable to use a discrete model. Divide time t by the typical time between two generations to obtain discrete dimensionless time steps, $\tau = 0, 1, 2, \dots$, such that N_τ denotes the population size at generation τ .

Rate of change of population (conservation condition):

$$\Delta N = \text{births} - \text{deaths} + \text{migration}.$$

The time evolution of N becomes:

Continuous

Instantaneous change

\dot{N} is rate of change per time unit

$$\dot{N} = \underbrace{\Delta N}_{\text{flow}}$$

\Rightarrow Smooth trajectory:

$$N(t) \text{ starting from } N(0) \equiv N_0$$

Discrete

Change from one generation to next

ΔN is change per generation

$$N_{\tau+1} = \underbrace{N_\tau + \Delta N}_{\text{map}}$$

\Rightarrow Sequence of points (orbit):

$$N_0, N_1, N_2, \dots$$

These are examples of continuous and discrete dynamical systems with the constraints $N(t) \geq 0$ and $N_\tau \geq 0$ (biologically relevant solutions). In one dimension the continuous system can be analytically solved in general. The discrete system has known solutions if ΔN is linear in N_τ , while non-linear ΔN rarely have analytical solutions.

1.2.1 Simplest example: Malthus model

Linear model: The change in population is proportional to size N with per capita birth rate b and death rate d (neglect migration)

$$\Delta N = bN - dN, \text{ with } b > 0 \text{ and } d > 0.$$

Continuous	Discrete
$\dot{N} = bN - dN$ $\Rightarrow N(t) = N_0 e^{rt}$	$N_{\tau+1} = N_\tau + bN_\tau - dN_\tau$ $\Rightarrow N_\tau = N_0(1+r)^\tau = N_0 e^{\tau \ln(1+r)}$

With initial condition $N(0) = N_0$ and $r = b - d$ is the continuous per capita growth rate (often simply denoted ‘growth rate’ or ‘birth rate’). Note that r is a rate (unit of inverse time) in continuous models, while it is dimensionless (per generation) in discrete models.

Both cases show exponential growth ($r > 0$) or decay ($r < 0$), but with different rates: r (continuous) and $\ln(1+r)$ (discrete) [to compare the two we assume that r and t are measured in units of generations]. Which rate is correct depends on the system we want to model: if generations are overlapping the continuous result is more likely to apply, while if generations are non-overlapping then the discrete result is more likely to apply. If r is small then $\ln(1 + r) \sim r$ and the results of the continuous and discrete models coincide (in this limit the population does not change much per time unit and thus discretization of the continuous system is well approximated by the discrete system).

For the Malthus model the qualitative behaviour is the same (exponential growth) in the discrete and continuous system. As we shall see in Lecture 2, for non-linear systems the qualitative behaviour can be completely different in continuous and discrete systems.

1.3 Example: Growth model for harvesting (M1.6)

The following example illustrates how a simple model can be used to find interesting and important points about a complex biological system. Harvesting of renewable resources such as fish, plants, forest, or bacteria in a bio-reactor, requires a sustainable strategy. We typically want to find a strategy that gives a maximum long-term yield with a minimum effort and possibly with the constraint to affect the ecosystem as little as possible. Consider the mathematical model

$$\dot{N} = \underbrace{rN \left(1 - \frac{N}{K}\right)}_{\text{Logistic growth}} - \underbrace{EN}_{\text{harvesting}} . \quad (1)$$

Assume $r, K > 0$ and $E \geq 0$. We remove population proportional to the number of individuals: the harvest yield is $Y \equiv EN$ with E being the harvest rate ('effort'). In the absence of harvest ($E = 0$) the system (1) has a per capita growth rate \dot{N}/N that depends on N :

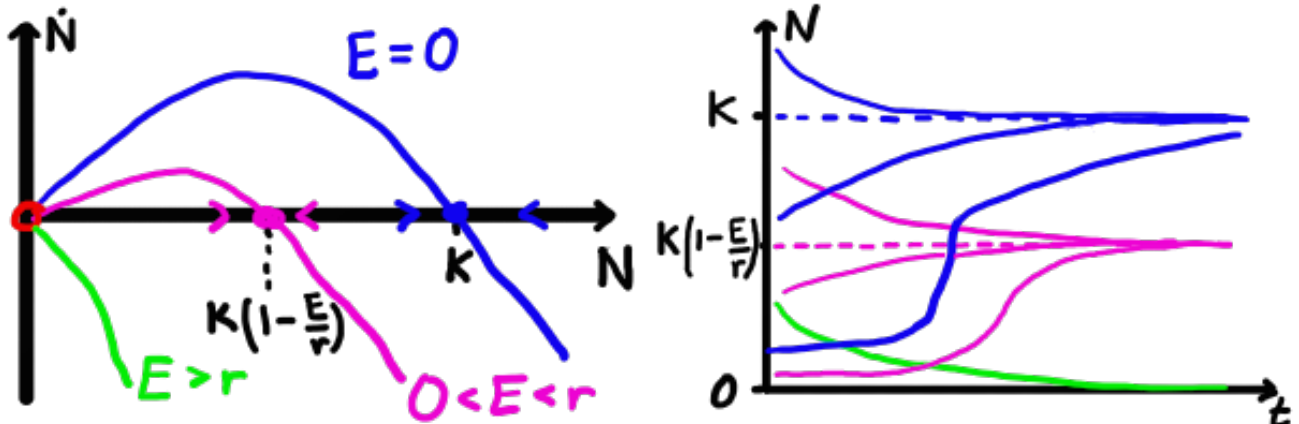
$$\frac{\dot{N}}{N} = r \left(1 - \frac{N}{K}\right) .$$

For small values of N this rate equals r and we obtain exponential growth as in the Malthus model in Section 1.2.1. To take into account the effects of limited resources or overcrowding, the growth rate decreases linearly with growing N until it reaches zero at the carrying capacity $N = K$. For values of $N > K$ the per capita growth rate is negative and the population decreases (births+deaths+migration < 0). This choice of \dot{N}/N decreasing linearly with N defines the logistic model (Verhulst model). Other growth models have other dependencies on N in their per capita growth rate.

Solving $\dot{N} = 0$ in Eq. (1) gives the steady states (fixed points):

$$N_1^* = 0 , \quad N_2^* = K \left(1 - \frac{E}{r}\right) .$$

Visualization of the flow (1) determines the stability of the fixed points:



Example trajectories are shown in the right panel. If $0 \leq E < r$, the population eventually ends up at the positive, attracting fixed point N_2^* . For the case without harvest ($E = 0$), this steady state is equal to the carrying capacity, $N_2^* = K$. If the harvest rate is too high, $E \geq r$, the fixed point $N_1^* = 0$ is attracting and the population eventually dies out. Solutions starting close to a stable fixed point approach it exponentially fast, while, if N_1^* is unstable, solutions starting close to zero initially grow exponentially, giving a sigmoidal shape of the solution.

The yield in the steady state is then

$$Y(E) = EN_2^* = EK \left(1 - \frac{E}{r}\right). \quad (2)$$

By solving $Y'(E) = 0 \Rightarrow E = r/2$ we obtain a maximal yield $Y_{\max} = Kr/4$ with population $N_2^* = K/2$.

This analysis shows that to obtain a maximal yield we should harvest at a rate $E = r/2$, but it does not say anything about how sensitive this strategy is against perturbations coming from stochastic fluctuations of the population or from neglected factors in the model.

One aspect not considered so far is the recovery time T_R , i.e. the time to move back to the steady state after a perturbation. We know that N_2^* is a stable steady state, the recovery time quantifies **how** stable it is. Write the system (1) as $\dot{N} = f(N)$ with $f(N) = rN(1 - \frac{N}{K}) - EN$. Taylor expansion around N_2^* gives

$$\dot{N} \approx \underbrace{f(N_2^*)}_{=0} + \underbrace{f'(N_2^*)}_{\lambda}(N - N_2^*) \Rightarrow N = N_2^* + \text{const.} \cdot e^{\lambda t}$$

close to N_2^* . Here $\lambda \equiv f'(N_2^*)$ is stability exponent, it evaluates to $\lambda = E - r < 0$ (fixed point is stable $\Leftrightarrow \lambda < 0$). Estimate the recovery time by the characteristic time scale close to the fixed point:

$$T_R(E) \equiv \frac{1}{|\lambda|} = \frac{1}{r - E}.$$

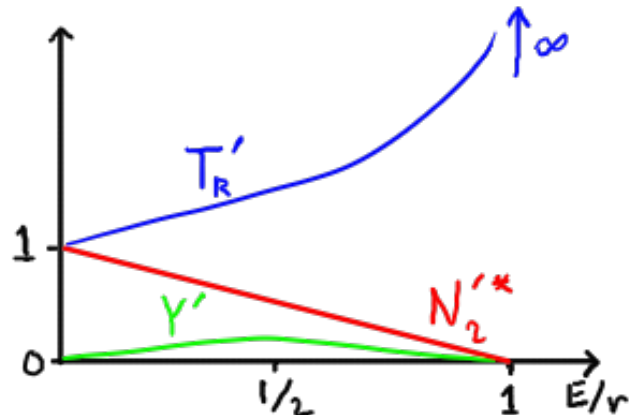
To reduce the number of parameters, we choose to measure population in units of K , $N' = N/K$ and time in units of $1/r$, $t' = rt$:

Steady state population size $N_2'^* = \frac{N_2^*}{K} = 1 - \frac{E}{r}$

Steady state yield $Y' = \frac{Y}{rK} = \frac{E}{r} \left(1 - \frac{E}{r}\right)$

Recovery time $T_R' = rT_R = \frac{1}{1-E/r}$

In these units everything is determined by the dimensionless parameter combination E/r :



The steady state approaches zero as E/r approaches 1. At the same time the recovery time approaches infinity. The yield reaches its maximum at $E/r = 1/2$ and thereafter declines.

Within this model, the best harvest strategy is to have a harvest rate $E=r/2$, giving the maximal yield. Further increase of E is counter-productive: it decreases the yield and may eventually lead to catastrophic consequences: the population may become extinct or need a long time to recover even if we stop harvesting (c.f. the sigmoidal shape of N plotted against t with $E = 0$ and small N_0 in the right panel of the first figure in this section). In conclusion, the simple example model (1) shows that it is possible to approach catastrophic outcomes if we mindlessly increase the harvest rate beyond the maximal sustainable yield when harvesting renewable resources.

Another, even more catastrophic approach to harvesting, is to have a constant yield Y_0 (e.g. a constant fishing quota). The model becomes

$$\dot{N} = rN \left(1 - \frac{N}{K}\right) - Y_0.$$

Analysing this model shows that the time to recovery is

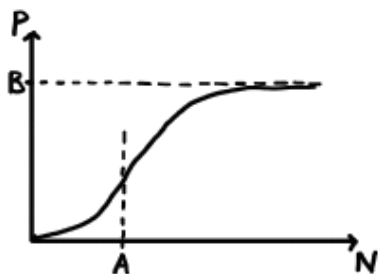
$$T_R(Y_0) = \frac{1}{r\sqrt{1 - Y_0/Y_{\max}}}.$$

This model is very sensitive close to the maximal yield: as $Y_0 \rightarrow Y_{\max}$ the recovery time becomes infinite (the fixed point becomes marginal) \Rightarrow this is not a good harvest strategy.

1.4 Example: Insect outbreak model (M1.2)

The following model for the population of spruce budworms subject to predation by birds illustrates hysteresis shown in many biological populations or ecosystems

$$\dot{N} = rN \left(1 - \frac{N}{K}\right) - \underbrace{\frac{BN^2}{A^2 + N^2}}_{\equiv p(N), \text{ predation}}.$$



When N is small, there is no predation (birds seek food elsewhere). When the number of budworms is large, the effects of predation saturates (birds eat as fast as they can). This system shows outbreaks and hysteresis as the carrying capacity is slowly changed (details in Murray 1.2).

If you need more training, you can have a look at the training question on an insect outbreak model. The solution will be presented as part of the first problem session.

2 Delay and discrete growth models (Murray Ch. 1,2)

Lecture 1 introduced the continuous logistic growth model and some variants thereof (harvesting and spruce budworm model). The logistic growth model agrees well with observations for simple organisms (bacteria, yeast,...) in lab environments. For species with more complex life cycles the logistic growth model often gives a qualitative agreement but fails to describe the quantitative behaviour. In particular, an initial logistic growth is often followed by large persistent fluctuations. These can be caused by time delays due to for example finite time to become fertile and finite time of gestation (time to evolve from fetus to birth). Such time delays can be modeled using a delay model.

2.1 Delay models (M1.3–1.4)

Introduce a single delay time scale $T \geq 0$

$$\dot{N}(t) = f(N(t), N(t - T)).$$

This is an example of a delay differential equation.

One example is the following extension to the logistic model (Hutchinson equation):

$$\dot{N}(t) = rN(t) \left(1 - \frac{N(t - T)}{K}\right), \quad (1)$$

complemented with initial condition $N(t)$ for all $-T \leq t \leq 0$. A Mathematica app for comparison of logistic growth with and without time delays is linked on the course page. Numerical solutions of Eq. (1) often show oscillatory behaviour. This is in contrast to systems without delay; an equation on the form $\dot{N} = f(N)$ cannot exhibit oscillatory dynamics (at each value of N the dynamics moves in a single direction $f(N)$).

Linear stability analysis Introduce dimensionless variables in Eq. (1), $\tau = rt$ and $u(\tau) = N(t)/K$, and let $D = rT$ to obtain

$$\frac{d}{d\tau}u(\tau) = \frac{1}{rK}\frac{d}{dt}N(t) = u(\tau)[1 - u(\tau - D)].$$

We have two steady states $u^* = 0$ and $u^* = 1$. Write $u(\tau) = u^* + \eta(\tau)$ where $\eta(\tau)$ is small at all τ considered. Expand dynamics to first order in η :

$$\begin{aligned} \frac{du^*}{d\tau} + \frac{d\eta}{d\tau} &= (u^* + \eta(\tau))[1 - u^* - \eta(\tau - D)] \\ \Rightarrow \frac{d\eta}{d\tau} &\approx u^*[1 - u^*] - u^*\eta(\tau - D) + \eta(\tau)[1 - u^*]. \end{aligned}$$

Case $u^* = 0$:

$$\frac{d\eta}{d\tau}(\tau) = \eta(\tau),$$

small perturbations η grow exponentially with τ . $u^* = 0$ is unstable and not of interest here.

Case $u^* = 1$:

$$\frac{d\eta}{d\tau}(\tau) = -\eta(\tau - D).$$

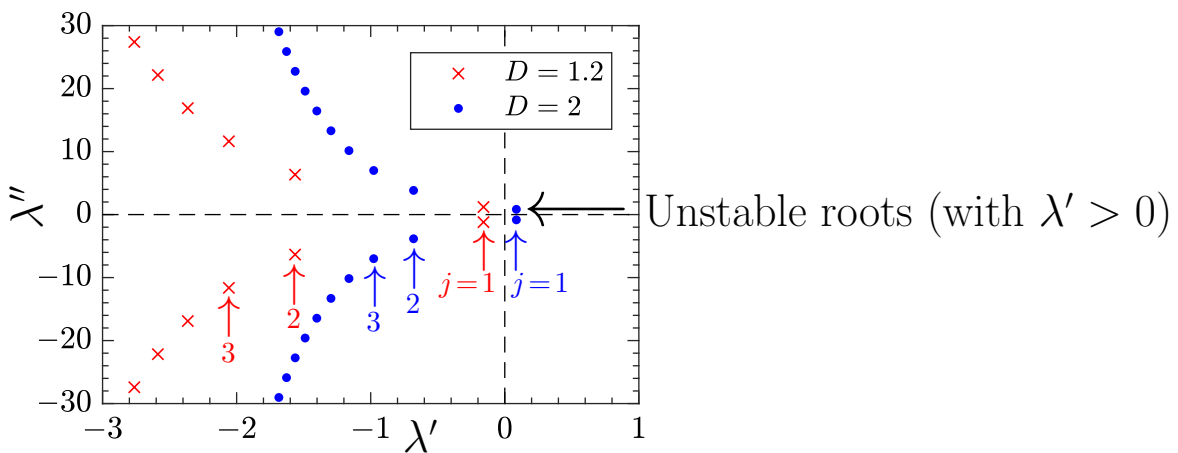
Search solution on the form

$$\eta(\tau) = Ae^{\lambda\tau}, \text{ with complex } \lambda = \lambda' + i\lambda''.$$

Inserting into the equation for η above gives

$$\begin{aligned} \lambda Ae^{\lambda\tau} &= -Ae^{\lambda(\tau-D)} \Rightarrow \lambda = -e^{-\lambda D} \\ \text{Real part: } \lambda' &= -e^{-\lambda'D} \cos(\lambda''D) \\ \text{Imaginary part: } \lambda'' &= +e^{-\lambda'D} \sin(\lambda''D) \end{aligned}$$

These equations for λ' and λ'' have an infinite amount of solutions for any positive value of the delay D :



Solutions come in complex conjugate pairs $\lambda_j = \lambda'_j \pm i\lambda''_j$, ordered such that $\lambda'_1 > \lambda'_2 > \dots$ and $j = 1, \dots, \infty$. The general solution is a superposition of the solutions corresponding to all conjugate pairs:

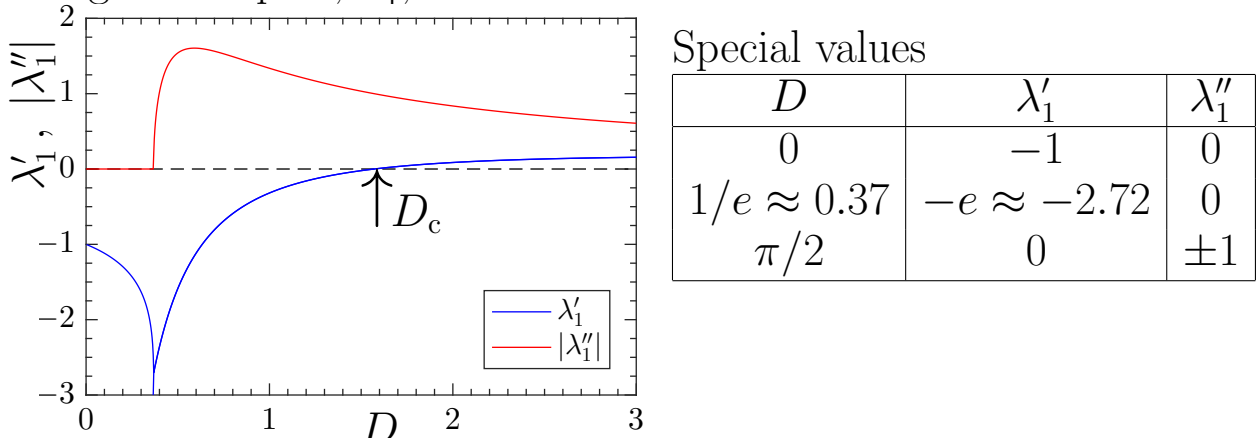
$$\eta(\tau) = \sum_j \left[\tilde{A}_j e^{(\lambda'_j + i\lambda''_j)\tau} + \tilde{B}_j e^{(\lambda'_j - i\lambda''_j)\tau} \right].$$

Choosing complex coefficients \tilde{A}_j and \tilde{B}_j to make $\eta(t)$ real, the solution can be written in terms of real coefficients A_j and B_j :

$$\eta(\tau) = \sum_j e^{\lambda'_j \tau} [A_j \cos(\lambda''_j \tau) + B_j \sin(\lambda''_j \tau)],$$

with A_j and B_j determined by initial condition $\eta(\tau)$ for $-D \leq \tau \leq 0$.

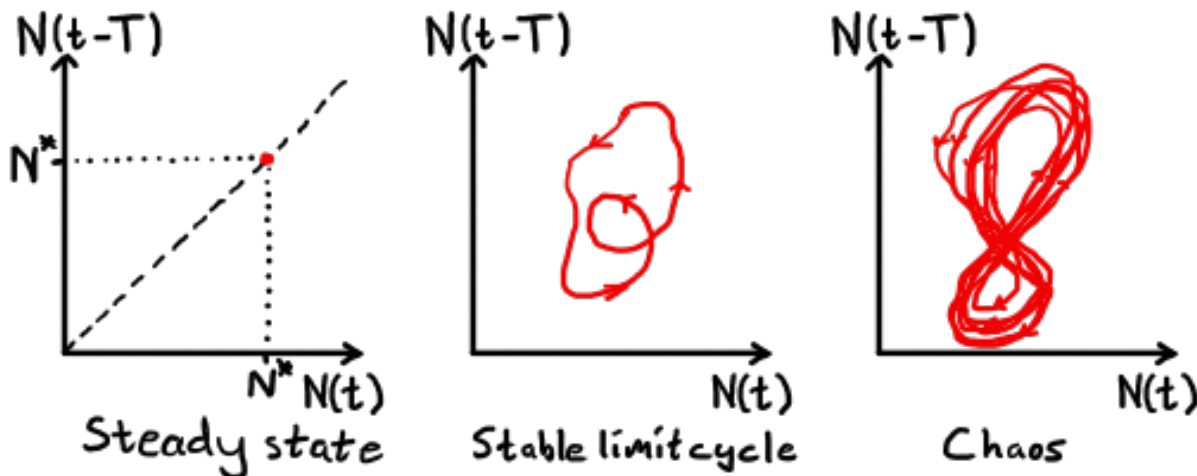
Plot the real and negative imaginary part of the solution λ_1 with largest real part, λ'_1 , as a function of D :



Inserting $\lambda'_1 = 0$ in the equations for λ' and λ'' above gives simple roots $\lambda''_1 = \pm 1$ at $D_c = \pi/2$. For $0 < D < D_c$ all roots have negative real parts, $\lambda'_j < 0$ and the solution is stable: small perturbations

η from the fixed point decay with time. For $D > D_c$ at least one unstable root with $\lambda'_j > 0$ exist. The system makes a qualitative transition (bifurcation) from stable to unstable at the bifurcation point $D_c = \pi/2$ where the maximal solution λ'_1 becomes positive.

In conclusion, linear stability analysis shows growing oscillations around the steady state $u^* = 1$ if the delay is large enough, $D > D_c$. This is a general conclusion: time delays typically destabilize a system. Plotting the dynamics in the $(N(t), N(t-T))$ space (delay embedding) shows a stable limit cycle if $D > D_c$ for the Hutchinson equation (1). The possible long-term dynamics in (bounded) delay models are:



Delay models other than the Hutchinson equation (1), may show chaotic behaviour (infinitely long aperiodic attractor). One example being formation of blood cell elements in the body, Murray 1.5.

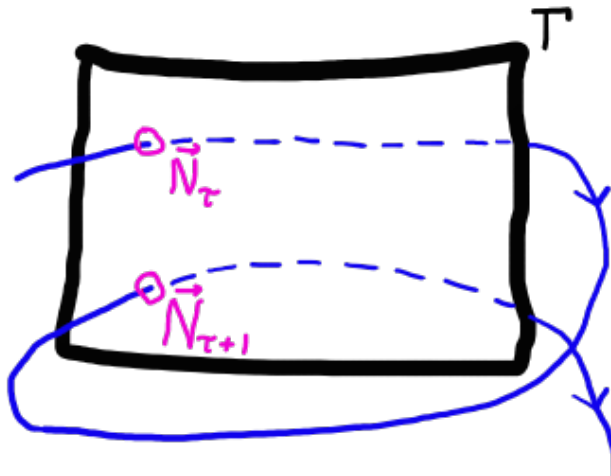
2.2 Discrete models (Murray Chapter 2)

As argued in Lecture 1 the population of non-overlapping generations can be modelled as a discrete dynamical system. This is an example of an inherently discrete dynamical system.

Discrete systems can also be obtained from continuous ones:

- **Stroboscopic map** Obtain discrete dynamics by strobining continuous flow at a sequence of times.
- **Using surface of section** Consider an n -dimensional continuous system and form an $n - 1$ -dimensional surface of section

Γ . Construct an orbit from all crossings of a trajectory with Γ (Poincaré map from \mathbf{x}_τ to $\mathbf{x}_{\tau+1}$). Example for $n = 3$:



Surface of sections are used to visualise 3D (or 4D) dynamics in 2 (or 3) dimensions, or to visualize and identify periodic motion.

- **Time discretisation** of continuous system $\dot{N} = f(N)$ to for example implement a continuous model on a computer. Get

$$N(t + \delta t) \approx N(t) + \delta t f[N(t)].$$

In terms of $\tau = t/\delta t$ we obtain a discrete dynamical system

$$N_{\tau+1} = \underbrace{N_\tau + \delta t f[N_\tau]}_{F(N_\tau)}. \quad (2)$$

Note that all continuous dynamical systems can be mapped on discrete dynamical systems, but the opposite is not true: not all discrete systems corresponds to a discretization of a continuous system.

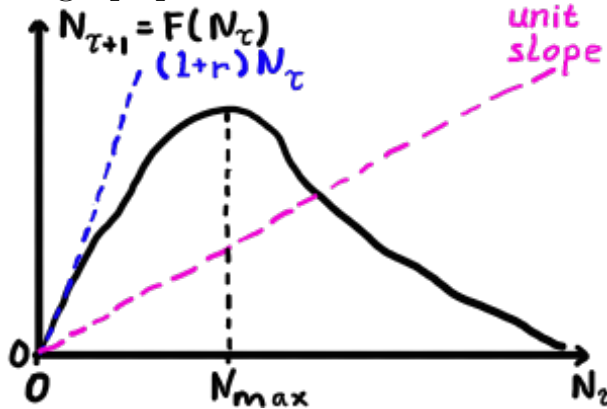
2.3 Discrete dynamics (M2.1,2.2)

Consider the system

$$N_{\tau+1} = F(N_\tau)$$

with some map on the form $F = N_\tau + \Delta N_\tau$ that preserves $N_\tau \geq 0$.

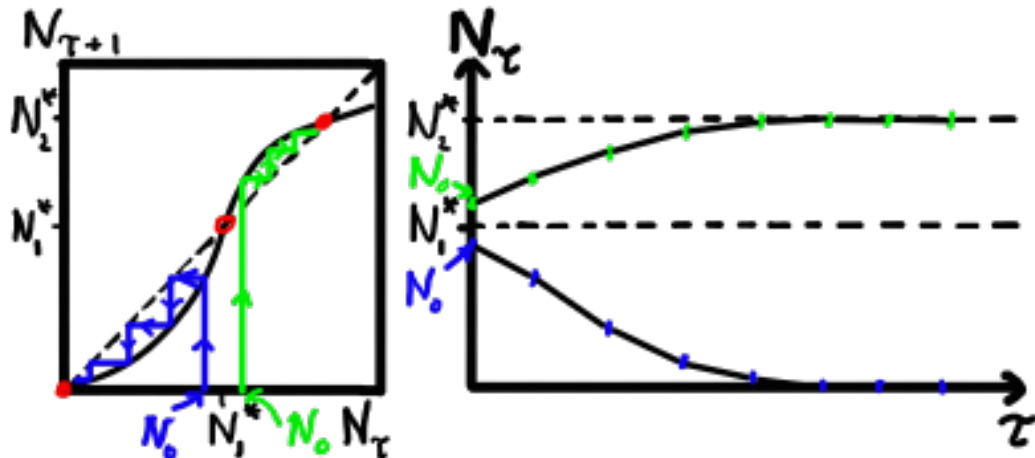
What are reasonable shapes of the map F for a growth model? For small population sizes we assume linear growth $F \sim (1+r)N$. Due to self-regulation when the system becomes overcrowded (finite carrying capacity), we expect F to reach some maximum and then decay for large population sizes:



Note that the population increases if $N_{\tau+1} = F(N_\tau)$ is larger than N_τ . Graphically this translates into being in a region where $F(N_\tau)$ lies above the line of unit slope, $F(N_\tau) = N_\tau$.

Similarly the population decreases if $F(N_\tau)$ lies below $F(N_\tau) = N_\tau$. Points where $F(N_\tau)$ cross $F(N_\tau) = N_\tau$ are fixed points (steady states). Applying the map on these points do not change the population. In growth models we often have a fixed point at $N_\tau = 0$ that can be either stable (attracting) or unstable (repelling).

The dynamics of one-dimensional maps are often visualized using cobweb plots (left panel):



The dynamics starting at two initial conditions (blue|green) are shown.

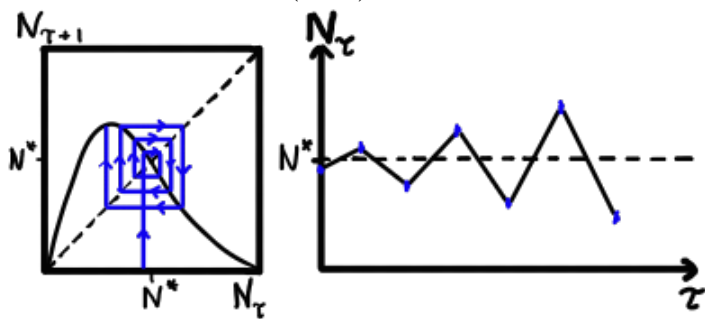
1. From a value N_τ , move vertically to $F(N_\tau)$.

2. Move horizontally to the line $F(N) = N$. The new coordinate is $(F(N_\tau), F(N_\tau)) = (N_{\tau+1}, N_{\tau+1})$, i.e. we have found the position of $N_{\tau+1}$ on the N_τ -axis.
3. Repeat step 1 from $N_{\tau+1}$

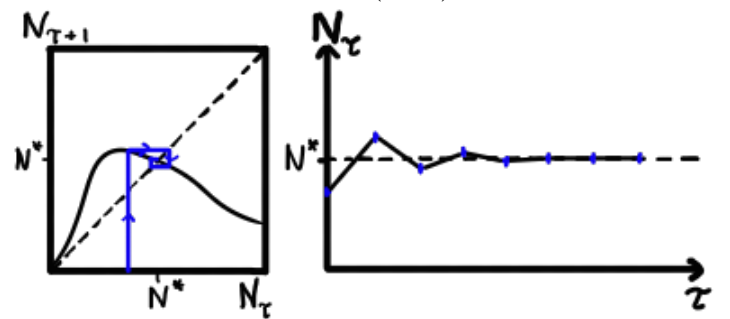
This procedure constructs the orbit of the map (right panel above). For the case illustrated there are three fixed points: two stable at $N^* = 0$ and N_2^* and one unstable at N_1^* .

Depending on the shape of F the dynamics in the vicinity of a fixed point N^* changes:

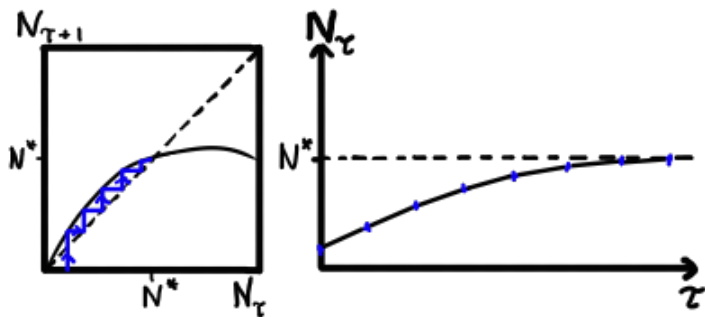
$$F'(N^*) < -1$$



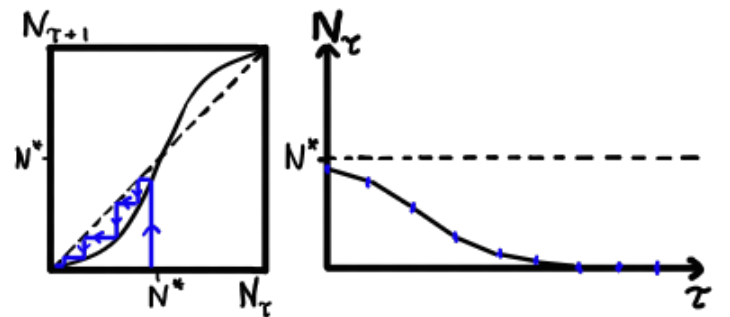
$$-1 < F'(N^*) < 0$$



$$0 < F'(N^*) < 1$$



$$1 < F'(N^*)$$



We have four distinct cases depending on the 'eigenvalue' $\Lambda \equiv F'(N^*)$:

Unstable
oscillations

Stable
oscillations

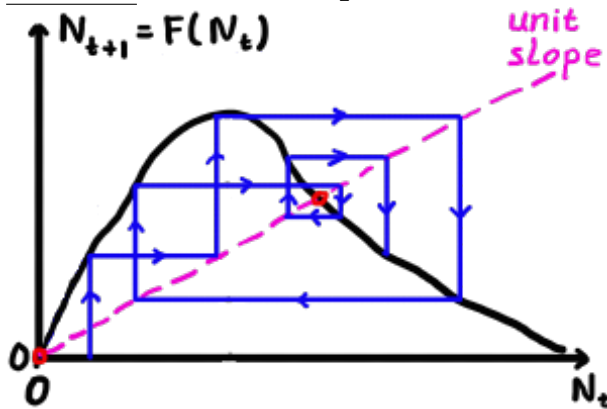
Stable
no oscillations

Unstable
no oscillations



Compare with the fixed points of a continuous dynamical system: stable if $f'(N^*) < 0$ and unstable if $f'(N^*) > 0$, oscillations are not possible in the continuous system because trajectories cannot intersect.

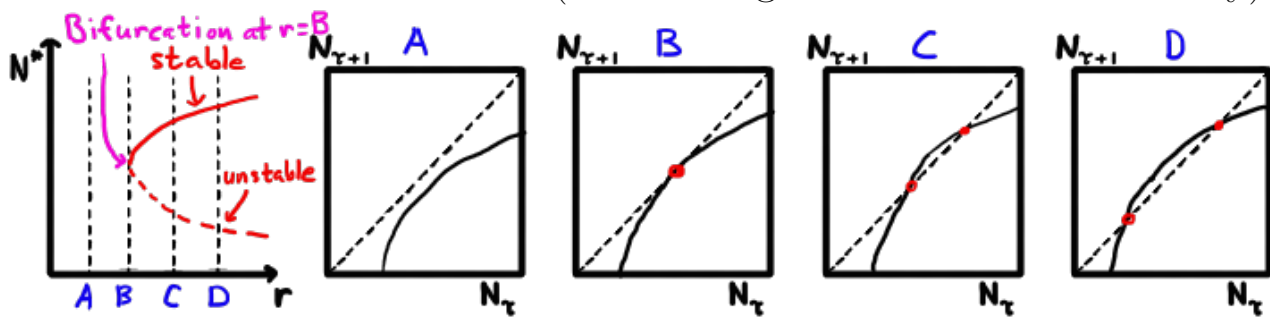
The global dynamics of a discrete one-dimensional system can be chaotic if all fixed points are unstable and if the dynamics is bounded:



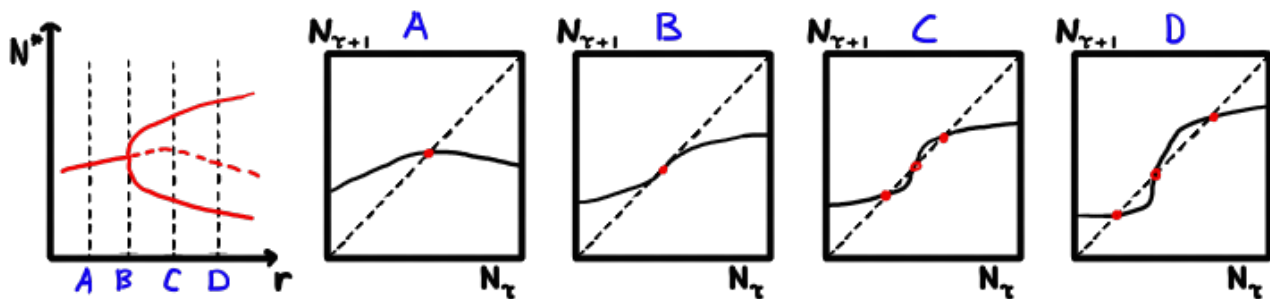
2.4 Bifurcations (M2.2,2.4)

Growth models exhibit control parameter such as the growth rate r . As the parameters change, the system may undergo bifurcations where fixed points change stability. Bifurcations occur as the eigenvalue $\Lambda = F'(N^*)$ passes through $+1$ or -1 upon variation of the control parameters. The following are examples of bifurcations with $\Lambda = +1$.

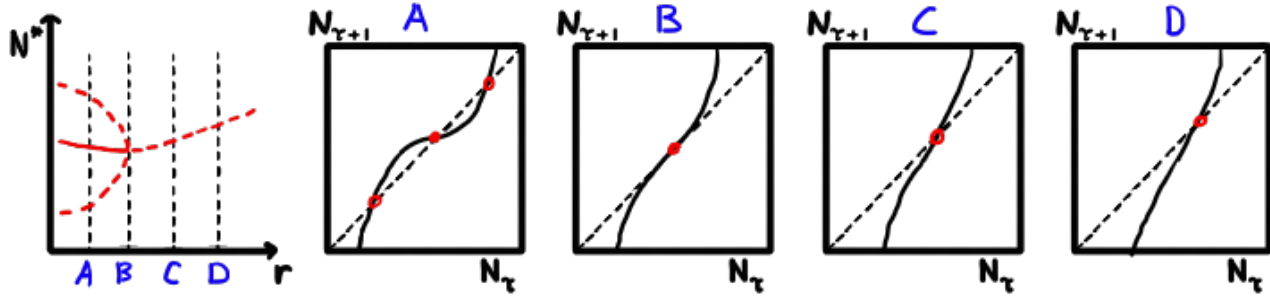
Saddle-node bifurcation (called ‘tangent bifurcation’ in Murray):



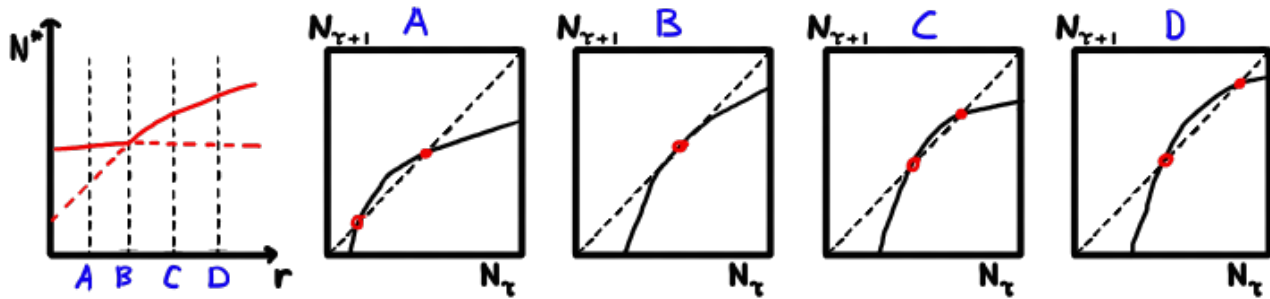
Supercritical pitchfork bifurcation



Subcritical pitchfork bifurcation



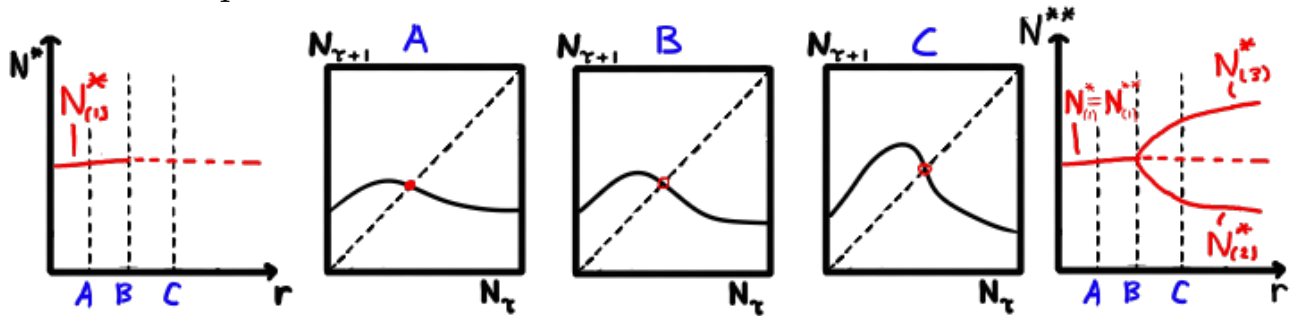
Transcritical bifurcation Stability changes as two fixed points ‘move through each other’



Bifurcations with $\Lambda = +1$ have counterparts in continuous dynamical systems: the time discretization (2): $F(N_\tau) = N_\tau + \delta t f(N_\tau)$ gives $F'(N_\tau^*) = 1 + \delta t f'(N_\tau^*)$. Thus, as the stability exponent $\lambda = f'(N_\tau^*)$ passes zero, the eigenvalue $\Lambda = F'(N_\tau^*)$ passes $+1$.

In addition to the examples above, discrete systems may also have bifurcations as Λ passes -1 , for example period-doubling bifurcations where a stable fixed point transforms into an attracting periodic cycle.

Period-doubling bifurcation Assume map $N_{\tau+1} = F(N_\tau)$ has an isolated fixed point $N_{(1)}^*$ and that $\Lambda = F'(N_{(1)}^*)$ passes through -1 at bifurcation point $r = B$



Denote fixed points of the second iterate of the map by $N_{(i)}^{**}$. One fixed

point is $N_{(1)}^{**} = N_{(1)}^*$ because $F(F(N_{(1)}^*)) = N_{(1)}^*$. It has eigenvalue

$$\frac{d}{dN}F(F(N))|_{N=N_{(1)}^{**}} = F'(F(N_{(1)}^*))F'(N_{(1)}^*) = \Lambda^2.$$

Thus, at $r = B$ the eigenvalue of the second iterate passes $\Lambda^2 = (-1)^2 = +1$ and the second iterate (typically) undergoes a pitchfork bifurcation, forming two new stable fixed points $N_{(2)}^{**}$ and $N_{(3)}^{**}$ (illustrated in right-most panel above). These form an alternating solution to the original map: $N_\tau = N_{(2)}^{**}, N_{(3)}^{**}, N_{(2)}^{**}, N_{(3)}^{**}, \dots$, i.e. a stable period-two cycle of the original map. Period-doubling bifurcations are frequent in the logistic map and other discrete growth models.

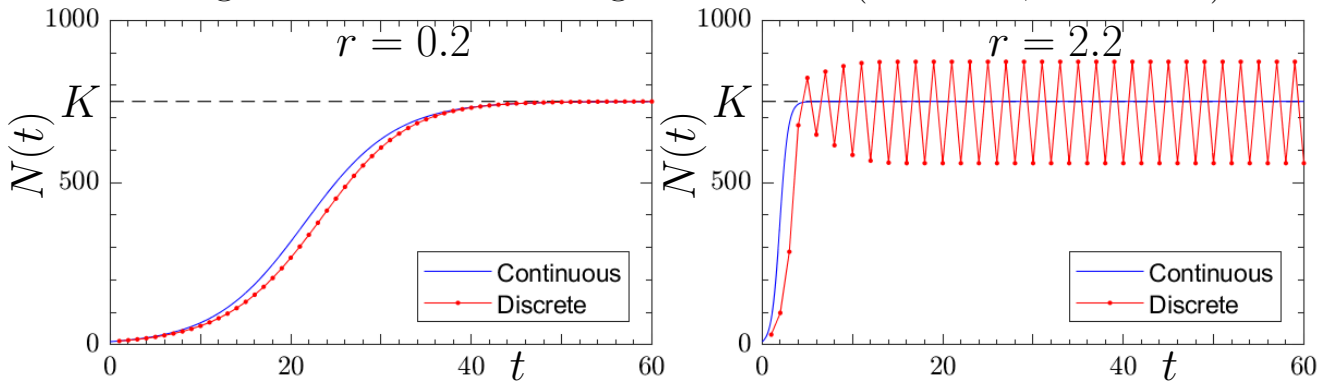
2.5 Example: Logistic map (M2.3)

The logistic map is a discrete system having the same form of the rate of change of population ΔN as the logistic equation from Lecture 1

$$N_{\tau+1} = N_\tau + rN_\tau \left(1 - \frac{N_\tau}{K}\right).$$

2.5.1 Comparison to logistic equation

The following figure shows a numerical comparison of continuous and discrete logistic models for two growth rates ($N_0 = 10$, $K = 750$):



The two models agree for small values of r . For larger values of r there can be significant difference. In the example shown the discrete model shows oscillations with period 2. A detailed analysis (below) shows that the discrete map has a fixed point at $N^* = K$, but that this fixed

point has undergone a period-doubling bifurcation at $r = 2$ and the dynamics is therefore attracted to a stable period-two cycle.

In conclusion, the inherent time delay of discrete models often give rise to unsteady or oscillatory behaviour similar to the effect of delay in continuous models above.

2.5.2 Analysis¹

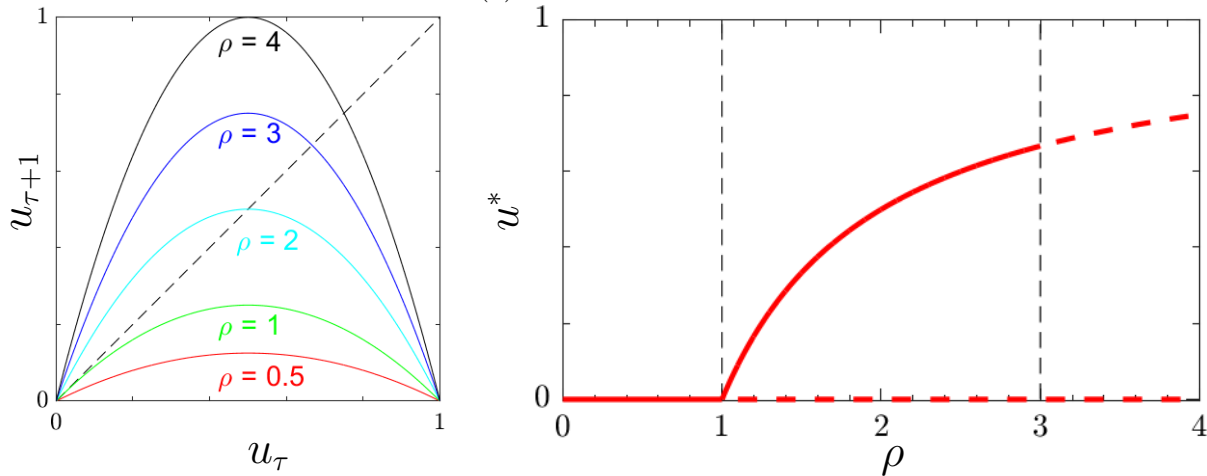
Introduce a dimensionless population size $u_\tau \equiv N_\tau r / (K(r + 1))$ and define $\rho \equiv r + 1$ in the logistic map:

$$u_{\tau+1} = \rho u_\tau (1 - u_\tau) . \quad (3)$$

Assume $0 < u_0 < 1$ and $0 < \rho \leq 4$ (population size may become negative if $\rho > 4$). The dimensionless logistic map (3) has two fixed points with corresponding eigenvalues Λ :

$$\begin{aligned} u_{(1)}^* &= 0 & \Lambda &= F'(0) = \rho \\ u_{(2)}^* &= 1 - \frac{1}{\rho} & \Lambda &= F'\left(1 - \frac{1}{\rho}\right) = 2 - \rho . \end{aligned}$$

For $0 < \rho < 1$, $u_{(1)}^* = 0$ is stable and the first bifurcation (transcritical) happens at $\rho = 1$ where $u_{(1)}^* = 0$ becomes unstable.



¹The details in this subsection are not part of the course content and can be skipped. They illustrate mathematically how the period-doubling cascade forms for the logistic map. Note that Section 2.5.3 on the qualitative features of the period-doubling cascade belong to the course content.

For $1 < \rho < 3$, $u_{(1)}^* = 0$ is unstable and $u_{(2)}^*$ is stable.

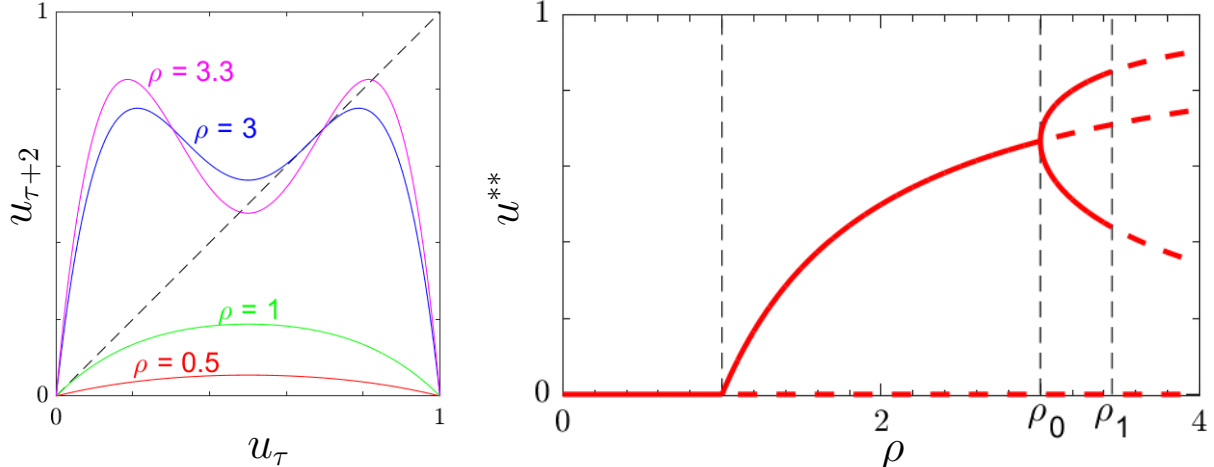
$\Lambda = -1$ for $u_{(2)}^*$ when $\rho = 3$ and the system has no stable fixed points when $\rho > \rho_1 = 3$. In order to understand the bifurcation, we must consider higher-order iterates of the map as follows. In general the points on an orbit are obtained by successive application of the map:

$$\begin{aligned} u_1 &= F(u_0) \\ u_2 &= F(F(u_0)) \equiv F^2(u_0) \\ &\vdots \\ u_\tau &= F^\tau(u_0). \end{aligned}$$

For the second iterate of F :

$$u_{\tau+2} = F^2(u_\tau) = \rho \underbrace{[\rho u_\tau (1 - u_\tau)]}_{u_{\tau+1}} \underbrace{(1 - \rho u_\tau (1 - u_\tau))}_{u_{\tau+1}} \quad (4)$$

Denote fixed points of the map F^2 by u^{**} . When ρ passes through 3, $F^2(u_\tau)$ undergoes a pitchfork bifurcation:



Note that all fixed points of $F(u_\tau)$ must also be fixed points of $F^2(u_\tau)$, $u_{(1)}^{**} \equiv u_{(1)}^* = 0$ and $u_{(2)}^{**} \equiv u_{(2)}^* = 1 - \rho^{-1}$, but the eigenvalue may be different. As we saw above, when ρ passes 3, the eigenvalue

$$\Lambda \equiv F'(u_{(2)}^*) = 2 - \rho$$

decreases through -1 and $u_{(2)}^*$ becomes unstable. At the same time

$$F'^2(u_{(2)}^{**}) = \frac{\partial}{\partial u} F(F(u)) \Big|_{u_{(2)}^*} = F'(\underbrace{F(u_{(2)}^*)}_{u_{(2)}^*}) F'(u_{(2)}^*) = [F'(u_{(2)}^*)]^2 = \Lambda^2$$

increases through $\Lambda^2 = (-1)^2 = +1$ and two new stable fixed points $u_{(3),(4)}^{**}$ of $F^2(u_\tau)$ are created in a pitchfork bifurcation:

$$u_{(3),(4)}^{**} = \frac{\rho + 1 \pm \sqrt{(\rho - 3)(\rho + 1)}}{2\rho}.$$

These are stable (if ρ is not too large) and satisfies

$$F^2(u_{(3)}^{**}) = u_{(3)}^{**} \text{ and } F^2(u_{(4)}^{**}) = u_{(4)}^{**}$$

but they are not fixed points of F :

$$F(u_{(3)}^{**}) \neq u_{(3)}^{**} \text{ and } F(u_{(4)}^{**}) \neq u_{(4)}^{**}.$$

It follows that $F(u_{(3)}^{**}) = u_{(4)}^{**}$ and $F(u_{(4)}^{**}) = u_{(3)}^{**}$, i.e. the system approaches a stable period-two cycle $u_{(3)}^{**}, u_{(4)}^{**}, u_{(3)}^{**}, u_{(4)}^{**}, \dots$

In conclusion: exactly when the period-one fixed point $u_{(2)}^* = 1 - \rho^{-1}$ becomes unstable a new period-two cycle is created (period-doubling bifurcation), c.f. Section 2.5.1.

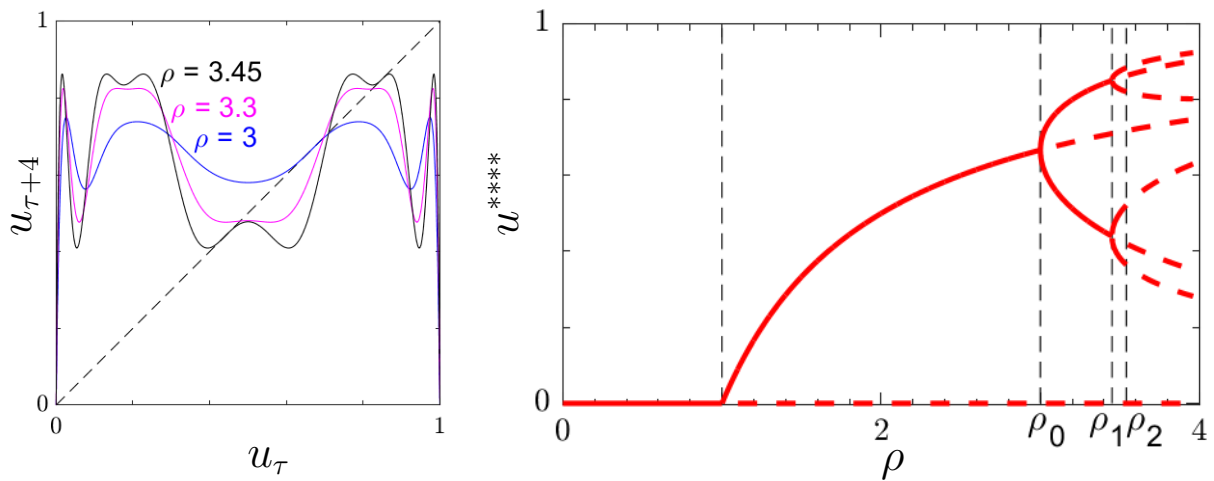
Note that the eigenvalues of $u_{(3),(4)}^{**}$ must be equal because they form a cycle for the original map:

$$\Lambda_3 \equiv F^{2'}(u_{(3)}^{**}) = \left. \frac{\partial}{\partial u} F(F(u)) \right|_{u_{(3)}^{**}} = F'(\underbrace{F(u_{(3)}^{**})}_{u_{(4)}^{**}}) F'(u_{(3)}^{**}) = F'(u_{(3)}^{**}) F'(u_{(4)}^{**}).$$

In the same way

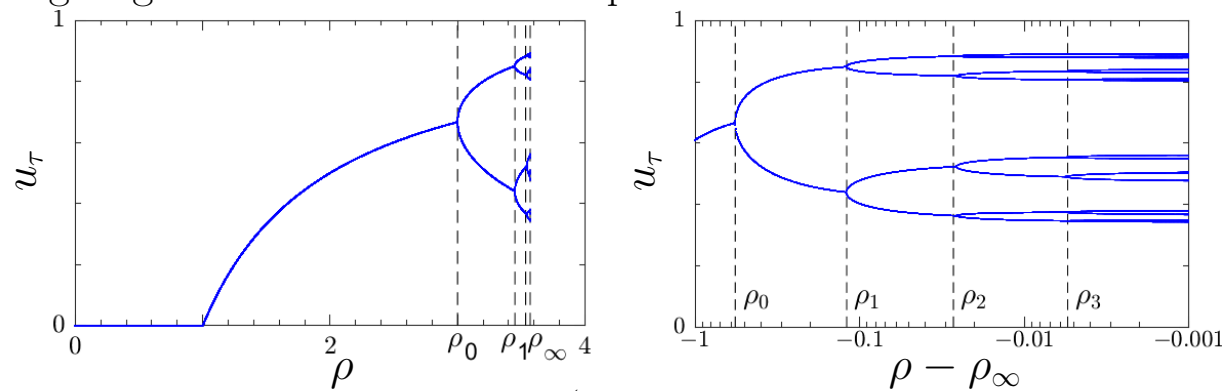
$$\Lambda_4 \equiv F^{2'}(u_{(4)}^{**}) = F'(u_{(3)}^{**}) F'(u_{(4)}^{**}).$$

As ρ passes $\rho_2 \approx 3.45$ the eigenvalues $\Lambda_3 = \Lambda_4$ simultaneously pass -1 and another period-doubling bifurcation occurs (four new stable fixed points are formed in the map F^4), creating an attracting period-four cycle in the original map (stable up to $\rho_3 \approx 3.54$):



2.5.3 Period-doubling cascade

Subsequent period doubling bifurcations give rise to a period-doubling cascade, consisting of bifurcation values ρ_i , $i = 1, 2, \dots$, where period 2^i -cycles are formed. The stable attracting cycle is obtained by plotting large-time iterates of the map:



The figure shows the attractor (long term limiting behaviour for most initial conditions) of the logistic map for different values of ρ on a linear (left) and logarithmic (right) scale. Unstable fixed points and cycles are only visited for a discrete set of isolated initial conditions and are not shown.

Feigenbaum (1978) showed that

$$\frac{\rho_n - \rho_{n-1}}{\rho_{n+1} - \rho_n} \rightarrow 4.669 \dots = \delta$$

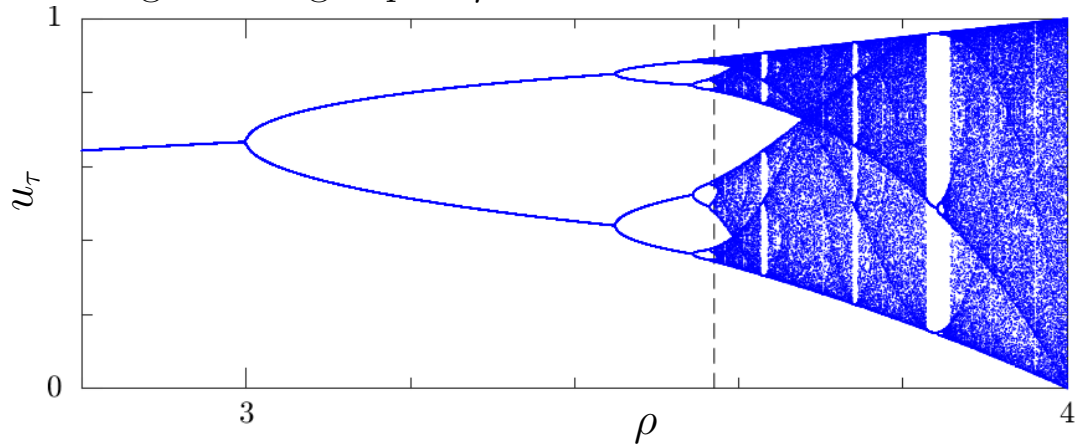
as $n \rightarrow \infty$. Also

$$\rho_n \rightarrow 3.56995 \equiv \rho_\infty$$

as $n \rightarrow \infty$. These results imply

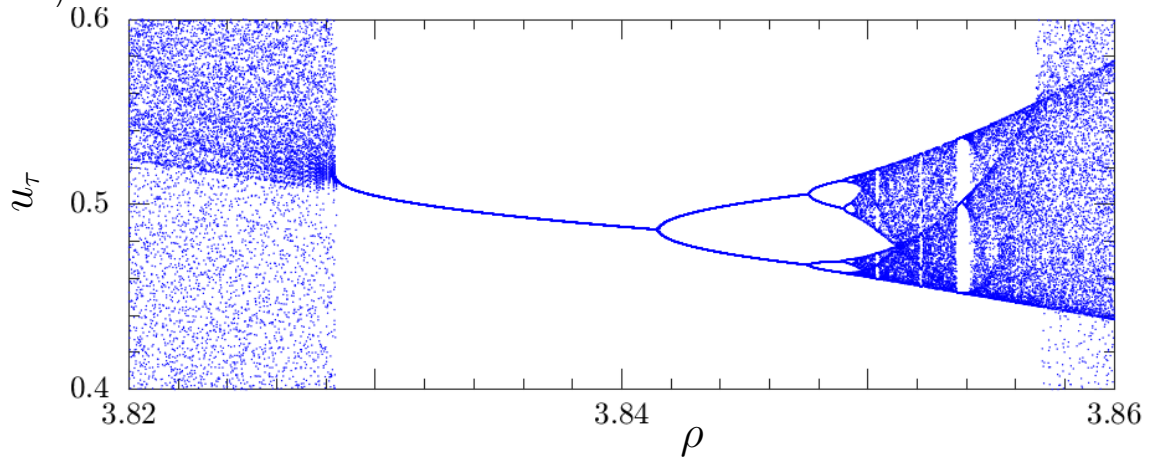
$$|\rho_\infty - \rho_n| \sim \delta^{-n}.$$

Extending the range up to $\rho = 4$:



reveals complicated dynamics: when $\rho > \rho_\infty$ attractors are either periodic cycles or aperiodic attractors. For $\rho = 4$ the aperiodic attractor fills the entire interval. For other values of ρ the aperiodic attractor splits to fill a number of smaller intervals, e.g. 2 bands at $\rho \approx 3.63$. Such aperiodic attractors are characterized by

1. Apparently irregular orbit
2. Re-appearance of the full pattern in small windows (fractal structure):



3. Enhanced sensitivity to changes in initial condition u_0

This behaviour is called deterministic chaos: the dynamics appears irregular despite being deterministic. More precisely: Deterministic

chaos describes aperiodic, bounded deterministic dynamics with enhanced sensitivity to small changes of initial conditions.

The period-doubling cascade leading to chaotic behavior shown here is a common route to chaos. It shows several universal features, for example $\delta = 4.669\dots$ takes the same value for many systems.

2.6 Higher dimensional discrete maps²

The graphical analysis for the one-dimensional discrete systems of the previous sections is here complemented with an analytical formulation, valid also for higher dimensions. Consider a general map

$$\mathbf{x}_{\tau+1} = \mathbf{F}(\mathbf{x}_\tau).$$

What happens to a small perturbation $\mathbf{x}^* + \delta\mathbf{x}$ after many iterations?

Let $\mathbf{F}^n(\mathbf{x}) \equiv \mathbf{F}(\mathbf{F}(\dots \mathbf{F}(\mathbf{x})))$ denote a map applied n times. First evaluate the derivative of $\mathbf{F}^n(\mathbf{x})$ at a fixed point \mathbf{x}^* . First $d = 1$:

$$\begin{aligned} \frac{\partial}{\partial x} F^n(x) \Big|_{x=x^*} &= \frac{\partial}{\partial x} F(F^{n-1}(x)) \Big|_{x=x^*} \\ &= \frac{\partial F}{\partial x} \underbrace{(F^{n-1}(x^*))}_{x^*} \frac{\partial}{\partial x} F^{n-1}(x) \Big|_{x=x^*} = \left[\frac{\partial F}{\partial x}(x^*) \right]^n \end{aligned}$$

General dimension

$$\frac{\partial}{\partial \mathbf{x}} \mathbf{F}^n(\mathbf{x}) \Big|_{\mathbf{x}=\mathbf{x}^*} = [\mathbb{J}(\mathbf{x}^*)]^n,$$

with \mathbb{J} the gradient matrix $\partial \mathbf{F} / \partial \mathbf{x}$.

\Rightarrow to first order we have

$$\mathbf{F}^n(\mathbf{x}^* + \delta\mathbf{x}) \approx \underbrace{\mathbf{F}^n(\mathbf{x}^*)}_{\mathbf{x}^*} + \underbrace{\frac{\partial}{\partial \mathbf{x}} \mathbf{F}^n(\mathbf{x}^*) \delta\mathbf{x}}_{[\mathbb{J}(\mathbf{x}^*)]^n} = \mathbf{x}^* + [\mathbb{J}(\mathbf{x}^*)]^n \delta\mathbf{x}$$

²Higher dimensional discrete maps is not part of the course content, but as a reference it could be good to have a hint of the theory which is outlined in this section (in particular the comparison between maps and flows on the last page could be relevant).

Let Λ_i and \mathbf{e}_i be eigenvalues and eigendirections of $\mathbb{J}(\mathbf{x}^*)$:

$$\mathbb{J}(\mathbf{x}^*)\mathbf{e}_i = \Lambda_i \mathbf{e}_i .$$

It follows

$$[\mathbb{J}(\mathbf{x}^*)]^n \mathbf{e}_i = \Lambda_i^n \mathbf{e}_i .$$

By decomposition of $\delta\mathbf{x}$ in terms of \mathbf{e}_i , i.e. $\delta\mathbf{x} = \sum_i a_i \mathbf{e}_i$ it follows

$$[\mathbb{J}(\mathbf{x}^*)]^n \delta\mathbf{x} = \sum_i a_i \Lambda_i^n \mathbf{e}_i .$$

- Eigendirections with $|\Lambda_i| < 1$ contracting for large n
- Eigendirections with $|\Lambda_i| > 1$ expanding for large n
- Eigendirections with $|\Lambda_i| = 1$ marginal for large n

The fixed point is stable if all $|\Lambda_i| < 1$.

If any $|\Lambda_i| > 1$ the fixed point is unstable.

2.6.1 p -cycles

As found above, discrete maps may show periodic motion. The fixed points of a map applied twice: $N_{\tau+2} = F(F(N_\tau))$ are 2-cycles i.e. the orbit is N_0, N_1, N_0, \dots

Any fixed point of the map satisfies $F^p(N^*) = N^*$ for any p .

Fixed points of $N_{\tau+p} = F^p(N_\tau)$ are cycles of period p .

The shortest cycle of N_τ is called prime cycle (p -cycle)

Summary: Comparison maps and flows

System	Flow \mathbf{f}	Map \mathbf{F}
Solution	Continuous ODE $\dot{\mathbf{x}} = \mathbf{f}(\mathbf{x})$ Trajectory $\mathbf{x}(t)$ Closed orbit $\mathbf{x}(t) = \mathbf{x}(t + T)$	Discrete difference equations $\mathbf{x}_{\tau+1} = \mathbf{F}(\mathbf{x}_\tau)$ Orbit $\{\mathbf{x}_0, \mathbf{x}_1, \dots\}$ Cycle $\mathbf{x}_{\tau+T} = \mathbf{x}_\tau$ (fixed point of $\mathbf{F}^T(\mathbf{x}_\tau)$)
Periodic solution	Fixed point cond. Chaos possible	$\mathbf{F}(\mathbf{x}^*) = \mathbf{x}^*$ If $d > 2$ otherwise $d > 1$
Jacobian	$J_{ij} = \partial f_i / \partial x_j$	$J_{ij} = \partial F_i / \partial x_j$ $\det \mathbb{J} = 1$
Area preserving if	$\nabla \cdot \dot{\mathbf{x}} = \text{tr } \mathbb{J} = 0$	$\lambda_i (\mathcal{R}e[\lambda_i] \text{ determines stability})$ $\lambda_1 < \lambda_2 < 0 \text{ and } \mathcal{I}m[\lambda_{1,2}] = 0$ $\lambda_1 > \lambda_2 > 0 \text{ and } \mathcal{I}m[\lambda_{1,2}] = 0$ $\lambda_1 < 0 < \lambda_2 \text{ and } \mathcal{I}m[\lambda_{1,2}] = 0$ $\lambda_{1,2} = \mu \pm i\omega \text{ and } \mu < 0$ $\lambda_{1,2} = \mu \pm i\omega \text{ and } \mu > 0$ $\lambda_{1,2} = \pm i\omega$
Eigenvalues at fixed point		$\Lambda_i (\Lambda_i \text{ determines stability})$ $ \Lambda_1 < \Lambda_2 < 1 \text{ and } \mathcal{I}m[\Lambda_{1,2}] = 0$ $ \Lambda_1 > \Lambda_2 > 1 \text{ and } \mathcal{I}m[\Lambda_{1,2}] = 0$ $ \Lambda_1 < 1 < \Lambda_2 \text{ and } \mathcal{I}m[\Lambda_{1,2}] = 0$ $\Lambda_{1,2} = \rho e^{\pm i\theta} \text{ and } \rho < 1$ $\Lambda_{1,2} = \rho e^{\pm i\theta} \text{ and } \rho > 1$ $\Lambda_{1,2} = e^{\pm i\theta}$
Stable node (2D)		
Unstable node (2D)		
Saddle (unstable) (2D)		
Stable spiral (2D)		
Unstable spiral (2D)		
Center (2D)		

3 Interacting species (Murray, Chapter 3)

Interactions between species may affect their growth rates. Here we will focus on two interacting species (while in nature often many species interact). The interaction is usually divided into three categories depending on how it affects the populations:

- **Predator-prey** if interaction increases growth rate of one species and decreases it for the other .
- **Competition** if interaction decreases growth rates of both populations.
- **Symbiosis** if interaction increases growth rates of both populations.

The general growth equations of two interacting species take the form

$$\begin{aligned}\dot{u} &= f(u, v) \\ \dot{v} &= g(u, v),\end{aligned}$$

where f and g depend on the sizes of the two populations u and v . Here these equations describe the interactions between two species, but they can also describe more general interactions, such as the kinetics of biochemical reactions (Lecture 4).

3.1 Predator-prey models

Predation or parasitism are examples of ecological interactions between species. While predators use their prey as a source of food, parasites use their hosts both as food and habitat. For many species, predation or parasitism dominate the size evolution. It is therefore of great interest to model predator-prey interactions.

3.1.1 Lotka-Volterra systems (M3.1)

We want to construct a model for predator-prey interactions between a prey population of size N and a predator population of size P . To this end, make the following assumptions:

- In absence of predation, prey has unbounded Malthusian growth $\dot{N} = aN$ with per capita growth rate $a > 0$.
- Prey population decays proportionally to the interaction rate with predator population. We often model the interaction rate as proportional to the product of population sizes, NP (rate of encounters between randomly moving individuals in homogeneous environment). We assume limitless appetite: interactions have the same outcome independent from the population sizes. This results in the following contribution to \dot{N} : $-bNP$ with constant $b > 0$.
- In absence of prey, predators have Malthusian decay $\dot{P} = -dP$ with per capita decay rate $d > 0$.
- Predator population increases proportional to their interaction rate with prey population (limitless appetite).

Combining these assumptions gives the simplest predator-prey model:

$$\begin{aligned}\dot{N} &= N(a - bP) \\ \dot{P} &= P(cN - d),\end{aligned}$$

All parameters a, b, c, d are positive. This model was proposed independently by Lotka (1920, chemical reactions) and Volterra (1926, populations).

These equations can be solved analytically. First, change to dimensionless units

$$\tau = at, \quad u(\tau) = \frac{c}{d}N(t), \quad v(\tau) = \frac{b}{a}P(t)$$

and let $\alpha = d/a$ to get:

$$\begin{aligned}\frac{du}{d\tau} &= u(1 - v) \\ \frac{dv}{d\tau} &= \alpha v(u - 1).\end{aligned}\tag{1}$$

Divide the equations:

$$\frac{dv}{du} = \frac{\alpha v(u-1)}{u(1-v)}.$$

These equations are separable:

$$\frac{1-v}{v} dv = \alpha \frac{u-1}{u} du.$$

Integrate:

$$[\log v - v]_{v_0}^v = \alpha [u - \log u]_{u_0}^u .$$

\Rightarrow the quantity

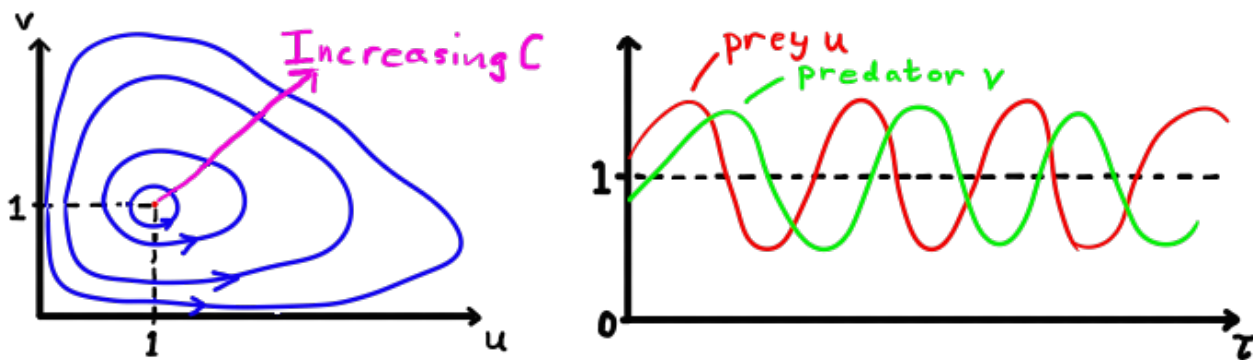
$$v + \alpha u - \log(vu^\alpha) = \underbrace{v_0 + \alpha u_0 - \log(v_0 u_0^\alpha)}_{\text{Const. } C} \quad (2)$$

is a conserved quantity (each trajectory has specific value of C that is determined by the initial condition v_0 and u_0).

- The minimal value $C_{\min} = 1 + \alpha$ for positive u and v is obtained at $u = v = 1$.
- $(u^*, v^*) = (1, 1)$ is also an isolated fixed point of Eq. (1).

That C has a local minimum at the fixed point implies that trajectories must orbit the fixed point, a ‘nonlinear center’ (Strogatz 6.5). The argument for this is as follows: different values of C correspond to different contour lines of Eq. (2). Since C increases in all directions around the isolated fixed point (where C is minimal), level curves for C slightly above C_{\min} must enclose the fixed point, forming closed orbits.

Since this is the only fixed point with $u > 0$ and $v > 0$, all solutions (with $C > 1 + \alpha$) are closed orbits in the u - v -plane (phase plane):



The system shows out-of phase oscillations between predator and prey populations. Note that direction of curves is such that prey grows if predator population is low and predators grow if prey population is high.

The closed orbits are not structurally stable (meaning a small perturbation may change the character of the solution), for example a small higher-order perturbation to the flow

$$\begin{aligned}\frac{du}{d\tau} &= u(1 - v) + \delta(u) \\ \frac{dv}{d\tau} &= \alpha v(u - 1),\end{aligned}$$

implies that the equations are no longer separable \Rightarrow no conserved quantity C \Rightarrow the center becomes a spiral (the formerly closed orbits either spiral into, or out from the fixed point).

Since the solution is structurally unstable, the Lotka-Volterra predator-prey equations should not be used as a model for interacting species. A refined model is needed.

3.1.2 More realistic predator-prey models (M3.3, 3.4)

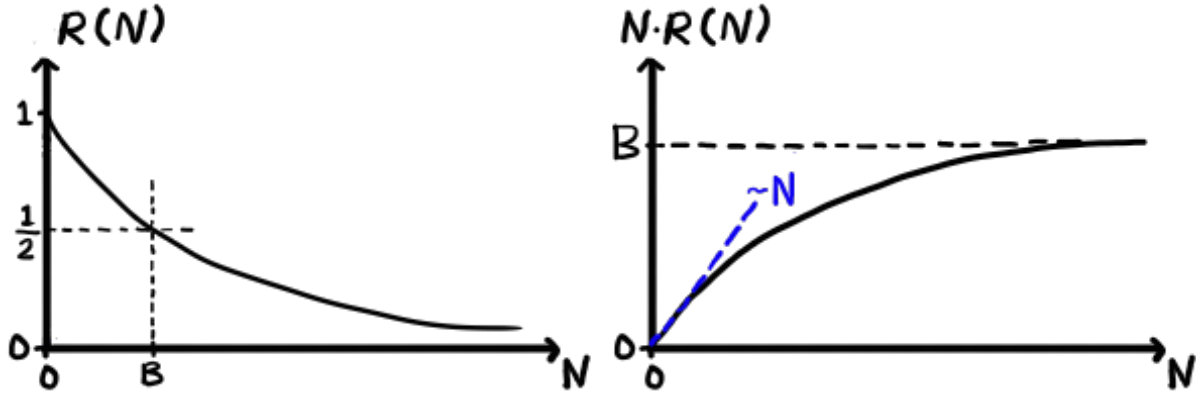
Two of the unrealistic assumptions of the Lotka-Volterra model is that the prey growth is unbounded in the absence of predation and that the predator appetite is unbounded. We therefore introduce a more realistic model. For the prey population, use logistic growth in absence of predators and modify the interaction rate:

$$\dot{N} = N \left[a \left(1 - \frac{N}{K} \right) - b P R(N) \right]$$

with $R(N)$ a decreasing function, for example:

$$R(N) = \frac{1}{1 + N/B}.$$

with saturation scale B :



The function $R(N)$ reduces the interaction rate in a way that models limited predator appetite: if N is small (compared to the parameter B), most encounters lead to reduction of prey, if N is large, only a few encounters lead to reduction of prey population. Larger values of B means larger appetite, as $B \rightarrow \infty$ the interaction of the Lotka-Volterra model is reobtained.

One possibility to model the predator growth is to replace the interaction cNP by $cNPR(N)$. An alternative which we consider below, is to replace the Lotka-Volterra interaction for P by a logistic growth with carrying capacity that is proportional to the prey population N :

$$\dot{P} = sP \left(1 - h \frac{P}{N}\right).$$

This model has 6 parameters a, b, K, B, s, h . Introduce dimensionless units

$$\tau = at, \quad u(\tau) = \frac{N(t)}{K}, \quad v(\tau) = \frac{h}{K}P(t)$$

and let

$$\alpha = \frac{bB}{ah}, \quad \beta = \frac{s}{a}, \quad \gamma = \frac{B}{K}$$

to get

$$\begin{aligned}\frac{du}{d\tau} &= u(1-u) - \alpha \frac{uv}{u+\gamma} \equiv f(u, v) \\ \frac{dv}{d\tau} &= \beta v \left(1 - \frac{v}{u}\right) \equiv g(u, v).\end{aligned}\tag{3}$$

The system has three positive dimensionless parameters α, β, γ . Fixed points are solutions to

$$f(u^*, v^*) = 0 \text{ and } g(u^*, v^*) = 0.$$

The only positive solution is

$$\begin{aligned}u^* &= \frac{1}{2} \left(1 - \alpha - \gamma + \sqrt{(1 - \alpha - \gamma)^2 + 4\gamma}\right) \\ v^* &= u^*.\end{aligned}$$

As in one dimension we classify the dynamics in the vicinity of the fixed point using linear stability analysis:

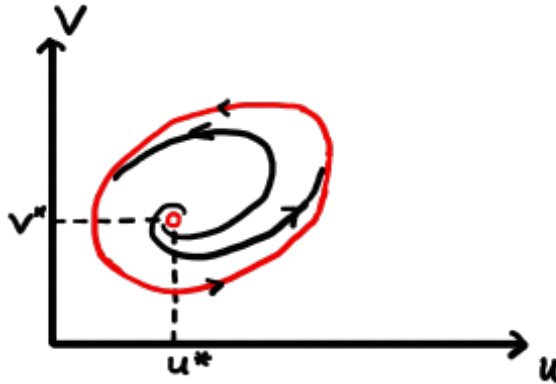
$$\begin{pmatrix} \frac{du}{d\tau} \\ \frac{dv}{d\tau} \end{pmatrix} \approx \underbrace{\begin{pmatrix} f(u^*, v^*) \\ g(u^*, v^*) \end{pmatrix}}_{=0} + \underbrace{\begin{pmatrix} \frac{\partial f}{\partial u}(u^*, v^*) & \frac{\partial f}{\partial v}(u^*, v^*) \\ \frac{\partial g}{\partial u}(u^*, v^*) & \frac{\partial g}{\partial v}(u^*, v^*) \end{pmatrix}}_{\mathbb{J}(u^*, v^*)} \begin{pmatrix} u - u^* \\ v - v^* \end{pmatrix} + \dots$$

The local dynamics around (u^*, v^*) is determined by the eigensystem of the stability matrix $\mathbb{J}(u^*, v^*)$ (denoted community matrix in population context).

The fixed point can be classified into different types depending on the eigenvalues λ_1 and λ_2 of $\mathbb{J}(u^*, v^*)$ (Murray, Appendix A).

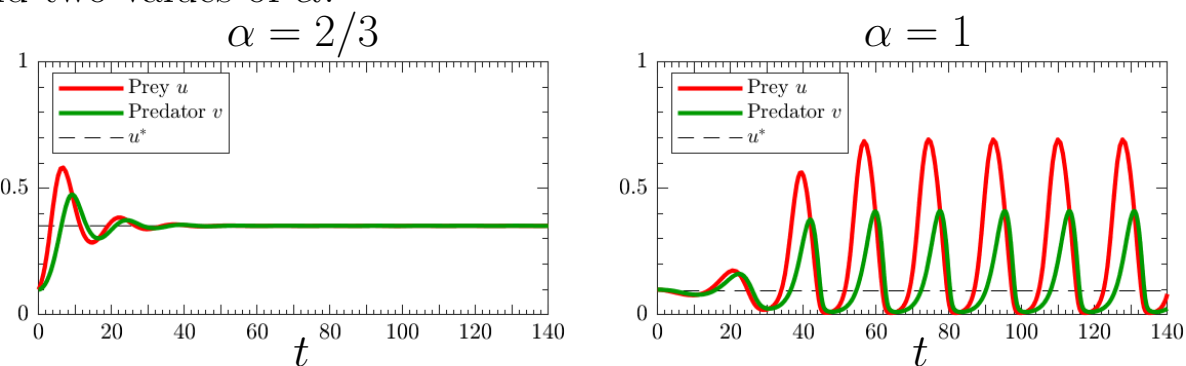
The fixed point is stable if both $\mathcal{R}e[\lambda_1] < 0$ and $\mathcal{R}e[\lambda_2] < 0$. and if either $\mathcal{R}e[\lambda_1] > 0$ or $\mathcal{R}e[\lambda_2] > 0$ the fixed point is unstable. An analysis (Murray 3.4) shows that there exists a volume in parameter space (α, β, γ space) for which the fixed point is stable and a complementary volume for which it is unstable. When the fixed point is stable, the system eventually settles at a constant population (u^*, v^*) . When the fixed point is unstable, it is possible to show (by constructing a

trapping region around the fixed point, see Murray 3.4 for details) that the system forms a limit cycle:



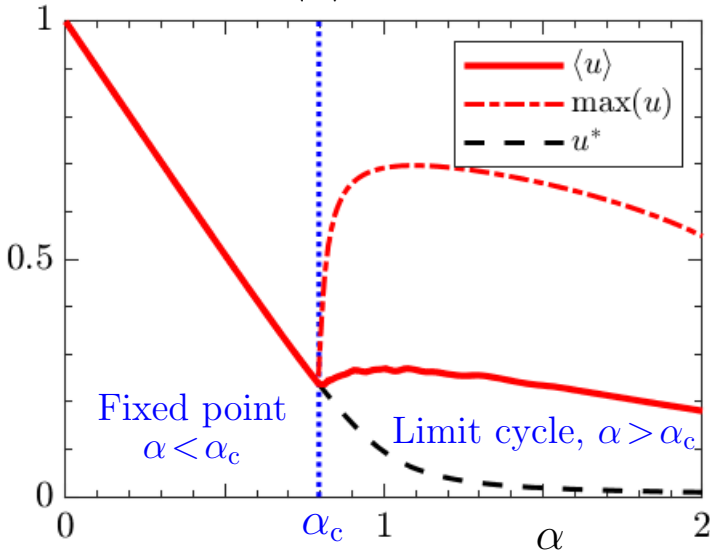
The population densities show oscillations with a phase lag, similar to the behaviour observed for the Lotka-Volterra model in Section 3.1.1 (the difference now is that the system has one single attracting periodic solution which is structurally stable).

Pest control The model described above can be used to model biological pest control which aims at controlling a pest population using its natural enemies. Assume that prey corresponds to pest and predators to a natural enemy. Simulations for $\beta = 0.5$, $\gamma = 0.01$ and two values of α :



In the absence of predators we have one stable steady state $u^* = 1$. When the natural enemy is present (with $\alpha = 2/3$) we obtain a steady state with reduced pest population $u^* \approx 0.3$. One might expect that a more effective predator [larger α , see Eq. (3)] gives more efficient pest control. This is not always so ($\alpha = 1$ in Figure above). Even though u^* decreases monotonously with increasing α , when α passes a bifurcation point the system shows high oscillations (limit cycle surrounding the fixed point). This is illustrated by plotting the average prey population

on the attractor, $\langle u \rangle$, against α with $\beta = 0.5$, $\gamma = 0.01$:



At $\alpha = \alpha_c \approx 0.8$ the system bifurcates from stable steady state ($\alpha < \alpha_c$) to stable limit cycle ($\alpha > \alpha_c$). The figure shows that the average prey population has a local minimum at the bifurcation point α_c .

3.2 Competing species (M3.5)

A simple model for competition for resources (e.g. nutrients, water, or territory) is to use logistic growth where a fraction b_{ij} of the other species contribute to the reduction of per capita growth rate (intrusion) due to finite carrying capacity:

$$\begin{aligned}\dot{N}_1 &= r_1 N_1 \left(1 - \frac{N_1 + b_{12} N_2}{K_1}\right) \\ \dot{N}_2 &= r_2 N_2 \left(1 - \frac{N_2 + b_{21} N_1}{K_2}\right),\end{aligned}$$

with growth rates $r_i > 0$, carrying capacities $K_i > 0$ and interactions $b_{ij} > 0$ (positive \Rightarrow competition). In dimensionless units

$$\tau = r_1 t, \quad u_1(\tau) = \frac{N_1(t)}{K_1}, \quad u_2(\tau) = \frac{N_2(t)}{K_2}$$

we have three dimensionless parameters

$$\rho = \frac{r_2}{r_1}, \quad a_{12} = b_{12} \frac{K_2}{K_1}, \quad a_{21} = b_{21} \frac{K_1}{K_2}$$

and the dimensionless dynamics:

$$\begin{aligned}\frac{du_1}{d\tau} &= u_1(1 - u_1 - a_{12}u_2) \\ \frac{du_2}{d\tau} &= \rho u_2(1 - u_2 - a_{21}u_1).\end{aligned}$$

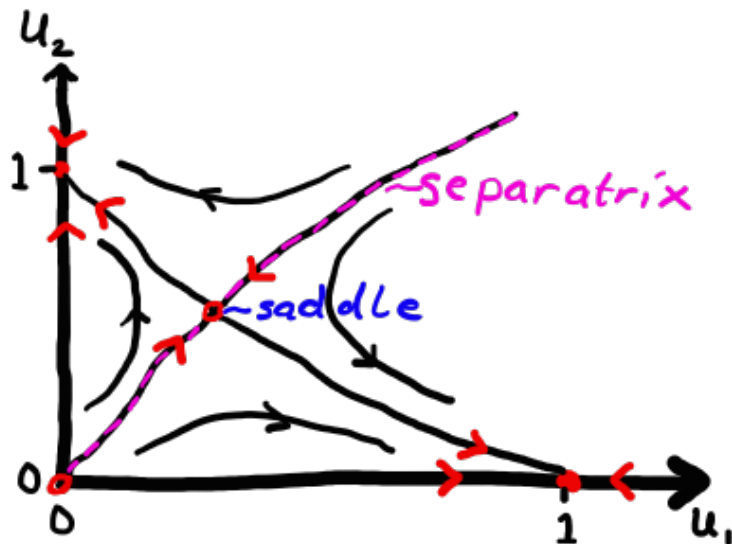
No interaction In the absence of the other species (or in the absence of competition, $a_{12} = a_{21} = 0$), the dynamics is one-dimensional along an axis and the population eventually reaches its carrying capacity ($u_1 = 1$ for species 1 or $u_2 = 1$ for species 2).

Weak interaction If both a_{12} and a_{21} are positive but smaller than unity the competition is weak and the populations reach a stationary state (stable node) with both population sizes below their carrying capacities.

Strong interaction If both a_{12} and a_{21} are larger than unity the competition is aggressive. Linear stability analysis for this case gives:

Fixed points	(0, 0)	(1, 0)	(0, 1)	$\frac{(a_{12}-1, a_{21}-1)}{a_{12}a_{21}-1}$
Sign of eigenvalues (eigenvalues real)	[+, +]	[-, -]	[-, -]	[+, -]
Type	Unstable node	Stable node	Stable node	Saddle

Flow moves along coordinate axes toward stable nodes $(0, 1)$ and $(1, 0)$ from unstable node at origin. Due to topological constraints (no crossing of trajectories along axes and negative flow for large u_1 or u_2) the saddle must connect to the other fixed points (heteroclinic orbits):



The separatrix separates regions of initial conditions ending up at a particular fixed point. For initial conditions below the separatrix, the population u_2 eventually get locally extinct (in the modelled ecosystem). Initial conditions above the separatrix implies local extinction of u_1 .

In general, if one or both of a_{12} and a_{21} are larger than unity, eventually one species dies out. This is the principle of competitive exclusion: if one species has the slightest advantage over another, it will dominate in the long term. This leads either to local extinction of the disadvantageous species, or to an evolutionary or behavioural adjustment to a different ecological niche [Gause (1934)] (reduction of a_{ij}). As a consequence, to avoid competition many species find their own niche, for example different species of birds foraging for insects in the same type of tree, with each species focusing on a different part of the tree.

The principle of competitive exclusion has been used to successfully treat infections of harmful bacteria by introducing a less harmful but more advantageous bacteria of the same strand. However, this method may backfire: if the target evolves to become more efficient when the competitor is introduced, it may make more damage (genetic evolution of one species to become better is not included in the competitive models).

3.3 Population dynamics of more species (M3.7)

The models for interacting species above can be extended to include additional species. The behaviours observed for two species (periodic oscillations of predator prey populations and extinction of competing species) are common, but there are also cases where more complex dynamics arise (limit tori, or strange attractors and chaos).

In conclusion, the study of interacting populations highlights the sensitivity of many ecosystems upon introduction of new species. One important example (among many) is the catastrophic consequences of implanting the Nile perch in Lake Victoria (Murray 3.7).

4 Reaction kinetics (Murray, Chapter 6)

In Lecture 3 we studied interaction models between populations of biological species. In this lecture we will see that these models show great similarity to simple models of chemical reactions.

4.1 Enzyme reactions (M6.1)

Most chemical reactions in living systems are very slow unless they are sped up by catalysts (substances that increase reaction rates without altering the reaction). In biological systems catalysts are called enzymes. There are thousands of examples of biochemical reactions that are sped up by enzymes. Usually catalysed reactions proceed in two steps. The substrate S reacts with the enzyme E to form a complex SE which is converted into a product P and the enzyme E



Here k_{-1} , k_1 , k_2 are rate constants (\rightleftharpoons denotes reversible reactions while \longrightarrow is a one-way reaction). The law of mass action states that the reaction rate R is proportional to the product of the concentrations of the reactants (assuming a well-mixed, not too fast reaction). Apply the law of mass action to the concentrations of reactants:

$$s = [S] \quad e = [E] \quad c = [SE] \quad p = [P]$$

to get:

$$\begin{aligned} \dot{s} &= -k_1 es + k_{-1}c, & s(0) &= s_0 \\ \dot{e} &= -k_1 es + (k_{-1} + k_2)c, & e(0) &= e_0 \\ \dot{c} &= k_1 es - (k_{-1} + k_2)c, & c(0) &= 0 \\ \dot{p} &= k_2 c, & p(0) &= 0. \end{aligned}$$

In systems described by law of mass action, linear combinations of the variables are often conserved. Add second and third equations

$$\dot{e} + \dot{c} = 0 \quad \Rightarrow \quad e + c = e_0.$$

This reflects that E acts as a catalyst: its concentration in free form (e) plus bound form (c) is constant. Using $e = e_0 - c$ and that the fourth equation is slave to the other three, two equations remain:

$$\begin{aligned}\dot{s} &= -k_1 e_0 s + (k_1 s + k_{-1})c \\ \dot{c} &= k_1 e_0 s - (k_1 s + k_{-1} + k_2)c.\end{aligned}$$

Go to dimensionless variables

$$\tau = k_1 e_0 t, \quad u(\tau) = \frac{s(t)}{s_0}, \quad v(\tau) = \frac{c(t)}{e_0}$$

and define dimensionless parameters

$$\lambda = \frac{k_2}{k_1 s_0}, \quad K = \frac{k_{-1} + k_2}{k_1 s_0}, \quad \epsilon = \frac{e_0}{s_0}$$

to get

$$\begin{aligned}\frac{du}{d\tau} &= -u + (u + \underbrace{K - \lambda}_{>0})v \equiv f(u, v), \quad u(0) = 1 \\ \frac{dv}{d\tau} &= \frac{1}{\epsilon} [u - (u + K)v] \equiv \frac{1}{\epsilon} g(u, v), \quad v(0) = 0.\end{aligned}\tag{1}$$

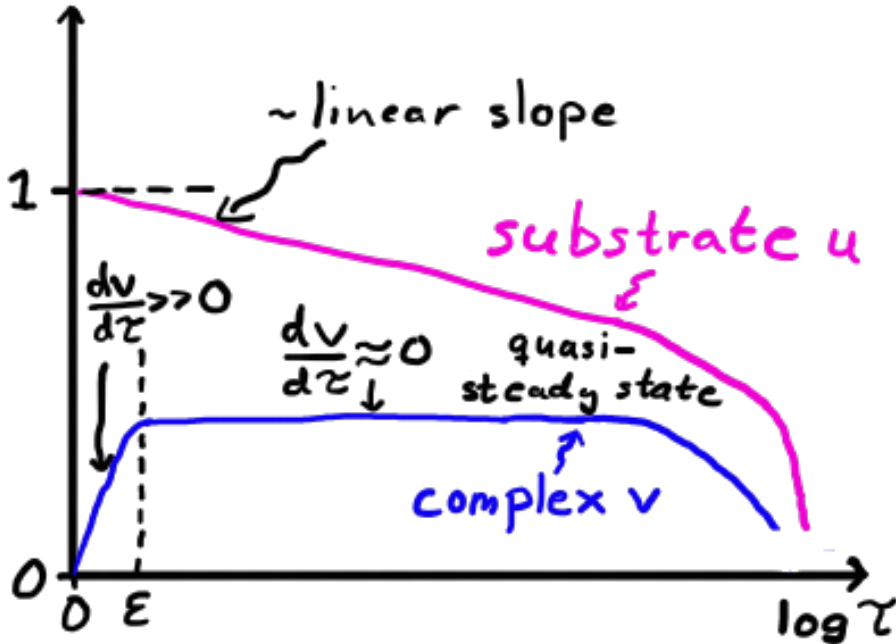
Usually only tiny enzymes concentrations are needed (compared to substrate concentrations): $\epsilon \sim 10^{-2} \dots 10^{-7}$. The Michaelis-Menten approximation exploits this observation.

4.1.1 Michaelis-Menten approximation (M6.3)

From Eq. (1) it follows that the reaction for the complex v is initially very fast (if $g(u, v)$ is not close to zero). Initially we have

$$\frac{dv}{d\tau} \gg 1.$$

It is therefore plausible that the v -reaction is more or less in equilibrium ($\frac{dv}{d\tau} \approx 0$) until the substrate is nearly all used up:



Strictly speaking this state is not a steady state, it is called Michaelis-Menten's quasi-steady state. It is valid until the substrate starts to get depleted. For $\tau \gg \epsilon$ approximate Eq. (1) by

$$\frac{du}{d\tau} = f(u, v), \quad g(u, v) = 0, \quad u(0) = 1. \quad (2)$$

Solving $g = 0$ for v gives

$$v = \frac{u}{u + K}$$

$$\frac{du}{d\tau} = -u + (u + K - \lambda) \frac{u}{u + K} = -\lambda \frac{u}{u + K}. \quad (3)$$

The relevant initial reaction rate r_0 is defined as the magnitude of the initial linear decay of the substrate u in the quasi-steady state:

$$r_0 \equiv \left| \frac{du}{d\tau} \right|_{\tau \approx 0} = \lambda \frac{u(0)}{u(0) + K} = \frac{\lambda}{1 + K}.$$

Here $\tau \approx 0$ means the start of the quasi-steady range, $\epsilon \ll \tau \ll 1$.

In dimensional variables

$$R_0 = \left| \frac{ds}{dt} \right|_{\tau \approx 0} = s_0 e_0 k_1 r_0 = \frac{Q s_0}{s_0 + K_m}$$

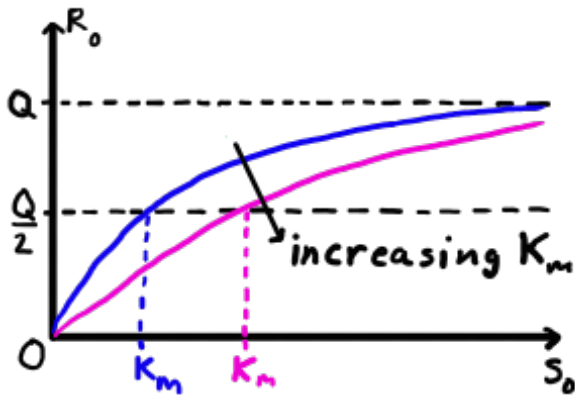
with Michaelis constant

$$K_m \equiv Ks_0 = \frac{k_{-1} + k_2}{k_1}$$

and maximal reaction rate (obtained for $s_0 \gg K_m$)

$$Q \equiv k_2 e_0 .$$

The reaction rate R_0 determines how efficient the enzyme is in converting the substrate. Parameter dependence:



Two remarks:

- In dimensional terms, Eq. (3) becomes

$$\dot{s} = -\frac{Qs}{s + K_m} .$$

If $s \ll K_m$ the right-hand side is approximately $-Qs/K_m$ (well known from Chemistry textbooks).

- $Q = k_2 e_0$ depends on the rate constant k_2 (for the conversion $\text{SE} \xrightarrow{k_2} \text{P} + \text{E}$). This conversion is called the rate-limiting step for the reaction.

Single-substrate biochemical reactions are often assumed to follow the Michaelis-Menten kinetics (even in situations where the law of mass action does not apply, such as unevenly distributed reactants in the gel-like structure of the protein-filled cytoplasm).

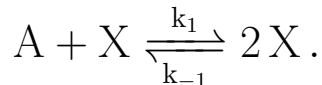
4.2 Examples of biochemical reactions (M6.6)

In addition to the two-step reaction above, living organisms host a large variety of biochemical reactions between enzymes and substrates. For example, the efficiency of an enzyme as a catalyst can be modified by other molecules: inhibitors decrease enzyme activity and activators increase activity.

The reactions can, similar to the growth models, be analyzed using a dynamical-system approach. Below, a few reactions are discussed.

4.2.1 Autocatalysis

Describes catalysis in which the products of the reaction act as a catalyst. Consider for instance



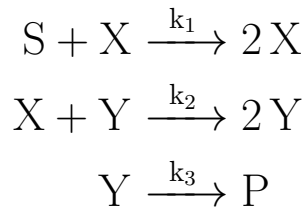
Assume that A is maintained at constant concentration $a = [A] = \text{const.}$. Law of mass action gives

$$\dot{x} = k_1ax - k_{-1}x^2.$$

This is a chemical equivalent to logistic growth.

4.2.2 Lotka reaction mechanism

Consider two coupled autocatalytic reactions giving one product:



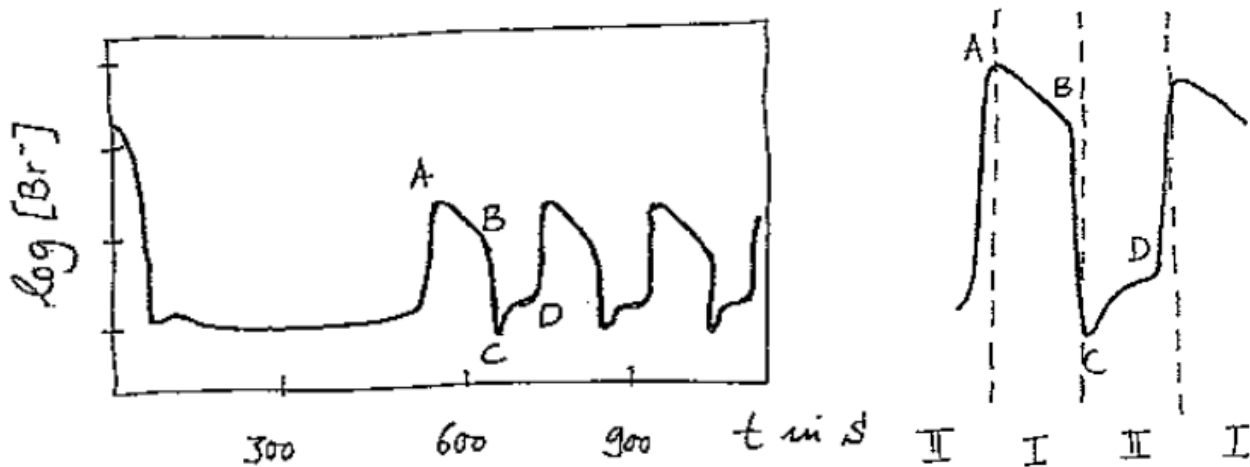
where $s = [S]$ is kept constant. Applying the law of mass action one obtains Lotka-Volterra's predator-prey dynamics:

$$\begin{aligned} \dot{x} &= \underbrace{k_1s}_a x - \underbrace{k_2}_b xy = x(a - by) \\ \dot{y} &= \underbrace{k_2}_c xy - \underbrace{k_3}_d y = y(cx - d). \end{aligned}$$

As seen in Lecture 3, these equations are solved by closed orbits in phase-space, leading to periodic oscillations of x and y . One may think that thermodynamics and chemical kinetics imply that chemical reactions quickly and monotonically reach equilibrium states. But, if the system is kept out of equilibrium (here by keeping s constant), complex or chaotic dynamics may emerge in chemical reaction systems. The Lotka example is not conclusive because the solutions are structurally unstable, but there are other examples where long-lasting concentration oscillations are observed in biochemical and chemical reactions, one being the Belousov-Zhabotinsky reaction.

4.2.3 Belousov-Zhabotinsky reaction (M8.4)

The most intensively studied chemical reaction exhibiting long-lasting oscillatory behaviour is the Belousov-Zhabotinsky reaction. It consists of two chemical processes in which bromide ions (Br^-) are consumed (process I) or created (process II). The reaction is kept out of equilibrium by constant supply of bromat (BrO_3^-). Experimental observation of $[\text{Br}^-]$ concentration:



After an initial transient the system shows periodic oscillations in the $[\text{Br}^-]$ concentration. Quick transitions occur between states where either process I ($A \rightarrow B$) or process II ($C \rightarrow D$) are dominant.

The experimental data is of the type of a relaxation oscillator (very slow build-up and sudden discharge). This is also what an analysis of the reaction equations shows.

5 Stochastic dynamics (Murray, Ch. 11)

So far we have considered simplified mathematical models for growth and interaction of populations, as well as chemical reactions. These have been deterministic models: the populations/concentrations are uniquely determined by the initial conditions. But in reality population sizes and chemical concentrations do not follow deterministic laws. More realistic stochastic models take into account of stochastic fluctuations of the population size and chemical concentrations.

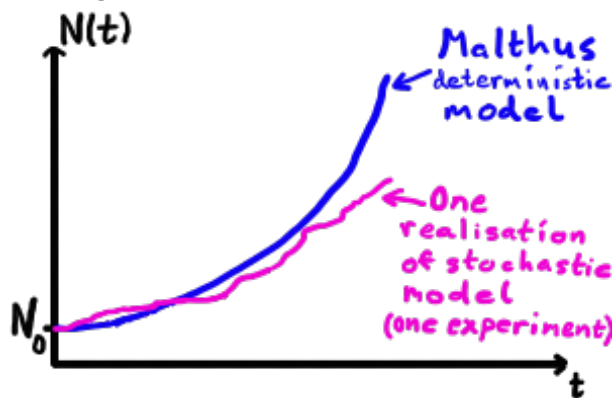
5.1 Deterministic versus stochastic growth models (Okubo, Chapter 1.3)

As an illustrative example, consider Malthus' growth model due to births only (per capita birth rate r , no deaths nor migration)

$$\dot{N} = rN \quad \Rightarrow \quad N(t) = N_0 e^{rt}.$$

If r is constant, then $N(t)$ is uniquely determined by the initial size N_0 .

Now consider an experiment (numerical or real-world) where the population increases due to births. Let $r \cdot \delta t$ denote the probability that in a small time interval, δt , one individual gives birth to another individual (r is an average per capita birth rate). In this formulation the size evolution $N(t)$ varies from experiment to experiment, even though r and N_0 are kept fixed:



Let $Q_N(t)$ be the probability to have N individuals at discrete time steps $t \in n\delta t$ with integer n . The following stochastic model deter-

mines how this probability changes with time:

$$Q_N(t) = Q_N(t - \delta t) + r\delta t(N - 1)Q_{N-1}(t - \delta t) - r\delta t N Q_N(t - \delta t).$$

The second term on the right-hand side is the gain in probability from the previous time step due to births causing transitions $N - 1 \rightarrow N$. The third term is the loss in probability due to births, $N \rightarrow N + 1$.

Move the term $Q_N(t - \delta t)$ to the left-hand side, divide by δt and take limit $\delta t \rightarrow 0$ to form a differential equation (Master equation)

$$\frac{dQ_N}{dt} = r(N - 1)Q_{N-1}(t) - rNQ_N(t) \quad (1)$$

with initial condition $Q_N(0) = \delta_{N,N_0}$.

As seen in the figure above, a realisation of the stochastic model in general differ from the deterministic model. To obtain the average result of the stochastic model, multiply Eq. (1) with N and sum over N

$$\begin{aligned} \frac{d}{dt} \sum_{N=0}^{\infty} N Q_N &= r \sum_{N=0}^{\infty} N(N - 1)Q_{N-1}(t) - r \sum_{N=0}^{\infty} N^2 Q_N(t) \\ &\quad [\text{Change of variable } N = N' + 1 \text{ in the first sum}] \\ &= r \sum_{N'=-1}^{\infty} (N' + 1)N' Q_{N'}(t) - r \sum_{N=0}^{\infty} N^2 Q_N(t) \\ &\quad [\text{First term is zero in first sum. Relabel } N' \rightarrow N] \\ &= r \sum_{N=0}^{\infty} N Q_N(t). \end{aligned}$$

Using that the expectation value of the population size N at time t is

$$\langle N(t) \rangle = \sum_{N=0}^{\infty} N Q_N(t)$$

we get

$$\frac{d}{dt} \langle N(t) \rangle = r \langle N(t) \rangle.$$

The average of the stochastic variable $N(t)$ follows the deterministic growth law (true for linear systems, but may fail for non-linear ones). As a result $\langle N(t) \rangle = N_0 e^{rt}$. A similar calculation gives the standard deviation:

$$\text{std}(N(t)) \equiv \sqrt{\langle N(t)^2 \rangle - \langle N(t) \rangle^2} = \sqrt{N_0} e^{rt} \sqrt{1 - e^{-rt}}.$$

For large t the relative standard deviation becomes

$$\frac{\text{std}(N(t))}{\langle N(t) \rangle} \sim N_0^{-1/2}.$$

Thus, a larger initial population gives better agreement between the deterministic law and one realization of the stochastic process. This latter result holds quite generally (also for non-linear systems). However, there are also critical differences between the models. If deaths were included in the models such that

$$r = \text{'rate of births'} - \text{'rate of deaths'} > 0$$

the population increases monotonously in the deterministic model. In a stochastic model with births and deaths there is always a finite (but in general small) probability that the population becomes extinct. Later in the course we will consider stochastic effects of finite population sizes in the context of disease spreading.

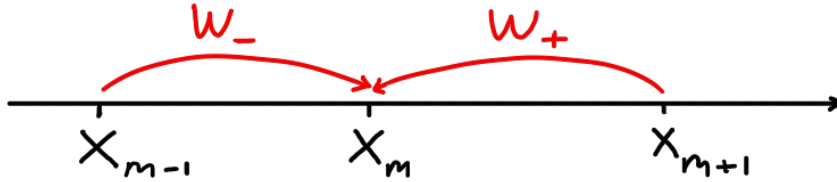
5.2 One-dimensional diffusion (M 11.1)

In the example above, a stochastic model was introduced to model temporal fluctuations in births. If the population size is large enough, this is not a problem and we can treat the growth deterministically.

Another stochastic aspect of the evolution of a population is spatial spread. As a simplest example the individuals of a population move randomly and independent of each other, a random walk.

5.2.1 One-dimensional random walk

Consider an individual, or a particle in general, moving at discrete coordinates $x_m \equiv m\delta x$ along the x -axis:



Assume that at each time step δt the particle makes a jump to a neighbouring discrete coordinate. Let w_- be the probability that the jump is $+\delta x$, i.e. w_- is the transition probability to move from $x_{m-1} \rightarrow x_m$. Analogously, w_+ is the transition probability from $x_{m+1} \rightarrow x_m$. The assumption that the particle jumps either $-\delta x$ or $+\delta x$ each time step gives $w_+ + w_- = 1$.

This process gives the possible particle positions $-n\delta x, \dots, n\delta x$ at time $n\delta t$. However, one should expect the probability to be higher close to $x = 0$. To find the time evolution of the spatial probability distribution, let $Q(x, t)$ be the probability to find the particle at discrete position $x \in m\delta x$ at discrete time steps $t \in n\delta t$ (m and n integers), given it was at $x = 0$ at $t = 0$. For the random walk we have:

$$Q(x, t) = w_- Q(x - \delta x, t - \delta t) + w_+ Q(x + \delta x, t - \delta t). \quad (2)$$

We want to find an equation for Q in the continuous limit $\delta t \rightarrow 0$ and $\delta x \rightarrow 0$. Series expand the Q :s on the r.h.s. in Eq. (2)

$$Q(x \pm \delta x, t - \delta t) = Q \pm \delta x \frac{\partial Q}{\partial x} - \delta t \frac{\partial Q}{\partial t} + \frac{\delta x^2}{2} \frac{\partial^2 Q}{\partial x^2} \mp \delta x \delta t \frac{\partial^2 Q}{\partial x \partial t} + \frac{\delta t^2}{2} \frac{\partial^2 Q}{\partial t^2} + \dots$$

where $Q \equiv Q(x, t)$. Insert this expansion into Eq. (2), using $w_+ = 1 - w_-$ and define $\epsilon \equiv w_- - w_+$:

$$\begin{aligned} Q &= Q - \epsilon \delta x \frac{\partial Q}{\partial x} - \delta t \frac{\partial Q}{\partial t} + \frac{\delta x^2}{2} \frac{\partial^2 Q}{\partial x^2} + \epsilon \delta x \delta t \frac{\partial^2 Q}{\partial x \partial t} + \frac{\delta t^2}{2} \frac{\partial^2 Q}{\partial t^2} + \dots \\ \Rightarrow \frac{\partial Q}{\partial t} &= -\frac{\epsilon \delta x \partial Q}{\delta t} + \frac{\delta x^2 \partial^2 Q}{2 \delta t} + \epsilon \delta x \frac{\partial^2 Q}{\partial x \partial t} + \frac{\delta t \partial^2 Q}{2} + \dots \end{aligned}$$

Take δt , δx and ϵ to zero such that

$$\frac{\delta x^2}{2\delta t} \rightarrow D \quad (3)$$

$$\frac{\delta x \epsilon}{\delta t} \rightarrow v, \quad (4)$$

where $D > 0$ and v are constants. This gives the continuous probability $Q(x, t)$ to find a particle at (continuous) position x and time t

$$\frac{\partial Q}{\partial t} = \underbrace{-v \frac{\partial Q}{\partial x}}_{\text{Advection (Drift)}} + \underbrace{D \frac{\partial^2 Q}{\partial x^2}}_{\text{Diffusion}}. \quad (5)$$

This is an example of an advection-diffusion equation. Eq. (5) is also satisfied for concentrations $n(x, t) = Q(x, t)N/V$ (here N is the total number of entities enclosed in a volume V).

5.2.2 Probability moments

To investigate Eq. (5), consider the moments

$$m_p(t) \equiv \langle x^p \rangle = \int_{-\infty}^{\infty} dx x^p Q(x, t).$$

$Q(x, t)$ is a probability distribution $\Rightarrow m_0(t) = 1$ at all times.
Assume that particle is initially localized at $x = 0$:

$$\begin{aligned} Q(x, t = 0) &= \delta(x) \\ \Rightarrow m_p(0) &= \begin{cases} 0 & \text{if } p > 0 \\ 1 & \text{if } p = 0 \text{ (normalisation)} \end{cases} \end{aligned}$$

Multiply Eq. (5) by x^p and integrate over x

$$\underbrace{\int_{-\infty}^{\infty} dx x^p \frac{\partial Q}{\partial t}}_{\frac{\partial m_p}{\partial t}} = -v \int_{-\infty}^{\infty} dx x^p \frac{\partial Q}{\partial x} + D \int_{-\infty}^{\infty} dx x^p \frac{\partial^2 Q}{\partial x^2} = [\text{P.I.}]$$

$$\begin{aligned}
&= \underbrace{\left[-vx^p Q + x^p \frac{\partial Q}{\partial x} \right]_{-\infty}^{\infty}}_0 + p v \underbrace{\int_{-\infty}^{\infty} dx x^{p-1} Q}_{m_{p-1}} - p D \underbrace{\int_{-\infty}^{\infty} dx x^{p-1} \frac{\partial Q}{\partial x}}_{m_{p-2}} \\
&= p v m_{p-1} - p D \underbrace{[x^{p-1} Q]_{-\infty}^{\infty}}_0 + p(p-1) D \underbrace{\int_{-\infty}^{\infty} dx x^{p-2} Q}_{m_{p-2}} \\
&\Rightarrow \partial_t m_p = p v m_{p-1} + p(p-1) D m_{p-2} \\
\text{Case } p = 0 : & \quad \partial_t m_0 = 0 \Rightarrow m_0 = 1 \text{ (normalisation)} \\
\text{Case } p = 1 : & \quad \partial_t m_1 = 1 \cdot v \cdot 1 + 0 \Rightarrow m_1 = vt \\
&\quad (\text{average position moves with const. velocity } v) \\
\text{Case } p = 2 : & \quad \partial_t m_2 = 2 \cdot v \cdot (vt) + 2 \cdot 1 \cdot D \cdot 1 \Rightarrow m_2 = v^2 t^2 + 2Dt
\end{aligned}$$

The mean square displacement (when $x_0 = 0$) becomes

$$\text{var}(x) = \langle (x - \langle x \rangle)^2 \rangle = \langle x^2 \rangle - \langle x \rangle^2 = m_2 - m_1^2 = 2Dt. \quad (6)$$

Eq. (6) is the characteristic law of diffusion, the mean square displacement grows linearly in time. The constant D is the diffusion coefficient. Note that Eq. (6) is a macroscopic equation (valid at macroscopic length and time scales), while Eq. (3) is a microscopic law.

5.2.3 Diffusion equation

For the special case $v = 0$ in Eq. (5) we get the diffusion equation:

$$\frac{\partial Q}{\partial t} = D \frac{\partial^2 Q}{\partial x^2}. \quad (7)$$

When $v = 0$, there is no net drift, $\langle x \rangle = 0$, but the mean square displacement increases with time: $\langle x^2 \rangle = 2Dt$ (diffusion).

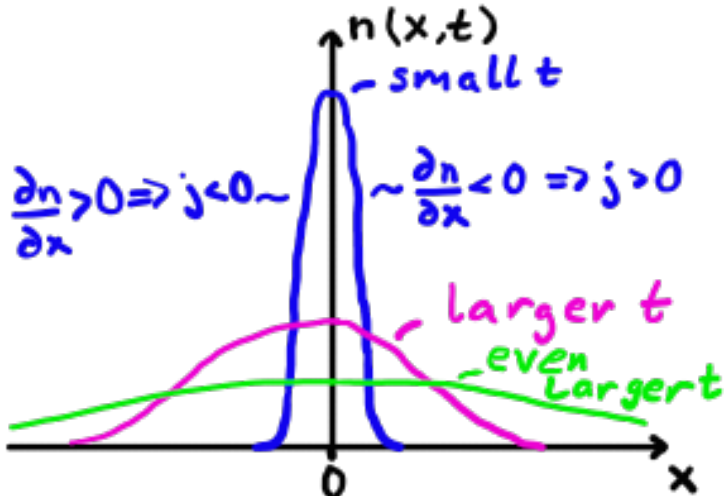
5.3 Macroscopic view of diffusion

The diffusion equation in the previous section was derived from a microscopic viewpoint, where the detailed motion of individual particles (the random walk) led to an equation for the macroscopic probability

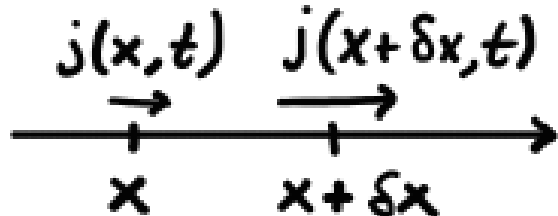
distribution Q . It is also possible to derive the diffusion equation starting from a macroscopic viewpoint. According to Fick's law matter is transported from high concentrations to low concentrations:

$$j(x, t) = -D \frac{\partial n}{\partial x}.$$

Here n is particle concentration, $n(x, t) = Q(x, t)N/V$ and the matter flux $j(x, t)$ denotes the transport of matter in the x -direction per ‘unit area’ and unit time. The effect of Fick’s law is to spread out sharp concentration gradients:



The change of concentration in a small interval δx



is

$$\frac{\partial}{\partial t} \int_x^{x+\delta x} dx' n(x', t) = j(x, t) - j(x + \delta x, t).$$

Divide by δx and let $\delta x \rightarrow 0$ to get

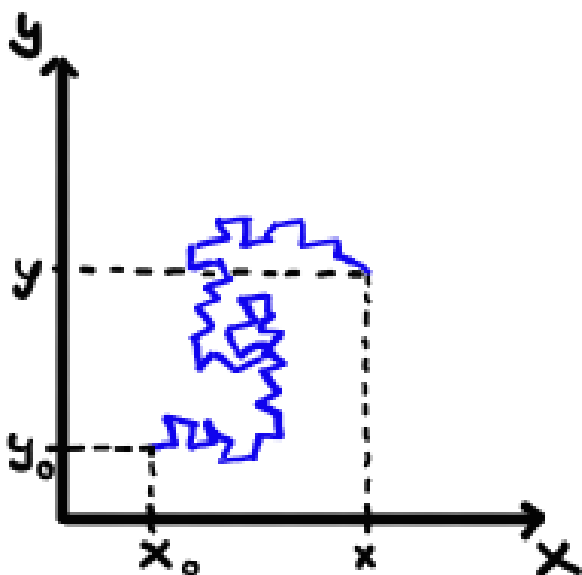
$$\frac{\partial n}{\partial t} = -\frac{\partial j}{\partial x} = D \frac{\partial^2 n}{\partial x^2}.$$

i.e. same as the diffusion equation Eq. (7).

6 Reaction-diffusion equations & travelling waves (Murray, Ch. 11, 13)

6.1 Diffusion

In lecture 5 we introduced one-dimensional random walks and derived a diffusion equation that determines the probability to find a random walker at position x at time t . The phenomenology of diffusion is similar in higher dimensions. Consider for example Brownian motion, i.e. the random motion of a particle induced by collisions with many smaller molecules:



Similar to the one-dimensional case, the mean square displacement for a particle initially localized at (x_0, y_0) grows linearly with time:

$$\text{var}(x - x_0) = 2Dt, \quad \text{var}(y - y_0) = 2Dt,$$

where D is the diffusion coefficient. Individual particles are unlikely to be found at their initial position after long times.

In general diffusion denotes an ‘irreversible’ process by which matter, particle groups, populations etc. spread out within a given space according to ‘random motion’ of individual particles. Here ‘irreversible’ means that the probability to go back to the initial configuration goes to zero as the number of particles goes to infinity. The ‘random motion’ can either be uncorrelated at different time steps, or there can

be some correlations that depend on which underlying mechanisms drives the particles. Three examples of underlying mechanisms important for biological applications are: molecular motion (molecular diffusion), turbulent flow (turbulent diffusion), and self-driven motion (motility) of biological species (population diffusion). As discussed below, the magnitude and spatial dependence of the diffusion coefficients may vary significantly depending on the underlying mechanism.

Example Molecular diffusion of proteins (diffusion coefficient $D \sim 10^{-11}\text{m}^2/\text{s}$) in a cell in the body (length scale $L \sim 10\mu\text{m}$). Time scale for diffusion to homogenise spatial variations of the protein: $T \sim L^2/D \sim 10\text{s}$.

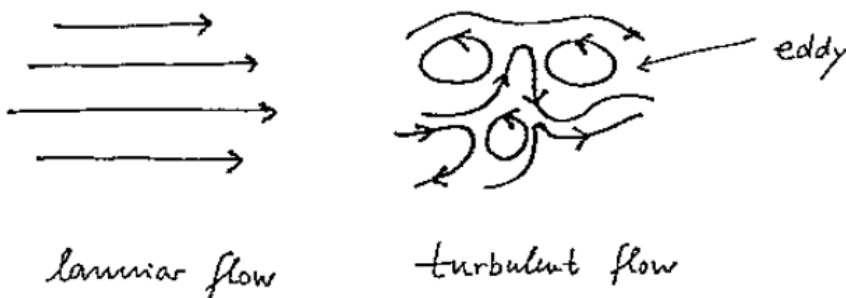
Example Sugar at the bottom of a cup of coffee may spread throughout the cup due to molecular diffusion. The diffusion coefficient for sugar dissolved in coffee is $D \sim 10^{-9}\text{m}^2/\text{s}$. The time T for sugar to get uniformly mixed due to diffusion in a cup of height $L = 5\text{cm}$ is $T \sim L^2/D \sim 30\text{days}$.

6.1.1 Turbulent diffusion (Okubo 2.4)

As seen by the second example above, molecular diffusion is often extremely slow at macroscopic scales. Diffusion due to turbulence is more efficient at these scales. The position of a small particle in a fluid flow evolves as $\dot{\mathbf{x}} = \mathbf{u}(\mathbf{x}, t)$

Laminar flow: low flow velocity \mathbf{u} , streamlines parallel

Turbulent flows: high flow velocity \mathbf{u} , irregular streamlines, chaotic



The accelerations of a particle in a (chaotic) turbulent flow can be viewed as random. The particle is governed by large-scale turbulent

diffusion (as opposed to the molecular-driven diffusion in Brownian motion). Some characteristic features of turbulent diffusion are:

1. Typical time-and length scales in turbulent diffusion are macroscopic (Brownian motion has microscopic length scale).
2. Turbulent flows consist of eddies with sizes that may vary over many orders of magnitude. Which eddies that contribute to the diffusion process varies with length scale ℓ , larger and larger eddies contribute as ℓ is increased. The effective diffusion coefficient D_{eff} grows with length scale ℓ as $D_{\text{eff}} \sim \ell^{4/3}$ according to experiments and theory (Richardson 1926). Turbulent diffusion becomes very efficient at the largest scales (dispersion of particles in the ocean, rain clouds, etc.)
3. Can in general not be modeled by simple random-walk models (need more general correlated random walks)

In conclusion: Turbulence is very good at mixing (tracer) particles.

6.1.2 Population diffusion (M11.3,11.4)

In population diffusion the particles (animals) are motile. The diffusion coefficient often depends on the population density. One example is models of migration of humans or animals (demic diffusion) from overcrowded areas into empty areas.

Population diffusion is often directed by chemicals (pheromones) that allow individuals to locate food and other individuals. This is particularly important for small animals that have limited sensing abilities. One example is the diffusion due to ‘run and tumble’ motion of bacteria (run and tumble is essentially a random walk, with alternating steps (run) and reorientations (tumble)). In the presence of a (diffusing) chemical, the run and tumble process may become directed and the bacteria climb the concentration gradient of the diffusing chemical (chemotaxis), leading to a concentration of bacteria close to the source of the chemical.

6.1.3 Importance of diffusion for biological systems

The mechanisms for diffusion discussed above are important in many biological applications. Some examples

- **Motility** All three mechanisms are important to describe the motility and spatial spread of small organisms as well as larger animals (for the latter molecular diffusion is not so important).
- **Reproduction** Spreading of pollen and spores using wind, water, or pollinators relies on all three diffusion mechanisms.
- **Chemical reactions** Molecular diffusion is often the mechanism in which large molecules (proteins and enzymes) are brought into contact with other reactants. Stirring (turbulent diffusion) may increase the reaction rate significantly.
- **Chemical communication** Pheromones from insects and other animals spread through diffusion.
- **Patchiness and pattern formation** can be driven by diffusion processes

This course focuses on population motility and on pattern formation.

6.2 Reaction-diffusion equations (M11.2)

Fick's law (from Lecture 5): diffusion occurs from high concentration to low concentration as to smoothen out concentration gradients. Matter flux (per unit area and unit time)

$$j = -D \frac{\partial n}{\partial x}.$$

Using conservation of mass in a small length segment (continuity equation) we found that Fick's law is equivalent to the one-dimensional diffusion equation.

Now consider a more general situation in three dimensions. Let S be a surface enclosing a volume V :



Apply the continuity equation (conservation equation):

'Change of concentration in volume V '

= 'Outflux of particles through boundary' + 'Particle production in volume'

$$\frac{\partial}{\partial t} \int_V d^3x n(\mathbf{x}, t) = - \int_S \underbrace{d\mathbf{S} \cdot \mathbf{j}(\mathbf{x}, t)}_{\text{flux of particles through } dS} + \int_V d^3x \underbrace{f(\mathbf{x}, t)}_{\text{source}}$$

Apply divergence theorem

$$\int_S d\mathbf{S} \cdot \mathbf{j}(\mathbf{x}, t) = \int_V d^3x \nabla \cdot \mathbf{j}(\mathbf{x}, t)$$

to get

$$0 = \int_V d^3x \left[\frac{\partial}{\partial t} n(\mathbf{x}, t) + \nabla \cdot \mathbf{j}(\mathbf{x}, t) - f(\mathbf{x}, t) \right].$$

This is true for any volume \Rightarrow integrand must vanish at all positions

$$0 = \frac{\partial}{\partial t} n(\mathbf{x}, t) + \nabla \cdot \mathbf{j}(\mathbf{x}, t) - f(\mathbf{x}, t). \quad (1)$$

This is the differential form of the continuity equation. It has many applications: n could denote mass, energy, electric charge, etc, and the forms of \mathbf{j} and f are determined by the mechanisms for local flux and production of n . Here, we let n denote a concentration of e.g. a chemical or a population, and we let the local flux \mathbf{j} be governed by diffusion (Fick's law)

$$\mathbf{j}(\mathbf{x}, t) = -D \nabla n(\mathbf{x}, t).$$

We have

$$\frac{\partial}{\partial t} n(\mathbf{x}, t) = \underbrace{f(\mathbf{x}, t)}_{\text{reaction}} + \underbrace{\nabla \cdot [D \nabla n(\mathbf{x}, t)]}_{\text{diffusion}}. \quad (2)$$

Commonly we let $D = \text{const.}$, but in general D can be anisotropic (a matrix) and depend on position (carefully taking into account which of the differential operators ∇ act on D).

Eq. (2) is an example of a reaction-diffusion equation: the reaction term describes how concentration n is transformed due to the source f , while the diffusion term describes spatial diffusion of n . The source $f(\mathbf{x}, t)$ is often a functional of concentration n and only implicitly depends on the coordinates \mathbf{x} and t through $n(\mathbf{x}, t)$.

6.2.1 Example: Population growth models

Let the source term $f(\mathbf{x}, t)$ represent birth-and-death processes and $n(\mathbf{x}, t)$ the population density. Assume constant D and logistic growth

$$f(\mathbf{x}, t) = rn \left(1 - \frac{n}{K}\right)$$

with linear growth rate r and carrying capacity K . Use Eq. (2) to get

$$\frac{\partial}{\partial t} n(\mathbf{x}, t) = rn(\mathbf{x}, t) \left(1 - \frac{n(\mathbf{x}, t)}{K}\right) + D \nabla^2 n(\mathbf{x}, t). \quad (3)$$

This is Fisher's equation, proposed by Fisher (1937) as a model for the spatial spread of an advantageous gene in a population. It is a natural generalisation of the logistic growth model to include spatial migration via diffusion.

6.2.2 Reaction-diffusion equations in Biological contexts

Reaction-diffusion equations are used to model population migration, infection outbreaks, wound healing, chemical reactions, etc. They also form prototype models for pattern formation. They are believed to

be essential for processes in which organisms develop their shape, and for patterns of animal coats and skin pigmentation.

Typical solutions of reaction-diffusion equations are: travelling waves, wave-like phenomena, self-organized patterns like stripes, spirals, etc.

6.2.3 More general reaction-diffusion equation for several interacting species or chemicals

Let $n_\alpha(\mathbf{x}, t)$ with $\alpha = 1, 2, \dots, m$ represent m different species. The reaction-diffusion equation Eq. (2) generalises to

$$\frac{\partial n_\alpha}{\partial t} = f_\alpha + \nabla \cdot \left[\sum_{\beta=1}^m D_{\alpha\beta} \nabla n_\beta \right]$$

The diffusion matrix $D_{\alpha\beta}$ is usually diagonal and interactions between species occur through f_α (each species has its own diffusivity $D_{\alpha\alpha}$).

6.2.4 Advection-diffusion equations

Advection denotes a deterministic transport of a substance with velocity $\mathbf{v}(\mathbf{x}, t)$, for example due to a turbulent fluid flow. The flux

$$\mathbf{j}(\mathbf{x}, t) = \underbrace{\mathbf{v}(\mathbf{x}, t)n(\mathbf{x}, t)}_{\text{Instantaneous flux generated by } \mathbf{v} \text{ (advection)}} - \underbrace{D\nabla n(\mathbf{x}, t)}_{\text{Contribution from diffusion (Fick's law)}}$$

inserted into the continuity equation (1) [neglect source, $f = 0$] gives

$$\frac{\partial}{\partial t} n(\mathbf{x}, t) = -\nabla \cdot \mathbf{j}(\mathbf{x}, t) = \nabla \cdot [-\mathbf{v}(\mathbf{x}, t)n(\mathbf{x}, t) + D\nabla n(\mathbf{x}, t)].$$

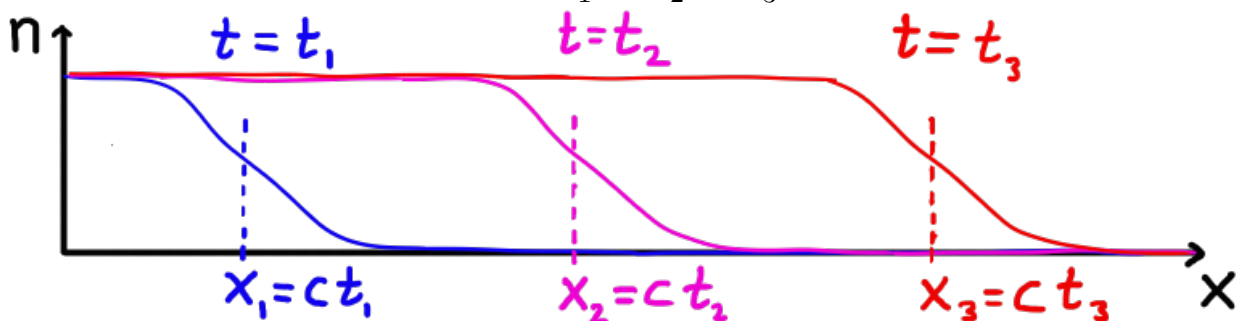
If $\mathbf{v}(\mathbf{x}, t) = \text{const.}$ this is the advection-diffusion equation of the one-dimensional random walk in Lecture 5. More generally when $\mathbf{f} \neq 0$, we have a combination: Reaction-Advection-Diffusion equation.

6.3 Travelling waves (M13.1,13.2,13.5)

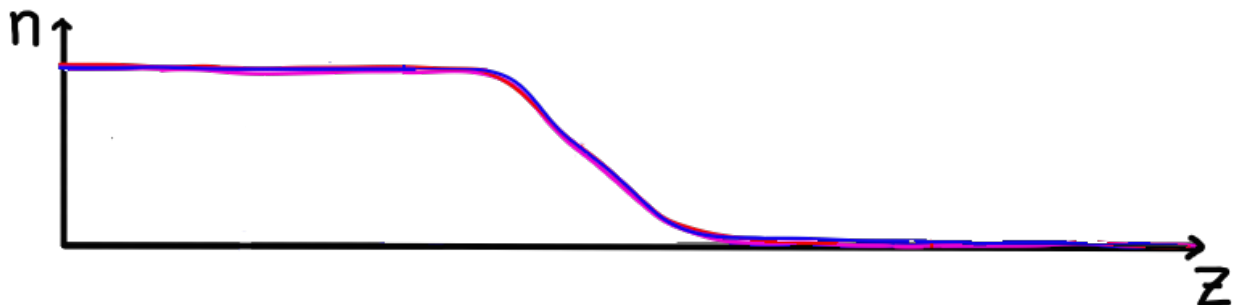
The reaction-diffusion equation in one dimension is

$$\frac{\partial}{\partial t} n(x, t) = f(x, t) + D \frac{\partial^2}{\partial x^2} n(x, t). \quad (4)$$

Assume $f = f(n(x, t))$, i.e. no explicit space-or time-dependence. Typical solutions (depending on f and boundary conditions): waves with continuously varying shape and speed of the wave front. Eq. (4) also allows for travelling-wave solutions: solutions which travel with constant shape and speed (and much faster than diffusion). Illustration for three successive times $t_1 < t_2 < t_3$:



Position of constant n moves with constant speed c . Change coordinates from (x, t) to moving coordinate (z, t) with wave variable $z = x - ct$. The concentration $n(z, t)$ is a travelling wave if it only depends on z (not explicitly on t). For the illustration above all curves collapse:



Depending on the initial condition, the solution may have an initial transient before reaching the travelling wave form. Often travelling waves are stable structures: for many initial conditions the travelling-wave solution is approached at large times.

Now search for travelling wave solutions to Eq. (4) by the ansatz

$$n(x, t) = u(x - ct) = u(z).$$

This coordinate change reduces the number of variables from 2 (x and t) to 1 (z). We have

$$\begin{aligned}\frac{\partial n}{\partial t} &= -c \frac{du}{dz} \\ \frac{\partial n}{\partial x} &= \frac{du}{dz}\end{aligned}$$

and Eq. (4) becomes

$$-c \frac{d}{dz} u(z) = f(u(z)) + D \frac{d^2}{dz^2} u(z), \quad (5)$$

i.e. an ordinary differential equation in z .

Boundary conditions For given boundary+initial conditions Eq. (4) has a unique solution. In contrast, for given boundary conditions Eq. (5) may have different solutions for different values of c .

To find allowed boundary conditions, integrate Eq. (5) over z

$$0 = \left[cu(z) + D \frac{d}{dz} u(z) \right]_{-\infty}^{\infty} + \int_{-\infty}^{\infty} dz f[u(z)].$$

Physical solutions have finite values of $u(z)$ and $u'(z)$ for all z . Therefore the integral must take a finite value. One condition for the integral to be finite is $f[u(z)] \rightarrow 0$ as $z \rightarrow \pm\infty$. Thus, for large $|z|$, $u(z)$ approaches fixed-points $f(u^*) = 0$ of the dynamical system obtained by letting $D = 0$ (homogeneous reaction) in Eq. (5).

6.3.1 Phase-plane analysis

Introduce help variable $v = \frac{du}{dz}$ to rewrite Eq. (5) as first-order system

$$\begin{aligned}\frac{du}{dz} &= v \\ \frac{dv}{dz} &= \frac{-cv - f(u)}{D}\end{aligned}$$

This is a flow with ‘time variable’ z and steady states at $v^* = 0$ and $f(u^*) = 0$. NB: If $c > 0$ then $z = x - ct$ may be of opposite sign compared to $t \Rightarrow$ steady states $f(u^*) = 0$ may show opposite stability compared to homogeneous steady states of Eq. (5) with $D = 0$. Classify the fixed point by evaluation of the Jacobian

$$\mathbb{J} = \begin{pmatrix} 0 & 1 \\ -f'(u^*)/D & -c/D \end{pmatrix}.$$

Eigenvalue equation

$$\begin{aligned} 0 &= \det(\mathbb{J} - \lambda \mathbb{I}) = \lambda(\lambda + c/D) + f'(u^*)/D \\ \Rightarrow \lambda_{\pm} &= \frac{1}{2D} \left(-c \pm \sqrt{c^2 - 4Df'(u^*)} \right) \end{aligned}$$

Depending on c , D and $f'(u^*)$ the fixed point can be of any type. Typically: Travelling waves are solutions that connects two steady states (heteroclinic orbit), joining an unstable manifold of the steady state where the wave originates ($z \rightarrow -\infty$) to the stable manifold of the steady state where the wave stops ($z \rightarrow \infty$).

6.3.2 Example: No reaction term

When $f = 0$ (the diffusion equation) no physically meaningful travelling wave exists to Eq. (5)

$$\begin{aligned} -c \frac{du}{dz} &= D \frac{d^2u}{dz^2} \\ \Rightarrow u(z) &= A + Be^{-cz/D} \end{aligned}$$

For the solution to be bounded as $z \rightarrow -\infty$ we must have $B = 0$. The remaining part of solution $n = A = \text{const.}$ is not a wave.

6.3.3 Example: Fisher’s equation (13.2)

$$\frac{\partial n}{\partial t} = \underbrace{rn \left(1 - \frac{n}{K}\right)}_{\text{logistic growth}} + \underbrace{D \frac{\partial^2 n}{\partial x^2}}_{\text{diffusion}}.$$

Change to dimensionless variables (units: $[r] = [t]^{-1}$, $[D] = [x]^2[t]^{-1}$, and $[K] = [n]$)

$$n = Kn', \quad t = \frac{t'}{r}, \quad x = x' \sqrt{\frac{D}{r}} \quad (6)$$

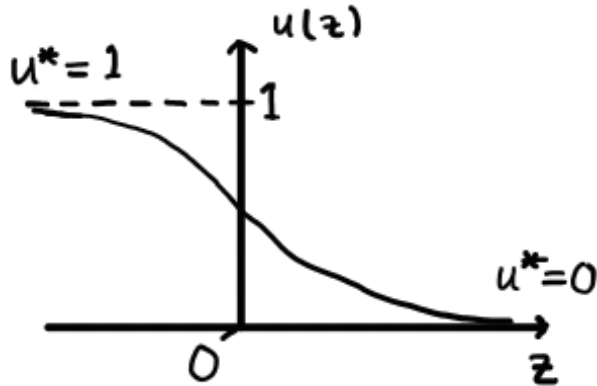
and for convenience drop the primes in what follows, to get

$$\frac{\partial n}{\partial t} = n(1-n) + \frac{\partial^2 n}{\partial x^2}.$$

If n is independent of x (homogenous solution) this is a dynamical system with two steady states:

$$\begin{aligned} n^* &= 0 \text{ (unstable)} \\ n^* &= 1 \text{ (stable).} \end{aligned}$$

Idea: Travelling wave connects these steady states:



Search for travelling waves connecting the steady states at large $|z|$ by the ansatz $z = x - ct$ (assume $c \geq 0$):

$$-c \frac{d}{dz} u(z) = u(z)(1-u(z)) + \frac{d^2}{dz^2} u(z)$$

with boundary conditions

$$\begin{aligned} \lim_{z \rightarrow -\infty} u(z) &= 1 \\ \lim_{z \rightarrow \infty} u(z) &= 0. \end{aligned}$$

Introduce help variable $v = \frac{du}{dz}$ to get first order system

$$\begin{aligned}\frac{du}{dz} &= v \\ \frac{dv}{dz} &= -cv - u(1-u).\end{aligned}$$

This ‘flow’ has two steady states

$$\begin{aligned}(u^*, v^*) &= (0, 0) \\ (u^*, v^*) &= (1, 0)\end{aligned}$$

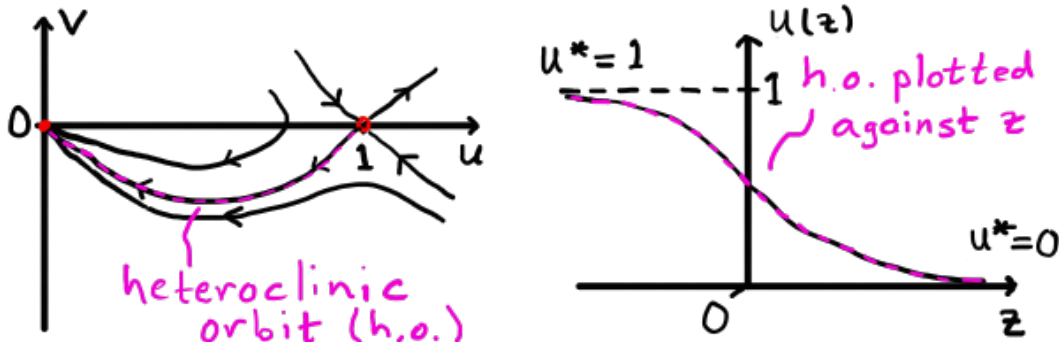
Linearisation

$$\mathbb{J} = \begin{pmatrix} 0 & 1 \\ 2u-1 & -c \end{pmatrix}.$$

Eigenvalue equation

$$\begin{aligned}0 &= \det(\mathbb{J} - \lambda \mathbb{I}) = \lambda(\lambda + c) - (2u - 1) \\ \Rightarrow \lambda_{\pm} &= \frac{1}{2} \left(-c \pm \sqrt{c^2 + 8u - 4} \right) \\ (u^*, v^*) = (0, 0) &: \begin{cases} \text{stable node} & \text{if } c > 2 \\ \text{stable spiral} & \text{if } c < 2 \end{cases} \\ (u^*, v^*) = (1, 0) &: \text{saddle point}.\end{aligned}$$

Solutions with $c < 2$ are unphysical (u becomes negative when dynamics spiral around $(0,0)$). Phase picture for $c > 2$ (left panel):



The heteroclinic orbit connects the two steady states $u^* = 1$ and $u^* = 0$. The corresponding trajectory is plotted against ‘time’ z in

the right panel starting at $u^* = 1$ as $z \rightarrow -\infty$, ending up at $u^* = 0$ as $z \rightarrow +\infty$, all the way with a negative slope $du/dz = v < 0$. In conclusion, a travelling wave solution exists (the heteroclinic orbit). This is the only physical solution of the system (all other trajectories approach infinity as $z \rightarrow -\infty$ or $z \rightarrow +\infty$).

The travelling-wave solution describes population spread from small values of x to larger values of x in a one-dimensional domain that is initially empty. Changing the sign of c the heteroclinic orbit goes from $u^* = 0$ to $u^* = 1$ in the figure above ($z \rightarrow -z$). This describes a population spread of an initial population at large x that populates an initially empty region at smaller x .

As a final remark, having a non-zero wave speed c always gives a more efficient spread than pure diffusion for large times:

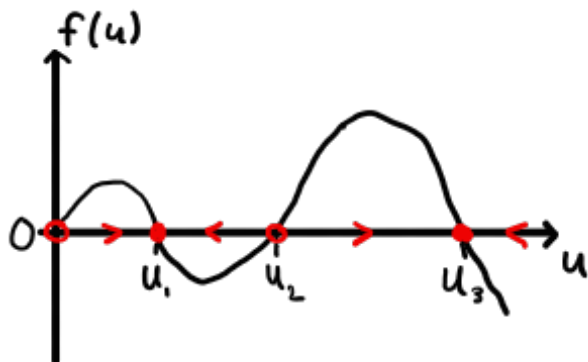
Dispersion mechanism	Diffusion	Travelling wave
Displacement L in time t	$L \sim \sqrt{2Dt}$	$L \sim ct$

6.3.4 Example: Spruce-budworm model (M13.5)

Consider a reaction-diffusion equation with

$$f(u) = \underbrace{ru(1 - u/q)}_{\text{Logistic growth}} - \underbrace{\frac{u^2}{1 + u^2}}_{\text{Predation}}.$$

Can have more than two fixed points (depending on the parameters):



Two stable steady states: u_1 small population, u_3 outbreak. How does outbreak propagate when spatial dispersion is included?

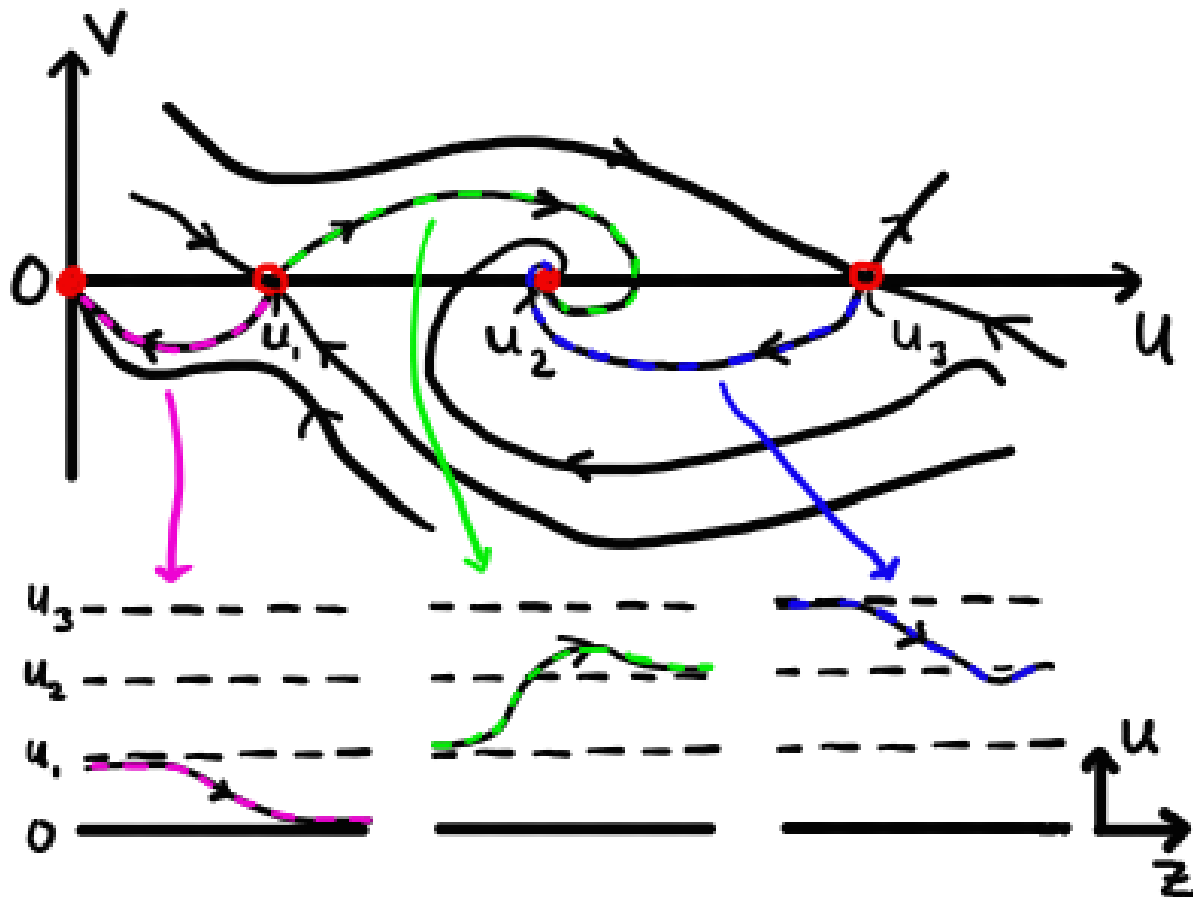
In the phase plane ($v = du/dz$) corresponding to Eq. (5):

$$\begin{aligned}\frac{du}{dz} &= v \\ \frac{dv}{dz} &= -cv - f(u).\end{aligned}$$

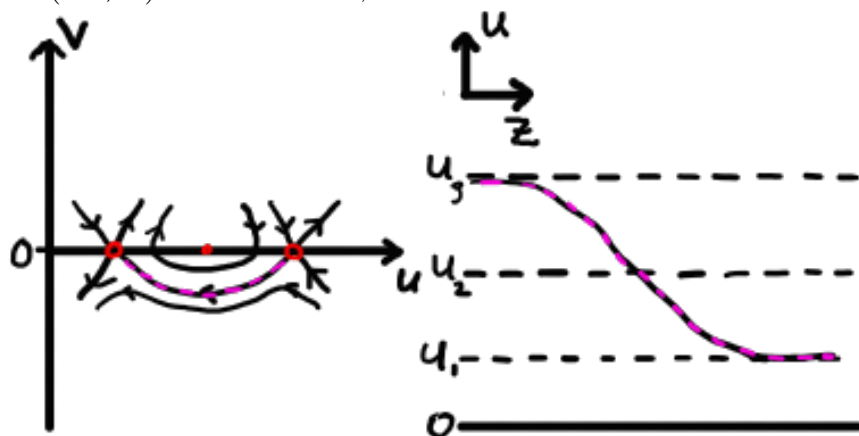
There are four steady states: (assume $c > 0$)

- $(u^*, v^*) = (0, 0)$: stable node/spiral
- $(u^*, v^*) = (u_1, 0)$: saddle point
- $(u^*, v^*) = (u_2, 0)$: stable node/spiral
- $(u^*, v^*) = (u_3, 0)$: saddle point

The types of fixed points obtained depend on c and the system parameters. Example (origin node, $(u_2, 0)$ spiral) allows for several travelling waves (which one of these is selected depends on initial + boundary conditions):



If $(u_2, 0)$ is a center, a connection between saddles 1 and 3 is possible:



If $c > 0$ outbreak spreads (case plotted, the wave leaves a population of size u_3 in its wake), if $c < 0$ outbreak is eliminated (the wave leaves a population of size u_1).

7 Pattern formation, diffusion-driven instability (Murray II: Ch. 2.1-2.4,3.1)

Biology is rich of patterns, some examples being

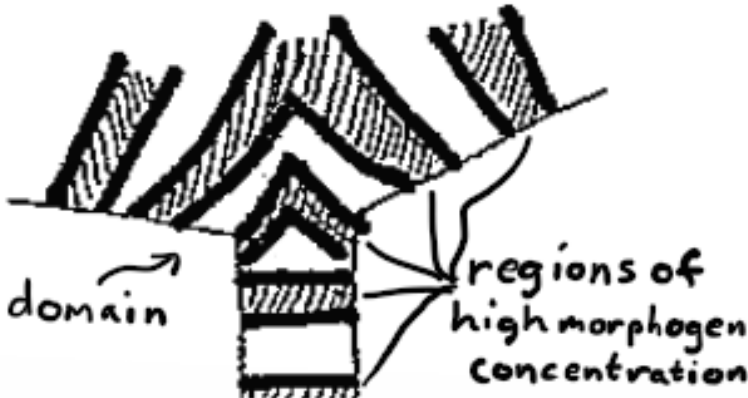
- Patterns in animal coating, snake skins, butterfly wings etc.
- Spatial organisation in initially homogeneous embryo to form an individual.
- Patterning principles of bacteria (forming complex patterns).
- Patchiness in ecology.

This lecture addresses formation of stationary patterns in reaction-diffusion systems. Wave-like spatio-temporal patterns are addressed in the next lecture.

7.1 Morphogenesis (MII 2.1)

The field of Morphogenesis concerns biological processes that determine biological shape and structure in an organism. These processes are in general poorly understood. It is clear that the processes must be genetically controlled, but the genes themselves cannot create the structure.

One possible mechanism for explaining the pattern formation of animal coating (and other morphogenesis) is the following: the genetic code gives the parameters for a reaction-diffusion process which show stationary non-homogeneous spatial patterns. The process describes the concentration of a morphogen at an early stage of the development of an organism. A morphogen is a chemical that is involved in morphogenesis, for example by creating black color in regions where morphogen concentration is high:



The mechanism that causes patterns in concentration to form from an initial close-to homogeneous concentration is the diffusion-driven instability (Turing instability, Turing 1952).

7.2 Diffusion-driven instability (MII 2.2)

Consider a reaction-diffusion model for coupled concentrations of two morphogens, an ‘activator’ $n_A(\mathbf{r}', t')$ and an ‘inhibitor’ $n_I(\mathbf{r}', t')$:

$$\begin{aligned} \frac{\partial n_A}{\partial t'} &= f_A(n_A, n_I) + D_A \nabla'^2 n_A \\ \frac{\partial n_I}{\partial t'} &= f_I(n_A, n_I) + D_I \nabla'^2 n_I \end{aligned},$$

where $0 < D_A < D_I$, t' and \mathbf{r}' are time and space in dimensional units, and $\nabla' = (\frac{\partial}{\partial r'_1}, \dots, \frac{\partial}{\partial r'_{\text{dim}}})$ is the Del operator in dim dimensions.

Initial condition Assume that $n_{A,I}(\mathbf{r}', t' = 0)$ are given functions

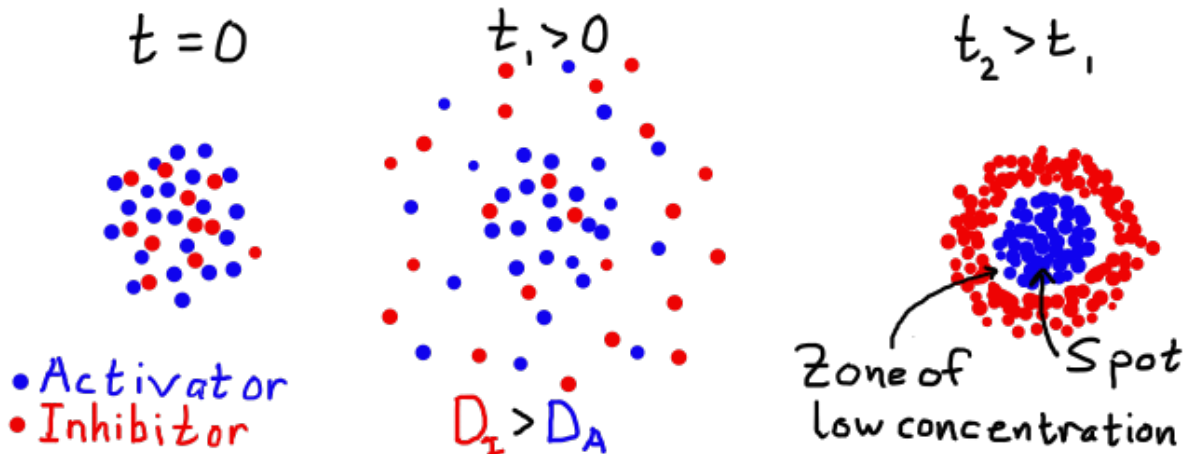
Boundary condition Assume no flux through system boundary:

$$\nabla'_e n_{A,I}(\mathbf{r}', t')|_{\mathbf{r}' \in \text{boundary}} = 0,$$

with \mathbf{e} the unit vector normal to the system boundary and $\nabla'_e \equiv \mathbf{e} \cdot \nabla'$ the directional derivative in direction \mathbf{e} . The no-flux boundary condition implies that the system is not influenced from the outside, i.e. emerging patterns are self-organising.

Basic mechanism Assume f_I, f_A chosen such that n_A (activator) stimulates production of n_I and n_I (inhibitor) slows production of n_A .

Assume that if the diffusion constants vanish, $D_A = D_I = 0$, the system tends to a linearly stable uniform steady state. Now, since $0 < D_A < D_I$ the inhibitor n_I spreads quicker than the activator n_A . Assume that a small spatial region initially has higher concentrations of n_A and n_I than its surroundings. Since $D_I > D_A$, n_I spreads faster and dominates and inhibits growth of the activator in the surroundings, but leaves an excess of n_A in the original area. As a result, we may obtain a concentration of n_A surrounded by n_I ; a spot is formed:



Several random initial regions of higher concentration may lead to spotted patterns (or channels if activators spread quick enough). This mechanism allows for spatially heterogeneous, time-independent, stable solutions (patterns). This may be unexpected, because without the reaction term, diffusion smoothens concentrations, here it is responsible for patterns.

7.3 Stability to spatial perturbations (MII 2.3)

To investigate the diffusion-driven instability mathematically, we make a perturbation around a stable homogeneous steady state.

7.3.1 Homogeneous steady states

Change to vector notation and dimensionless units: $\mathbf{r} = \mathbf{r}'/L$ and $t = t'D_A/L^2$, where L is the linear size of the spatial domain:

$$\frac{\partial \mathbf{n}}{\partial t} = \mathbf{f}(\mathbf{n}) + \nabla^2 \mathbb{D} \mathbf{n}, \quad \mathbb{D} = \begin{pmatrix} 1 & 0 \\ 0 & d \end{pmatrix}. \quad (1)$$

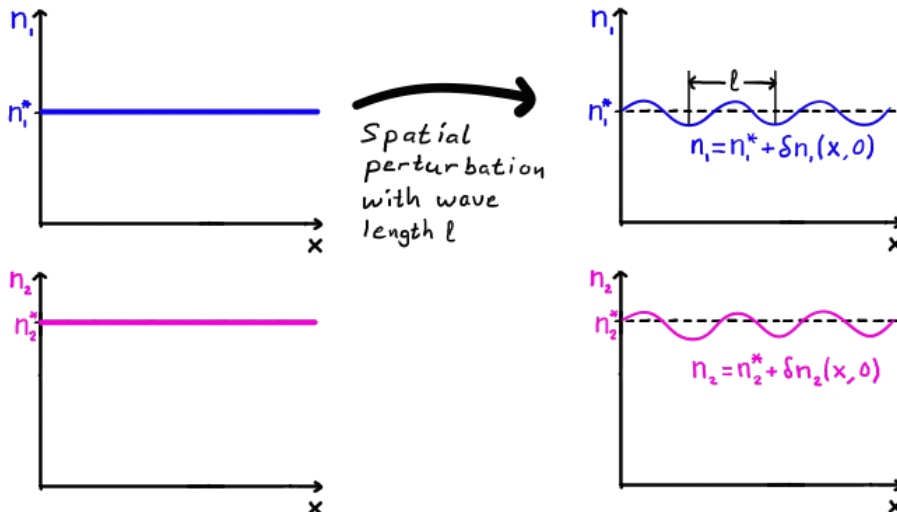
Here $\mathbf{n} = (n_A, n_I)L^{\text{dim}}$, $\mathbf{f} = (f_A, f_I)L^{2+\text{dim}}/D_A$ and $d = D_I/D_A > 1$. Interchanging n_A and n_I gives the case $d < 1$. Homogeneous solutions (no spatial dependence in \mathbf{n}) to Eq. (1) are governed by $\dot{\mathbf{n}} = \mathbf{f}(\mathbf{n})$. Relevant steady states are given by positive zeroes \mathbf{n}^* such that $\mathbf{f}(\mathbf{n}^*) = 0$. Their linear stability is determined by the eigenvalues $\lambda_{\pm}^{(\mathbb{J})}$ of the stability matrix $\mathbb{J}(\mathbf{n}^*)$:

$$\mathbb{J}(\mathbf{n}^*) = \left(\begin{array}{cc} \frac{\partial f_1}{\partial n_1} & \frac{\partial f_1}{\partial n_2} \\ \frac{\partial f_2}{\partial n_1} & \frac{\partial f_2}{\partial n_2} \end{array} \right) \Bigg|_{\mathbf{n}=\mathbf{n}^*}, \quad \lambda_{\pm}^{(\mathbb{J})} = \frac{1}{2} \left(\text{tr}\mathbb{J} \pm \sqrt{(\text{tr}\mathbb{J})^2 - 4 \det \mathbb{J}} \right). \quad (2)$$

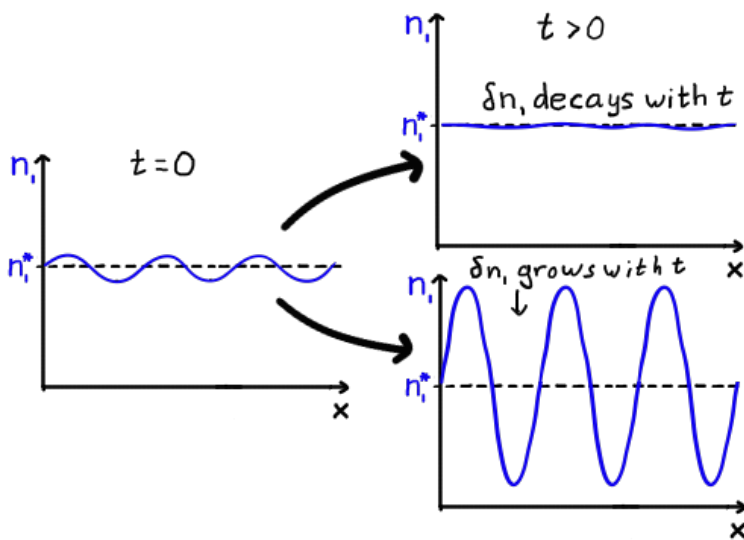
Since the steady state is stable, all eigenvalues have negative real part, i.e. $\text{tr}\mathbb{J} < 0$ and $\det \mathbb{J} > 0$ must be satisfied for our steady state.

7.3.2 Small spatial perturbation

Assume \mathbf{n}^* is stable and consider a small spatio-temporal perturbation $\delta\mathbf{n}(\mathbf{r}, t)$ to the homogeneous steady state, $\mathbf{n} = \mathbf{n}^* + \delta\mathbf{n}(\mathbf{r}, t)$. Example in one spatial dimension:



The perturbations δn_1 and δn_2 may grow or decay with time:



The stability could depend on the wave length ℓ : when $\ell \rightarrow \infty$ (homogeneous case) the system is stable.

Insert $\mathbf{n} = \mathbf{n}^* + \delta\mathbf{n}(\mathbf{r}, t)$ into Eq. (1), keeping only terms to first order in $\delta\mathbf{n}$:

$$\begin{aligned} \frac{\partial}{\partial t}(\mathbf{n}^* + \delta\mathbf{n}) &= \mathbf{f}(\mathbf{n}^* + \delta\mathbf{n}) + \nabla^2 \mathbb{D}(\mathbf{n}^* + \delta\mathbf{n}), \\ \Rightarrow \frac{\partial}{\partial t} \delta\mathbf{n} &= \mathbb{J}(\mathbf{n}^*) \delta\mathbf{n} + \nabla^2 \mathbb{D} \delta\mathbf{n} \end{aligned} \quad (3)$$

with $\mathbb{J}(\mathbf{n})$ being the stability matrix in Eq. (2).

Separation of variables This equation is separable, make ansatz $\delta\mathbf{n}(\mathbf{r}, t) = T(t)R(\mathbf{r})\delta\mathbf{n}_0$ with constant $\delta\mathbf{n}_0$

$$\begin{aligned} \frac{\partial}{\partial t} T(t) R(\mathbf{r}) \delta\mathbf{n}_0 &= T(t) R(\mathbf{r}) \mathbb{J}(\mathbf{n}^*) \delta\mathbf{n}_0 + T(t) \nabla^2 R(\mathbf{r}) \mathbb{D} \delta\mathbf{n}_0 \\ \Rightarrow \frac{1}{T(t)} \frac{\partial}{\partial t} T(t) \delta\mathbf{n}_0 &= \mathbb{J}(\mathbf{n}^*) \delta\mathbf{n}_0 + \frac{\nabla^2 R(\mathbf{r})}{R(\mathbf{r})} \mathbb{D} \delta\mathbf{n}_0. \end{aligned} \quad (4)$$

Since the right-hand side does not depend on t we must have

$$\frac{1}{T(t)} \frac{\partial}{\partial t} T(t) = \lambda = \text{const.} \Rightarrow T(t) = T(0) e^{\lambda t}.$$

Similarly we must have

$$\frac{\nabla^2 R(\mathbf{r})}{R(\mathbf{r})} = -k^2 = \text{const.} \quad (5)$$

This is the Helmholz equation. The choice of the form $-k^2$ for the separation coefficient is natural for most zero-flux boundary conditions. Solutions $R(\mathbf{r})$ describe spatial waves with wave number k . Eq. (5) can be solved by separation of variables, 2D example: $R(\mathbf{r}) = X(x)Y(y) \Rightarrow R(\mathbf{r}) \sim e^{i(k_x x + k_y y)}$. This solution is natural for rectangular domains, but for other shapes (circular etc.) it may be useful to first change coordinates before separation of the spatial variables.

7.3.3 Eigenvalue analysis

As the following analysis shows, we do not need to explicitly solve Eq. (5) to find the stability conditions due to spatial perturbations. Using $\partial T / \partial t = \lambda T$ and $\nabla^2 R = -k^2 R$ in Eq. (4), we find an equation relating the constants λ , and k

$$\lambda \delta \mathbf{n}_0 = \mathbb{J}(\mathbf{n}^*) \delta \mathbf{n}_0 - k^2 \mathbb{D} \delta \mathbf{n}_0 = [\underbrace{\mathbb{J}(\mathbf{n}^*) - k^2 \mathbb{D}}_{\mathbb{K}(k)}] \delta \mathbf{n}_0$$

This is the equation for the eigenvalues $\lambda(k)$ and eigenvectors $\delta \mathbf{n}_0(k)$ of the matrix $\mathbb{K}(k)$. The eigenvalues are given by

$$\det[\lambda \mathbb{I} - \mathbb{K}] = 0 \quad \Rightarrow \quad \lambda^2 - \text{tr} \mathbb{K} \lambda + \det \mathbb{K} = 0.$$

with solutions $\lambda_{\pm}(k)$. Since $\text{tr} \mathbb{K}$ is negative for all values of k :

$$\text{tr} \mathbb{K} = \underbrace{\text{tr} \mathbb{J}}_{<0} - k^2 \text{tr} \mathbb{D} < 0.$$

one eigenvalue $\lambda_-(k)$ has negative real part. For the second eigenvalue $\lambda_+(k)$ to be positive, corresponding to unstable perturbations, we search for values of k such that $\det \mathbb{K}(k) < 0$. Write

$$\det \mathbb{K} = \det(\mathbb{J} - k^2 \mathbb{D}) = dk^4 - (dJ_{11} + J_{22})k^2 + \det \mathbb{J}. \quad (6)$$

Find range of k such that $\det \mathbb{K}(k) < 0$ by solving $\det \mathbb{K} = 0$ in Eq. (6)

$$k_{\pm}^2 = \frac{1}{2d} \left(dJ_{11} + J_{22} \pm \sqrt{(dJ_{11} + J_{22})^2 - 4d \det \mathbb{J}} \right). \quad (7)$$

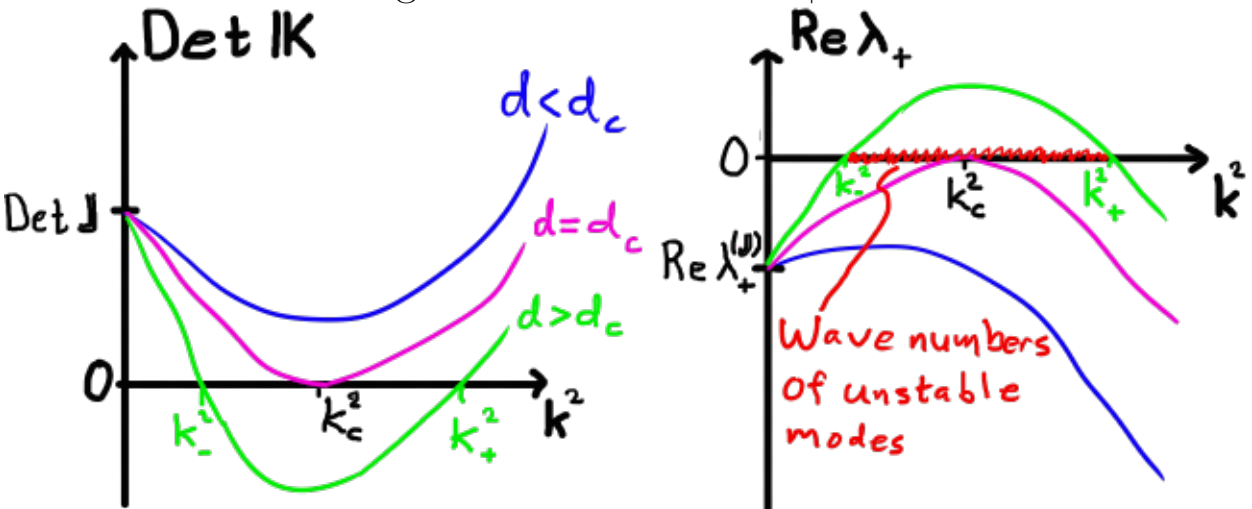
For k_{\pm}^2 to be real in Eq. (7), the square root must be real:

$$(dJ_{11} + J_{22})^2 - 4d \det \mathbb{J} \geq 0. \quad (8)$$

For k_{\pm}^2 to be positive in Eq. (7) (so that k_{\pm} real) use that $\det \mathbb{J} > 0 \Rightarrow$ the square root is smaller than $dJ_{11} + J_{22}$, i.e. $k_{\pm}^2 \geq 0$ if

$$dJ_{11} + J_{22} > 0. \quad (9)$$

When $k = 0$ in Eq. (6), $\det \mathbb{K} = \det \mathbb{J} > 0$ and for large k , $\det \mathbb{K} \sim dk^4 > 0$. If Eqs. (8) and (9) are satisfied, then $\det \mathbb{K}$ has two crossings with zero and it is negative for $k_- < k < k_+$:



In this range, the maximal eigenvalue λ_+ of \mathbb{K} is positive. A bifurcation occurs at $d = d_c$ where $k_+ = k_- \equiv k_c$. For $d > d_c$ the homogeneous steady state is unstable to spatial perturbations in the range $k_- < k < k_+$. The condition $k_+ = k_-$ in Eq. (7) is obtained by setting the discriminant to zero:

$$(d_c J_{11} + J_{22})^2 - 4d_c \det \mathbb{J} = 0$$

The largest solution ($d_c > 1$) defines d_c . At this bifurcation point

$$k_c^2 = \frac{1}{2d_c} (d_c J_{11} + J_{22}).$$

Note that $J_{ij} = \partial f_i / \partial n_j \propto L^2 \partial f_{A|I} / \partial n_{A|I} \Rightarrow k_{\pm} \propto L$ in Eq. (7), i.e. the range of wave numbers $k_- < k < k_+$ giving rise to instabilities takes smaller values and becomes narrower if the system size L is decreased. Consequently, a small system can only have few waves (if any), and they must have low wave numbers.

7.3.4 Summary of conditions to have Turing instability

Conditions for the homogeneous steady state to be stable:

$$\text{tr} \mathbb{J} < 0 \text{ and } \det \mathbb{J} > 0.$$

Conditions for system to be unstable for a range of wave numbers ($\det \mathbb{K} < 0$) is given by Eqs. (8) and (9) (remove equality in Eq. (8) since it corresponds to a marginal case)

$$dJ_{11} + J_{22} > 0 \text{ and } \frac{(dJ_{11} + J_{22})^2}{4d} > \det \mathbb{J}.$$

Here \mathbb{J} is evaluated at the stable homogeneous steady state:

$$\mathbb{J} = \begin{pmatrix} J_{11} & J_{12} \\ J_{21} & J_{22} \end{pmatrix} = \left. \begin{pmatrix} \frac{\partial f_1}{\partial n_1} & \frac{\partial f_1}{\partial n_2} \\ \frac{\partial f_2}{\partial n_1} & \frac{\partial f_2}{\partial n_2} \end{pmatrix} \right|_{\mathbf{n}=\mathbf{n}^*}.$$

From these conditions it follows that $d \neq 1$ (hence $d > 1$ as assumed earlier) and that the signs of the elements of \mathbb{J} take one of the forms

$$\begin{pmatrix} + & + \\ - & - \end{pmatrix}, \begin{pmatrix} + & - \\ + & - \end{pmatrix}.$$

If the conditions above are fulfilled there exist a range of wave numbers for which the system is unstable. But depending on the boundary conditions we do not yet know if any of these ($k_- < k < k_+$) are allowed solutions.

7.4 Boundary conditions

We have found the following solutions to Eq. (3):

$$\delta \mathbf{n}_k(\mathbf{r}, t) = e^{\lambda(k)t} R_k(\mathbf{r}) \delta \mathbf{n}_0(k),$$

where $\lambda(k)$ are eigenvalues and eigenvectors to $\mathbb{K}(k)$, and $R_k(\mathbf{r})$ are solutions to the Helmholtz equation $\nabla^2 R_k(\mathbf{r}) + k^2 R_k(\mathbf{r}) = 0$. Now we want to apply the initial condition $\delta \mathbf{n}(\mathbf{r}, t = 0)$ and the boundary condition

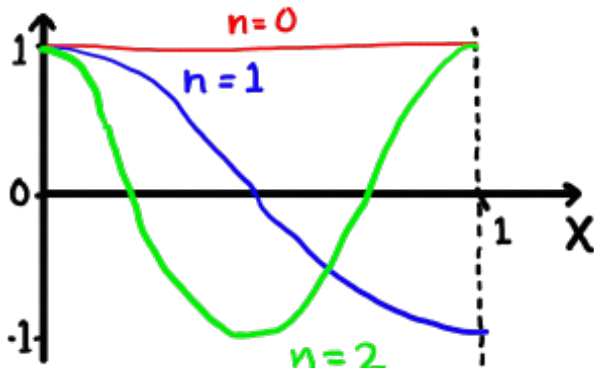
$$\nabla_{\mathbf{e}} \delta \mathbf{n}|_{\mathbf{r} \in \text{boundary}} = 0. \quad (\text{from } \nabla_{\mathbf{e}} (\mathbf{n}^* + \delta \mathbf{n})|_{\mathbf{r} \in \text{boundary}} = 0)$$

7.4.1 Example: One-dimensional box between $0 \leq x \leq 1$

The solutions to Helmholtz equation with no-flux boundary condition,

$$-\frac{\partial}{\partial x} R_k(x=0) = \frac{\partial}{\partial x} R_k(x=1) = 0,$$

are $R_k(x) = \cos(kx)$ with $k = 0, \pi, 2\pi, \dots$



Thus only discrete values of k are allowed: $k = n\pi$ with $n = 0, 1, 2, \dots$. Note that the upper bound is $x = 1$ because x was scaled with system size L in the dedimensionalization.

7.4.2 Example: Two-dimensional box with unit side length

$$R_{k_{n,m}}(x, y) = \underbrace{\cos(n\pi x)}_{k_x} \underbrace{\cos(m\pi y)}_{k_y}$$

Solutions are labelled by $k_{n,m} = |\mathbf{k}| = \pi\sqrt{n^2 + m^2}$ with integer n, m .

General boundary conditions on a finite domain Other shapes of the system boundary give more complicated solutions, but still only discrete values of k are allowed (assuming a finite domain). In general the solution satisfying the boundary condition is

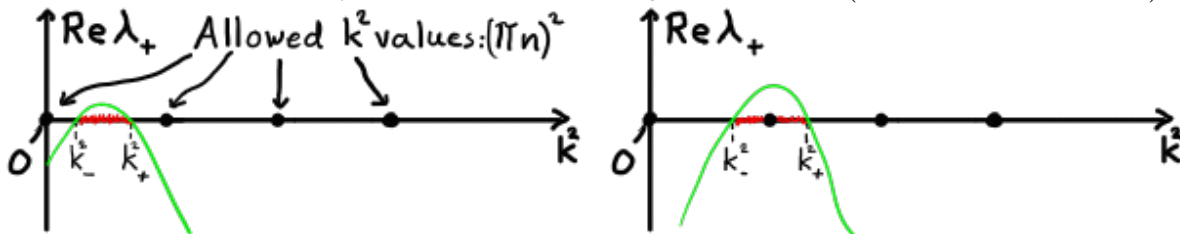
$$\delta \mathbf{n}(\mathbf{r}, t) = \sum_k c_k e^{\lambda(k)t} R_k(\mathbf{r}) \delta \mathbf{n}_0(k),$$

where the sum runs over all allowed values of k and where the coefficients c_k are chosen so that the initial condition $\delta \mathbf{n}(\mathbf{r}, 0)$ is satisfied.

If any k with $k_- < k < k_+$ has non-zero c_k , the system is linearly unstable and spatial perturbations to the homogeneous stable state grow. When perturbations grow large, the system is assumed to be stabilized by non-linear contributions that determine the final pattern in the system. This pattern is related to the pattern created by the linear contribution, but not necessarily the same. Thus, the final pattern depends on a combination of the initial condition, the linear perturbation theory, and the non-linear effects of the system. If no k in $k_- < k < k_+$ has non-zero c_k , the system decays back to the spatially homogeneous solution after a small perturbation.

7.4.3 One-dimensional box revisited

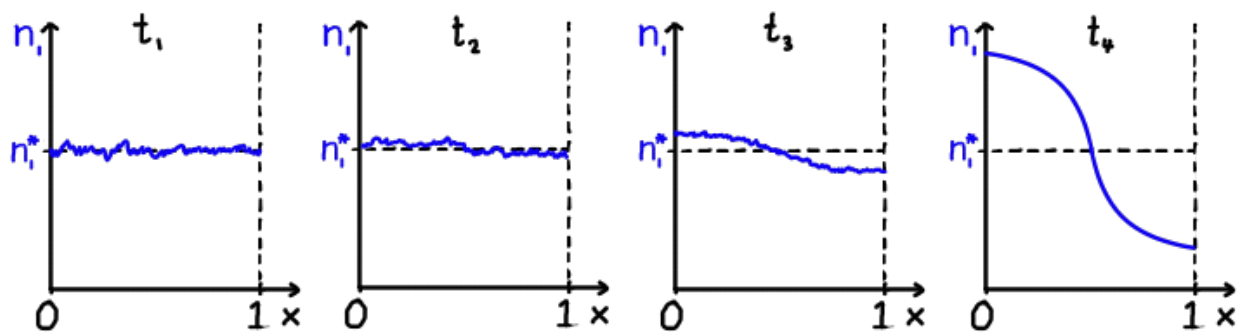
As seen above, solutions satisfying the boundary conditions in 1D are $R_k(x) = \cos(kx)$, where k takes discrete values $k = n\pi$ with $n = 0, 1, 2, \dots$. Does any of these correspond to an unstable mode? $k = 0$ never leads to instability (stable homogeneous solution). What about $k = \pi$? As observed above, $k_+ \sim \sqrt{J_{ij}} \sim L$, so if the system size L is small enough then $k_+ < k = \pi$ and no allowed k -values exist between k_- and $k_+ \Rightarrow$ no instability possible (left panel below).



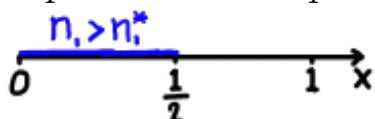
Increasing L so that exactly one mode, $k = \pi$, lies in $k_- < k < k_+$ (right panel above) we have

$$\mathbf{n} = \mathbf{n}^* + \delta\mathbf{n}, \text{ with } \delta\mathbf{n} \sim e^{\lambda_+(\pi)t} \cos(\pi x) \delta\mathbf{n}_0^+(\pi)$$

where $\lambda_+(\pi)$ and $\mathbf{n}_0^+(\pi)$ are the positive eigenvalue and corresponding eigenvector of \mathbb{K} when $k = \pi$. A small random perturbation decays in all modes except $k = \pi$ where it grows, illustrated below at successive times $t_1 < t_2 < t_3 < t_4$ (assume first component of $\delta\mathbf{n}_0^+(\pi)$ is positive)

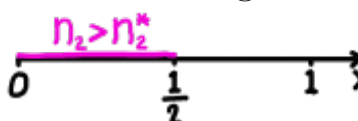


A pattern develops in n_1 :

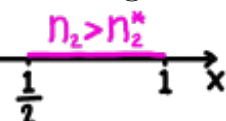


Similarly a pattern for n_2 emerges (which depends on the relative sign of the components in the eigenvector $\delta \mathbf{n}_0^+(\pi)$):

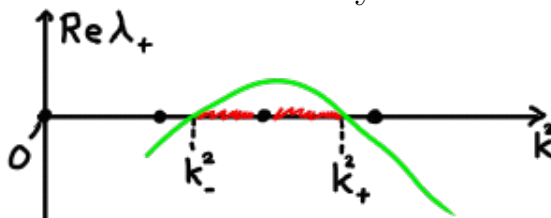
Same sign



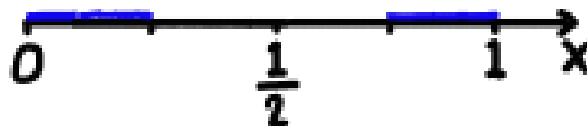
Opposite sign



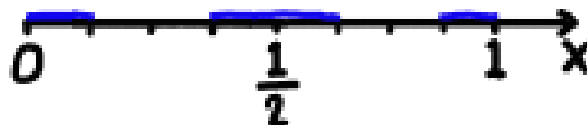
Now assume that only the mode $n = 2$ lies in $k_- < k < k_+$:



The corresponding pattern is ($n = 2$):

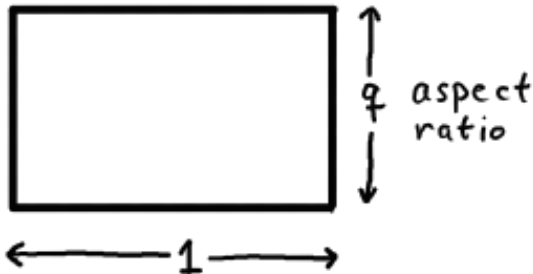


and so forth ($n = 4$):



7.5 Two-dimensional patterns (MII 2.4, 3.1)

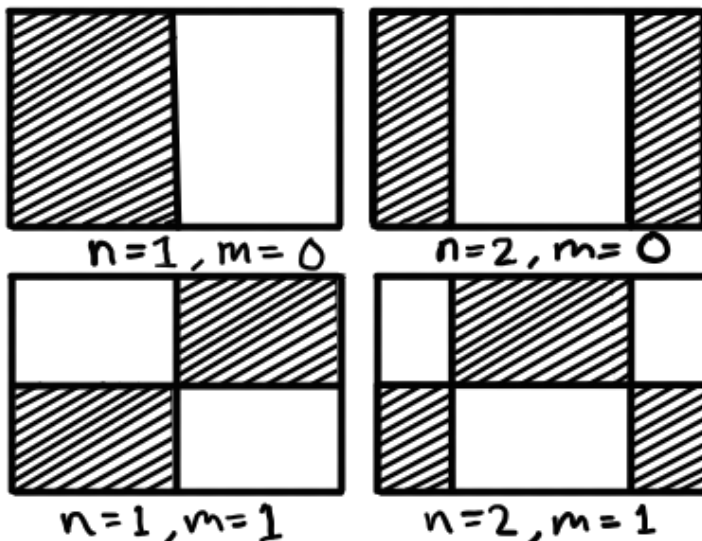
Two-dimensional rectangular boundary



Allowed solutions for the boundary conditions of this geometry are

$$R_{k_{n,m}}(x, y) = \cos(\underbrace{n\pi}_{k_x} x) \cos\left(\frac{m\pi}{\underbrace{q}_{k_y}} y\right).$$

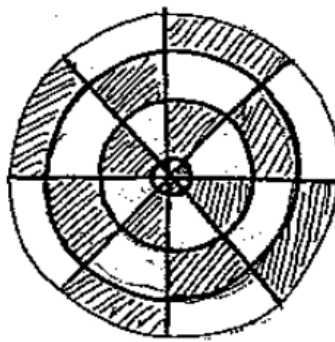
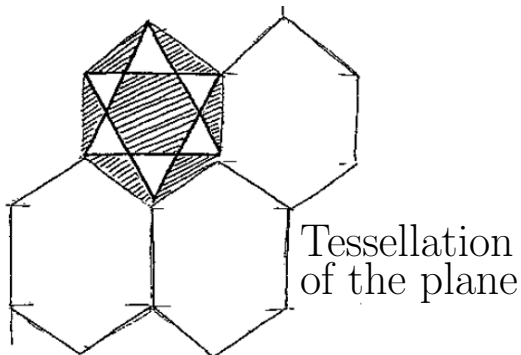
To have a Turing instability, we must have $k_- < \pi\sqrt{n^2 + (m/q)^2} < k_+$. Some patterns corresponding to a single wave vector $\mathbf{k} = (k_x, k_y) = \pi(n, m/q)$ in this range are (shaded regions corresponds to $n_1 > n_1^*$):



Less simple domains require the solution of the Helmholtz equation (5)

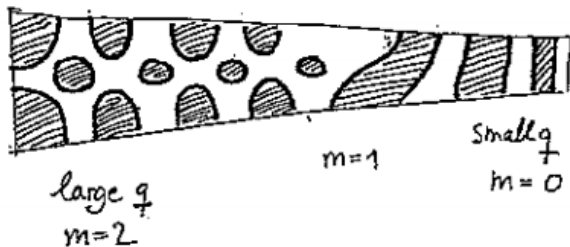
$$\nabla^2 R(\mathbf{r}) = -k^2 R(\mathbf{r}), \quad \nabla_e R(\mathbf{r})|_{\mathbf{r} \in \text{boundary}} = 0. \quad (10)$$

Some symmetric domains have explicit solutions, such as the left panel below:



However, for most domains solutions must be found numerically, as for the circular domain (right panel above).

The linear stability theory outlined in this Lecture works well when the unstable modes have small wave numbers (large wave length). For example, consider shapes of tails or legs of animals:



As the aspect ratio q becomes smaller, the possible values of m that fits the range $k_- < \pi\sqrt{n^2 + (m/q)^2} < k_+$ becomes smaller. The resulting patterns have small wave numbers and remind of coating on spotted animals: striped tails. The following figure compares the patterns obtained from simulations of reaction diffusion equations on three domains (a)–(c) to typical tail markings of members of the cat family (d)–(g):

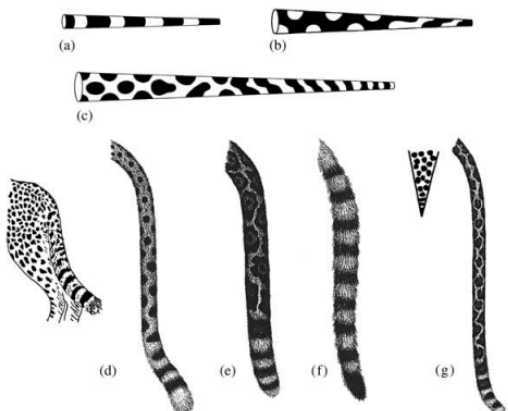


[Figure taken from Murray,
Mathematical Biology II
(2003)]

If you need more training, you can have a look at the training question on instabilities in activator inhibitor systems.

8 Spatiotemporal patterns (Murray: Ch. 12.1; Murray II: Ch. 1.8-1.9)

In Lecture 6 we saw that a one-dimensional reaction diffusion equation may show wave-like solutions. The reaction-diffusion equation for two coupled concentrations $n_1(\mathbf{x}, t)$ and $n_2(\mathbf{x}, t)$, reaction terms f_1 and f_2 , and diffusion constants D_1 and D_2

$$\begin{aligned} \frac{\partial n_1}{\partial t} &= f_1(n_1, n_2, \mathbf{x}, t) + D_1 \nabla^2 n_1 \\ \frac{\partial n_2}{\partial t} &= f_2(n_1, n_2, \mathbf{x}, t) + D_2 \nabla^2 n_2 \end{aligned} , \quad (1)$$

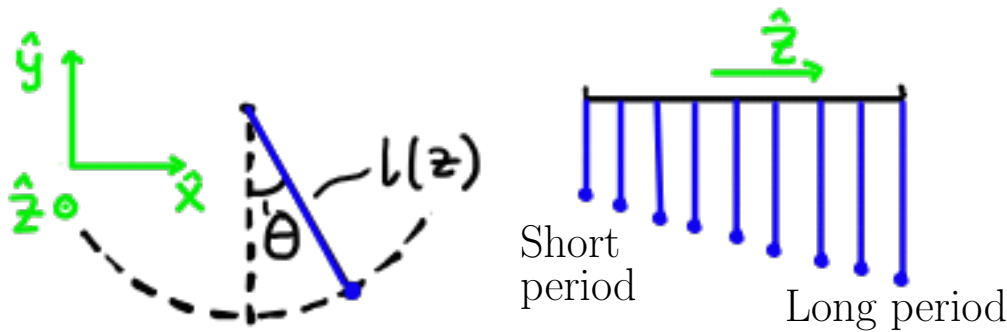
often has even more intricate dynamics. As seen in the last lecture, it allows for spontaneous formation of stationary patterns via the diffusion-driven instability. In this lecture we will consider formation of spatiotemporal patterns in the form of spiral waves.

8.1 Waves in uncoupled oscillators (M 12.1)

As a simplest example of a mechanism for spatio-temporal wave formation of the concentrations n_1 and n_2 in Eq. (1), consider a case where diffusion is negligible ($D_1 = D_2 = 0$) and where f_1 and f_2 depend explicitly on a single spatial coordinate z . At each value of z , the system has an independent growth equation. A simple example from mechanics is obtained by denoting $n_1 = \theta$, $n_2 = \omega$ and letting $f_1 = \omega$, $f_2 = -\frac{g}{l(z)}\phi$ (g is gravitational acceleration):

$$\frac{\partial \theta}{\partial t} = \omega, \quad \frac{\partial \omega}{\partial t} = -\frac{g}{l(z)}\theta. \quad (2)$$

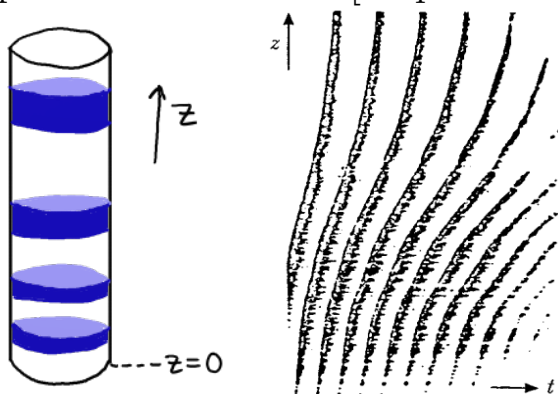
For each value of z these equations describe the angular motion of a simple pendulum of length $l(z)$.



By choosing $l(z)$ appropriately, this system shows wave patterns. Similar behaviour is observed in spatial distributions of biological (limit-cycle) oscillators. These oscillators are often coupled to some degree, a case we will consider in a later lecture. An example of a system consisting of uncoupled oscillators is given by the Belousov-Zhabotinsky reaction, which we study in detail below.

8.1.1 Example: Belousov-Zhabotinsky reaction

The BZ reaction was introduced in Lecture 4. It is a chemical oscillator: the ratio of concentrations of the reactants oscillates (in contrast to the spatial angular coordinate in the pendulum above). Adding an appropriate dye allows for visualization of the concentration of one of the reactants. If stirred, the color of the entire sample periodically changes due to oscillations in the concentration of the reactant. If instead left unstirred in a vertical cylinder, spatial patterns form: coloured bands form at the bottom of the cylinder, and rise slowly to eventually fill the cylinder with non-homogeneously distributed bands. Illustration of band positions after some time (left) and experimental space-time dependence of bands [Kopell and Howard (1973)] (right):



[Right panel from Fig. 12.1b in Murray, *Mathematical Biology I* (2003)]

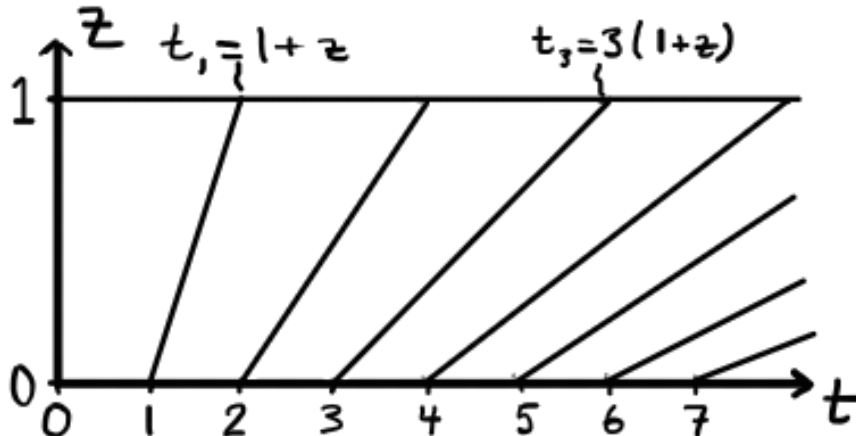
Model: Let each position z in the cylinder be an independent chemical oscillator (undergoing the Belousov-Zhabotinsky reaction) with period time T that depends on z (for instance due to temperature variation, or a concentration gradient in one of the chemicals in the z -direction).

Use the phase of oscillation $\phi(z, t)$ to characterise the state of each oscillator. An oscillator of period time T forms a closed periodic orbit γ in phase space (the space of chemical concentrations n_1, n_2). Assuming an initial coordinate $(n_1(0), n_2(0))$ on γ when $t = 0$, all succeeding points $(n_1(t), n_2(t))$ on γ can be parameterized by t . Use the phase $\phi(z, t) = \phi_0(z) + 2\pi t/T(z)$ to parameterize the state of the oscillator at z . $\phi(z, t)$ increases with 2π as t increases by a multiple of the period time $T(z)$:

$$\phi(z, t + nT(z)) = 2\pi n + \phi(z, t),$$

with integer n . To understand the structure of bands, introduce wave fronts: Regions of constant phase (points in this one-dimensional case).

As an explicit example, assume initial phase $\phi_0(z) = 0$, and $T(z) = 1 + z$. At times $t_n = nT(z) = n(1 + z)$ the n :th wave front (the wave front with $\phi = 2\pi n$) reaches the height $z = 1$ in the cylinder:



- The oscillator at $z = 0$ is in phase (returns to the original concentration) every time unit [$T(z=0)=1$], the oscillator at $z = 1$ is in phase every second time unit [$T(z = 1) = 2$].
- The speed $v_n(z)$ at which the n :th wave front move is given by

the slopes of the lines in the figure above:

$$v_n(z) \equiv \left[\frac{dz}{dt} \right]_{\phi=2\pi n} = \frac{1}{n}.$$

- For fixed t there will be more and more bands in the cylinder the larger t is, and the bands are denser at small z . This essentially explains the observed pattern in the experiment.

This is an example of purely kinematic pattern formation (diffusion, convection etc. are negligible). Nothing actually moves, it is just the relative phases that varies. In contrast, in systems with coupled oscillators the phase and frequency of individual oscillators may change due to the interaction. Such systems often exhibit synchronisation (next lecture).

8.2 Spiral waves (MII 1.8)

In addition to travelling waves and the kinematic waves above, reaction-diffusion equations in higher dimensions can show spiral waves. These occur naturally in many biological, physiological and chemical systems, some examples are:

1. Belousov-Zhabotinski reaction
2. Neural activity in brain
3. Electrical impulses in heart
4. Signalling patterns of slime mould

Example: Spiral wave in concentration in a BZ reaction



- For a fixed time, contour lines of concentration form a spiral.
- As time goes, the spiral is rotating.
- Curves of constant concentration (phase) describe wave-fronts of the wave.

8.2.1 Simple rotating spiral

It is natural to describe a rotating spiral in two spatial dimensions by polar coordinates r, θ at time t . The phase ϕ of a simple rotating spiral is

$$\phi(r, \theta, t) = \frac{2\pi t}{T} + \underbrace{\psi(r)}_{\phi_0(r, \theta)} \pm m\theta \quad (3)$$

with constant angular frequency $\Omega = 2\pi/T$ (change sign of first term to change direction of rotation), radial dependence $\Psi(r)$, number of arms m , and \pm in front of m decides chirality of the spiral. Analogous to the patterns in Section 8.1, regions of constant phase describe wave fronts of the spiral wave (one-dimensional curves here).

A concentration showing a simple rotating spiral can be written as $n(r, \theta, t) = F(\phi)$, where F is a 2π -periodic function. The following examples show lines of constant concentration (wave fronts) at $t = 0$ (curves show $\phi = 0, 2\pi, 4\pi, \dots$):



1. **Archimedian spiral** $\psi \propto r$, $m = 1$, ‘-’ sign in Eq. (3)
2. **Logarithmic spiral** $\psi \propto \ln r$, $m = 1$, ‘-’ sign in Eq. (3)
3. **3-armed Archimedian spiral** $\psi \propto r$, $m = 3$, ‘+’ sign in (3)
4. **Target pattern** $\psi \propto r$, $m = 0$

Some observations:

- For fixed r and t , the spiral has an m -fold symmetry
- For fixed (r, θ) , a wave front passes through every $\frac{T}{m}$ time unit.

8.2.2 Spiral waves in oscillatory reaction systems (MII 1.9)

In the previous section a mathematical description of wave fronts of spiral waves was introduced. This description in terms of a phase $\phi(r, \theta, t) = \Omega t \pm m\theta + \psi(r)$ can be used to search for spiral waves in reaction-diffusion equations in two spatial dimensions, similar to how we used the wave variable $z = x - ct$ to search for travelling waves in reaction diffusion equations in one spatial dimension. An example of a reaction diffusion equation for two concentrations n_1 and n_2 allowing spiral-wave solutions is the ‘ λ - ω reaction system’

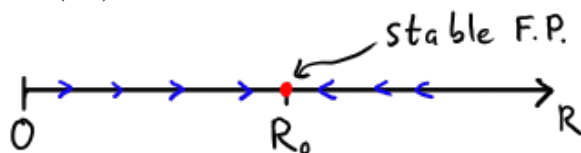
$$\frac{\partial}{\partial t} \begin{pmatrix} n_1 \\ n_2 \end{pmatrix} = \begin{pmatrix} \lambda(R) & -\omega(R) \\ \omega(R) & \lambda(R) \end{pmatrix} \begin{pmatrix} n_1 \\ n_2 \end{pmatrix} + D \nabla^2 \begin{pmatrix} n_1 \\ n_2 \end{pmatrix}$$

with $R = \sqrt{n_1^2 + n_2^2}$ and λ, ω are real functions of R .

Homogeneous solutions (n_1 and n_2 independent of the spatial coordinates) to this system often show oscillations. To see this, transform the concentrations (n_1, n_2) to polar coordinates $n_1 = R \cos \phi, n_2 = R \sin \phi$

$$\begin{aligned} \frac{\partial R}{\partial t} &= \frac{n_1 \frac{\partial n_1}{\partial t} + n_2 \frac{\partial n_2}{\partial t}}{R} = \lambda(R)R + D(\nabla^2 R - R|\nabla \phi|^2) \\ \frac{\partial \phi}{\partial t} &= \frac{n_1 \frac{\partial n_2}{\partial t} - n_2 \frac{\partial n_1}{\partial t}}{R^2} = \omega(R) + D \left(\frac{2}{R} \nabla R \cdot \nabla \phi + \nabla^2 \phi \right) \end{aligned} \quad (4)$$

In the homogeneous case ($D \rightarrow 0$), the n_1 - n_2 -system has a limit-cycle if $\lambda(R)R$ has a stable steady state at some $R = R_0$



The limit-cycle oscillator has phase $\phi(\mathbf{x}, t) = \phi_0(\mathbf{x}) + \omega(R_0)t$.

Adding diffusion, the system allows for travelling plane wave solutions along the x -axis on the form $R = \alpha = \text{const.}$ and $\phi = \omega(\alpha)t - \sqrt{\lambda(\alpha)/D}x$ (follows by insertion into Eq. (4)). The stability of these travelling wave solutions depends on the form of λ and ω and analysis is in general non-trivial.

Adding diffusion may also allow for spiral wave solutions. Search for rotating spirals on the form

$$\begin{aligned} R(r, \theta, t) &= f(r) \\ \phi(r, \theta, t) &= \Omega t + m\theta + \psi(r) \end{aligned}$$

with spatial polar coordinates $x = r \cos \theta$, $y = r \sin \theta$ (the angular coordinate in n_1 - n_2 -space is the phase ϕ) and with suitable boundary conditions. Using numerical solutions of the resulting partial differential equations, rotating spirals have been found for different choices of $\lambda(R)$ and $\omega(R)$, one simple example being $\lambda(R) = 1 - R^2$ and $\omega(R) = -\beta R^2$ with $\beta > 0$ showing 1-armed or 2-armed spirals when $\beta = 1$ (Kuramoto & Koga 1981). For higher values of β the wave fronts become chaotic.

Spiral waves are also observed in many reaction-diffusion models that are not on the form of the λ - ω reaction system above. See for example the work of Dwight Barkley or the classification of the Gray-Scott model.

These notes are an excerpt of H. Stroetzel, Physica D 193
(2005)

7. Synchronisation of coupled oscillators

7.1. Introduction

Collective synchronisation: network of oscillators locks into a common mode despite the fact that the frequencies of the individual oscillators are all slightly different.

This mechanism is thought to operate in a wide variety of biological and engineering systems

- networks of pacemaker cells in (human) heart
- network of circadian pacemakers cells in (human) brain
- metabolic synchronisation of yeast-cell suspension
- synchronously flashing fireflies
- synchronously chirping crickets

- synchronous motion of ant colonies

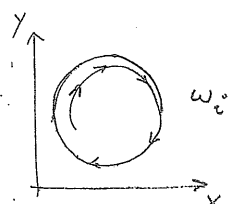
→ E.OH

- synchronisation of laser arrays
- synchronisation of metronomes on a flexible shelf
- Millennium bridge (reinforcement vs. damping)

→ E.OH

7.2. Formulation of the problem

Consider ensemble of limit-cycle oscillators i (see for example p. 175) with nearly identical frequencies ω_i and weak interactions.



Weak interactions, small detuning → Separation of time scales: the oscillators rapidly relax to their limit cycles and can therefore be characterised by their phases ϕ_i . On a much longer time scale the phase dynamics is influenced by the interactions.

Numerical observations: phase transition

detuning large w.r.t. coupling

incoherent phase
each oscillator moves at its own frequency

detuning small w.r.t. coupling

clusters of oscillators freeze into synchrony

Hypothesis: individual phases ϕ_i are "pulled towards mean-field phase ψ " (and not to the phase of any other oscillator). The magnitude of this effect is proportional to the extent of coherence, i.e., to the fraction of oscillators frozen into synchrony.

positive-feedback loop

Problem: derive mathematical model supporting this hypothesis.

Two tasks

- ① derive model from realistic microscopic dynamics
- ② analyse model (mean-field approach → lecture notes on neural networks and stability analysis)

In the following concentrate on ②.

7.3. Kuramoto's model

Ensemble of nearly identical, weakly interacting limit-cycle oscillators.

Approximate equation for phase dynamics at large times

$$\dot{\theta}_i = \omega_i + \sum_{j=1}^N \Gamma_{ij} (\theta_j - \theta_i) \quad i=1, \dots, N$$

(Kuramoto 1984).

Nobody has yet succeeded in solving or analysing these equations in their most general form (as quoted above):

- $\Gamma_{ij}(\theta) = \underbrace{\sum_k a_k^{(ij)} e^{ik\theta}}_{\text{arbitrary}}$
- network connectivity
 - fully connected
 - nearest-neighbour coupling on square lattice
 - random partial connectivity
 - scale-free networks

Kuramoto simplified the problem further by assuming $\Gamma_{ij}(\theta_j - \theta_i) = \frac{K}{N} \sin(\theta_j - \theta_i)$

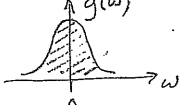
- retain just one Fourier mode
- weight all couplings equally, K.
- network fully coupled (each oscillator is connected to all others)

Kuramoto's model

$$\dot{\theta}_i = \omega_i + \frac{K}{N} \sum_{j=1}^N \sin(\theta_j - \theta_i),$$

proper normalization
when $N \rightarrow \infty$

- frequency distribution $\text{Prob}(\omega_i = \omega) = g(\omega)$
- mean frequency $\bar{\omega} = \frac{1}{N} \sum_{j=1}^N \omega_j$ ↗ p. 3
- assume that $g(\omega)$ is unimodal and symmetric, $g(\bar{\omega} + \omega) = g(\bar{\omega} - \omega)$.

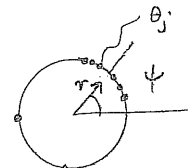


Go to frame rotating at frequency Ω : $\theta_i \rightarrow \theta_i + \Omega t$.
Eq. (*) is invariant and $g(\omega) = g(-\omega)$.

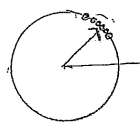
7.4. Order parameter (\rightarrow Neural networks p. 45)

Order parameter:

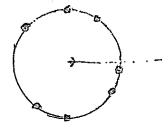
$$r(t) = \frac{1}{N} \sum_{j=1}^N e^{i\theta_j} \quad (**)$$



$r(t)$ measures phase-coherence, $\phi(t)$ is average phase.



$r \approx 0$



Population in collective rhythm

Individual oscillations add incoherently in (**)
no macroscopic rhythm

Mean-field form of eq. (*)
Multiply eq. (*) with $e^{-i\theta_i}$

$$r e^{i(\psi - \theta_i)} = \frac{1}{N} \sum_{j=1}^N e^{i(\theta_j - \theta_i)}$$

Take imaginary part

$$r \sin(\psi - \theta_i) = \frac{1}{N} \sum_{j=1}^N \sin(\theta_j - \theta_i)$$

Insert into eq. (*) to obtain

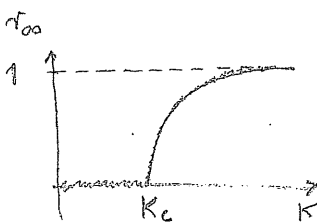
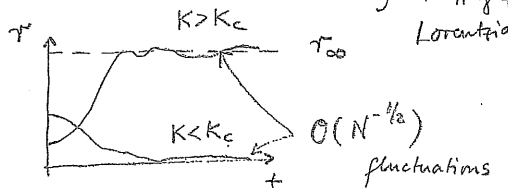
$$\dot{\theta}_i = \omega_i + K r \sin(\psi - \theta_i)$$

Coupling only through mean fields r and ψ .

This form appears to be consistent with hypothesis on p. 40.

7.5. Results of computer simulations for kuramoto's model (large N)

$$g(\omega) = \frac{\gamma}{\pi} \frac{1}{\omega^2 + \omega^2}$$



Questions

- compute K_c and $r_\infty(K)$
- compute apparent stability of $r_\infty=0$ -branch below K_c and the bifurcating branch above K_c
- finite N results, convergence as $N \rightarrow \infty$?

7.6. Mean-field analysis

$$\dot{\theta}_i = \omega_i + K r \sin(\psi - \theta_i)$$

$$r(t) e^{i\psi(t)} = \frac{1}{N} \sum_{j=1}^N e^{i\theta_j(t)}$$

Consider limit of $N \rightarrow \infty$ and seek steady-state solution

$$r(t) = \text{const.} \equiv r$$

$$\psi(t) = \text{const.} \quad (\text{can take } \psi = 0)$$

Equation of motion $\dot{\theta}_i = \omega_i - K r \sin(\theta_i)$ rotates at frequency $\frac{1}{2}$, go to rotating frame.

$$\dot{\theta}_i = \omega_i - K r \sin(\theta_i) \quad (*) \text{ frame}$$

Self-consistency condition: compute θ_i and determine $r(t) e^{i\psi(t)}$. Must find that $r(t) = \text{const.}$ and $\psi = 0$.

Linear stability analysis of (*)

Steady-state condition:

$$\omega_i - K r \sin \theta_i = 0$$

Steady states for

$$|\omega_i| \leq Kr,$$

$$\text{since } |\sin \theta_i| \leq 1.$$

Steady states are stable.

$$\frac{d}{d\theta} (-\sin \theta) < 0 \text{ for } |\theta| < \frac{\pi}{2}$$

For much oscillators $\theta_i = \text{const.}$

They are called phase-locked because they are rotating rigidly at frequency $\frac{1}{2}$ in the original frame.

The remaining oscillators are unstable. They rotate in a non-uniform manner, and are called drifting.

locked oscillators $\hat{=}$ centre of g

drifting oscillators $\hat{=}$ tails of g

Assume that drifting oscillators are described by stationary distribution

$$p(\omega, \theta) d\theta = \frac{\text{fraction of oscillators}}{\text{with frequency } \omega \text{ with phase between } \theta \text{ and } \theta + d\theta}$$

Stationarity requires that $p(\omega, \theta)$ must be universally proportional to speed $|\dot{\theta}|$

$$\frac{dp}{dt} + \frac{\partial}{\partial \theta} (v p) = 0$$

$$p(\omega, \theta) = \frac{C}{|w - Kr \sin \theta|}$$

where C is determined so that $\int d\theta g(\omega, \theta) = 1$

Find

$$C = \frac{\sqrt{w^2 - Kr^2}}{2\pi}$$

Now check for self-consistency

$$\langle e^{i\theta} \rangle = \langle e^{i\theta} \rangle_{\text{drift}} + \langle e^{i\theta} \rangle_{\text{lock}}$$

$$\langle e^{i\theta} \rangle = r e^{i\psi} = r \quad \text{since } \psi = 0 \text{ was assumed}$$

Since $\psi = 0$ was assumed, $\langle e^{i\theta} \rangle = r$
(remember $\langle e^{i\theta} \rangle = r e^{i\psi}$).

Evaluate the two contributions separately.

First locked contribution

$$\sin \theta^* = \frac{w}{Kr} \quad |w| \leq Kr$$

In the limit of $N \rightarrow \infty$ there are just as many oscillators at θ^* as there are at $-\theta^*$ (since $g(w)$ is symmetric)

So

$$\langle \sin \theta \rangle_{\text{lock}} \xrightarrow{\text{average over oscillators}} 0$$

Thus

$$\langle e^{i\theta} \rangle_{\text{lock}} = \langle \cos \theta \rangle_{\text{lock}}$$

$$= \int_{-Kr}^{Kr} dw g(w) \cos[\theta(g(w))]$$

Change variables from w to θ

$$\langle e^{i\theta} \rangle_{\text{lock}} = \int_{-\frac{\pi}{2}}^{\frac{\pi}{2}} d\theta \underbrace{Kr \cos \theta}_{\frac{dw}{d\theta}} g(Kr \sin \theta) \cos \theta$$

$$= Kr \int_{-\frac{\pi}{2}}^{\frac{\pi}{2}} d\theta \cos^2 \theta g(Kr \sin \theta)$$

Now consider the contribution from the drifting oscillators.

$$\langle e^{i\theta} \rangle_{\text{drift}} = \int_{-\pi}^{\pi} d\theta \int dw g(w) e^{i\theta} p(\theta, w)$$

Make use of symmetry (see p. 320)

$$g(w) = g(-w)$$

$$p(\theta + \pi, -w) = p(\theta, w)$$

to show that $\langle e^{i\theta} \rangle_{\text{drift}} = 0$.

Self-consistency condition

$$r = Kr \int_{-\frac{\pi}{2}}^{\frac{\pi}{2}} d\theta \cos^2 \theta g(Kr \sin \theta)$$

Trivial solution $r = 0$: incoherent state with $p(\theta, w) = (2\pi)^{-1}$.

Second solution, partially synchronised state given by

$$1 = K \int_{-\frac{\pi}{2}}^{\frac{\pi}{2}} d\theta \cos^2 \theta g(Kr \sin \theta)$$

Determine K_c (p. 317) by letting $r \rightarrow 0^+$

$$K_c = \frac{1}{g(0) \int_{-\frac{\pi}{2}}^{\frac{\pi}{2}} d\theta \cos^2 \theta} = \frac{2}{\pi g(0)}$$

What is the functional form of $r(K)$ for $K > K_c$? Expand self-consistency condition in powers of r .

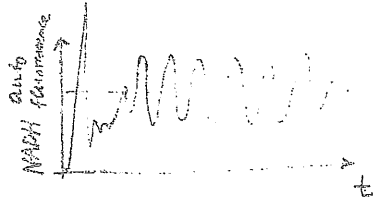
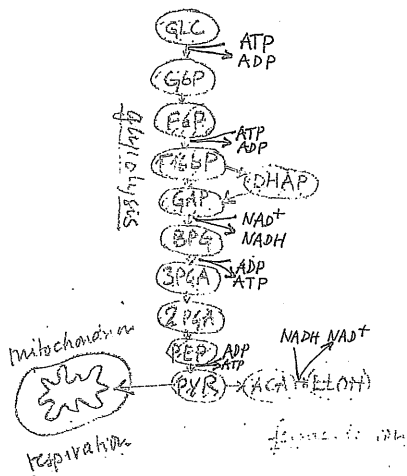
$$1 = \frac{K}{K_c} + \frac{K(Kr)^2 g''(0)}{2} \int_{-\frac{\pi}{2}}^{\frac{\pi}{2}} d\theta \cos^2 \theta \sin^2 \theta + \dots$$

First order vanishes since $g'(0) = 0$.

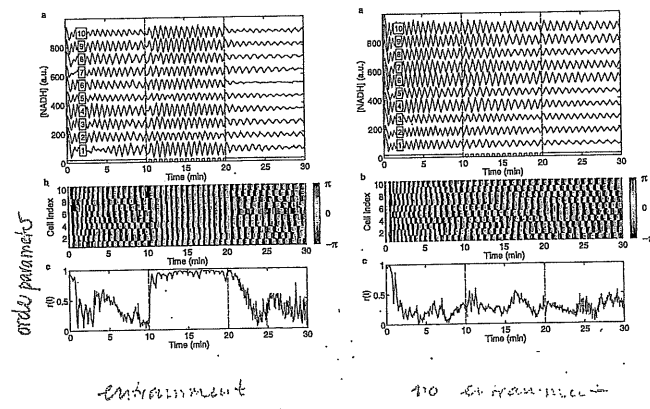
$$= \frac{\pi}{8}$$

7.3. glycolytic oscillations in yeast cells

glycolysis in yeast cells. Metabolic oscillations.



Entrainment of NADH oscillations by cyanide concentration oscillations



A.-K. Guimaraes et al. Sci. Rep. 5 (2015)

6. Models for the spreading of disease

6.1. An epidemic model (SIR model)

Consider disease which upon recovery gives rise to immunity.

Divide population (N) into three classes

$$\text{susceptibles} \quad S(t) \geq 0$$

$$\text{infectives} \quad I(t) \geq 0$$

$$\text{removed} \quad R(t) \geq 0$$

(recovered and immune, recovered and isolated, or dead)

$$S \rightarrow I \rightarrow R$$

Assumptions concerning transmission of infection and incubation period:

① gain in I is given by rSI with $r > 0$ a constant (infection rate)

② rate of $I \rightarrow R$ is αI with $\alpha > 0$ a constant (removal rate of infectives)
 α^{-1} is average infectious period

Question: given r, α, S_0, I_0 will infection spread or not? Show that $I_0 > I(t) \rightarrow 0$ if population of susceptibles at $t=0$ is below a critical value.

$$\frac{dI}{dt} \Big|_{t=0} = (rS_0 - \alpha)I_0 \begin{cases} < 0 & \text{if } S_0 < \frac{\alpha}{r} \\ > 0 & \text{if } S_0 > \frac{\alpha}{r} \end{cases}$$

The parameter $\frac{\alpha}{r}$ is called relative removal rate, and $\beta = \frac{\alpha}{r}$ is called the infection contact rate. Write

$$r_0 = \frac{rS_0}{\alpha} = \beta \cdot S_0 = \frac{S_0}{\frac{\alpha}{r}}$$

which is called reproductive rate (of the infection).

From (*)

$$\frac{dS}{dt} \leq 0 \quad \Rightarrow S(t) \leq S_0$$

So if $S_0 < \frac{\alpha}{r}$ (ie. $\frac{S_0}{\frac{\alpha}{r}} < 1$ or $r_0 < 1$) then

$$\frac{dI}{dt} = (rS - \alpha)I \leq (rS_0 - \alpha)I \leq 0.$$

③ incubation period sufficiently short to be ignored

Rate equations

$$\frac{dS}{dt} = -rSI \quad (*)$$

$$\frac{dI}{dt} = rSI - \alpha I \quad (**)$$

$$\frac{dR}{dt} = \alpha I \quad (***) \quad \text{Kermack-McKendrick (1927)}$$

Initial conditions

$$S(0) = S_0, \quad I(0) = I_0, \quad R(0) = 0$$

Conservation law

$$\frac{d}{dt}(S + I + R) = 0$$

so

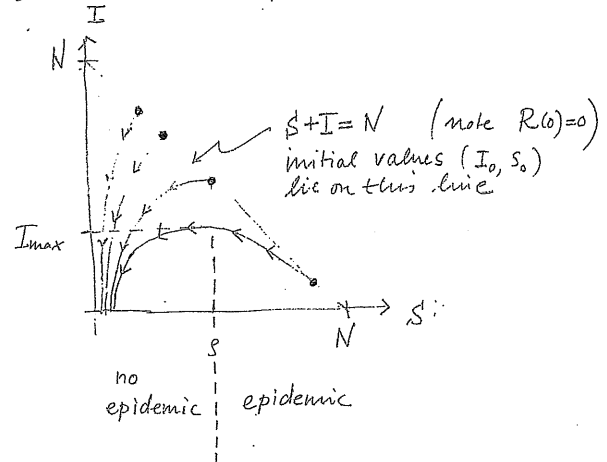
$$S(t) + I(t) + R(t) = \text{const.} = N$$

In this case

$I_0 > I(t) \rightarrow 0$ as $t \rightarrow \infty$,
infection does not spread.

If by contrast $r_0 > 1$ have an epidemic:
 $I(t)$ initially increases so that for some $t > 0$ find $I(t) > I_0$.

Phase-space diagram. Equation for R is solved to eqns. for S and I . Consider dynamics in phase plane (S, I) .



-5-

(A) Dynamics doesn't leave triangular region

Use same trick as for Lotka-Volterra model (p. 81): divide (**) by (***)

$$\frac{dI}{dS} = \frac{\frac{dI}{dt}}{\frac{dS}{dt}} = -\left(\frac{rS-\alpha}{rS-\alpha}\right) = \frac{S}{S-1}$$

Assume
 $I \neq 0$

Integrate

$$I + S - S \log S = \text{const.}$$

$$= I_0 + S_0 - S \log S_0$$

So

$$I + S = I_0 + S_0 + S \log \frac{S}{S_0}$$

$$\leq I_0 + S_0 = N$$

↑

$$\text{Since } S < S_0 \text{ have } \log \frac{S}{S_0} \leq 0$$

So phase-plane dynamics never leaves triangular region sketched on previous page.

-6-

(B) Determine maximal number of infections

Find I_{\max} for given initial conditions (S_0, I_0) by determining value of S for which

$$\frac{dI}{dt} = 0$$

Since $\frac{dI}{dt} = (rS-\alpha)I$ this occurs for

$$S = S^* \quad I_{\max} \text{ at } S^* \quad rS^* = \frac{\alpha}{r}$$

$$\text{From } I + S = I_0 + S_0 + S \log \frac{S}{S_0} \text{ obtain}$$

$$I_{\max} = I_0 + S_0 - S^* + S^* \log \frac{S^*}{S_0}$$

$$= N - S^* + S^* \log \frac{S^*}{S_0}$$

(C) Time to reach $I=0$

As $I \rightarrow 0$, $\frac{dI}{dt} \rightarrow 0$ and $\frac{dS}{dt} \rightarrow 0$. So

it takes infinitely long to reach $I=0$.

-7-

(D) Total # of susceptibles infected

What is the total number of susceptibles infected during epidemic?

$$I_{\text{tot}} = I_0 + (S_0 - S(\infty))$$

So to answer this question need to determine $S(\infty)$. Divide (*) by (***)

$$\frac{dS}{dR} = \frac{\frac{dS}{dt}}{\frac{dR}{dt}} = -\frac{rS}{\alpha} = -\frac{S}{S-1}$$

$$\Rightarrow S(t) = S_0 e^{-\frac{R(t)}{S}} \geq S_0 e^{-\frac{N}{S}} > 0$$

$S_0 < S(\infty)$. The figure on p. 244 shows $S(\infty) < S$. In summary

$$0 < S(\infty) < S$$

Since $I(\infty) = 0$, $S(t) + I(t) + R(t) = N$ implies

$$R(\infty) = N - S(\infty)$$

So $S(\infty)$ is the positive root $0 < z < S$ of

$$z = S_0 e^{-\frac{N-z}{S}}$$

$$z = S(\infty)$$

This determines I_{tot} .

-8-

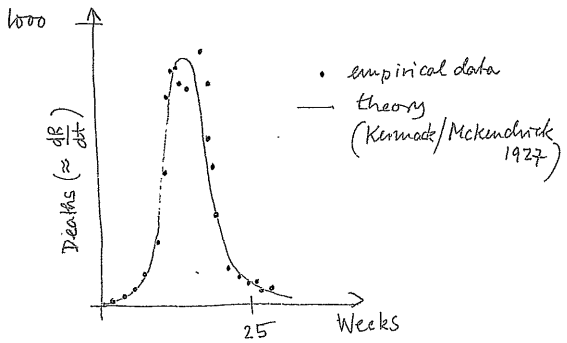
Have as $t \rightarrow \infty$

$$I(t) \rightarrow 0$$

$$S(t) \rightarrow S(\infty) > 0$$

So epidemic dies out due to lack of infectives and not due to lack of susceptibles.

Public health records record rate $\frac{dR}{dt}$ at which infectives are removed, due to death for example (Bombay plague epidemic of 1905/06).



Theory. Take

$$\frac{dR}{dt} = \alpha I = \alpha (N - R - S)$$

$$S = S_0 e^{-\frac{R}{S}}$$

$$= \alpha \left[N - R - S_0 \exp\left(-\frac{R}{S}\right) \right]$$

Solution can be found numerically.
Instead assume $R/S \ll 1$ and expand

$$\exp\left(-\frac{R}{S}\right) \approx 1 - \frac{R}{S} + \frac{R^2}{2S^2}$$

to get

$$\frac{dR}{dt} = \alpha \left(N - S_0 + \left(\frac{S_0}{S} - 1\right) R - \frac{S_0 R^2}{2S^2} \right)$$

Obtain

$$R(t) = \frac{S^2}{S_0} \left[\left(\frac{S_0}{S} - 1 \right) + \beta \tanh\left(\frac{\beta \alpha t}{2} - \phi\right) \right],$$

$$\phi = \left[\left(\frac{S_0}{S} - 1 \right)^2 + \frac{2S_0(N-S_0)}{S^2} \right]^{1/2},$$

$$\phi = \frac{1}{\beta} \tanh^{-1} \left(\frac{S_0}{S} - 1 \right).$$

Check by differentiating $R(t)$.

In particular

$$\frac{dR}{dt} = \frac{\alpha \beta^2 S^2}{2 S_0} \operatorname{sech}^2\left(\frac{\alpha \beta t}{2} - \phi\right)$$

Fitting parameters

$$\left. \begin{aligned} A_1 &= \frac{\alpha \beta^2 S^2}{2 S_0} \approx 890 \\ A_2 &= \frac{\alpha \beta}{2} \approx 0.2 \\ A_3 &= \phi = 3.4 \end{aligned} \right\} \text{for plot on p. 8}$$

Problems:

- ① if duration of epidemic is too long must include birth & death terms,
- ② incubation period
- ③ age classes
- ④ Spatial spreading

6.2 A model for the spatial spread of an epidemic

Consider model from section 6.1,

$$\frac{dI}{dt} = (\gamma S - \alpha) I$$

$$\frac{dS}{dt} = -\gamma S I$$

γ life expectancy of an infective
 α measures transmission efficiency
Assume diffusive spreading with diffusion constant D

Note: same D for I and for S

$$\frac{\partial I}{\partial t} = (\gamma S - \alpha) I + D \Delta I$$

$$\frac{\partial S}{\partial t} = -\gamma S I + D \Delta S$$

$I = I(\xi, t)$ and $S = S(\xi, t)$ with $\xi = (\vec{x})$.

Consider one-dimensional case to keep algebra simple. Proceed in usual fashion: dimensionless variables

$$I' = \frac{I}{S_0}, \quad S' = \frac{S}{S_0}$$

$$t' = rS_0 t, \quad \lambda = \frac{\alpha}{rS_0}$$

$$x' = \sqrt{\frac{rS_0}{D}} x$$

Now drop primes for notational convenience

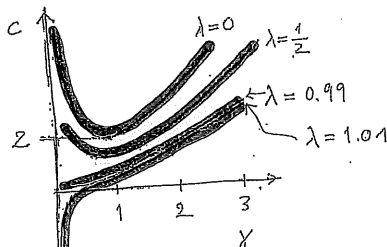
$$\frac{\partial S}{\partial t} = -IS + \frac{\partial^2 S}{\partial x^2} \quad (*)$$

$$\frac{\partial I}{\partial t} = IS - \lambda I + \frac{\partial^2 I}{\partial x^2}$$

Only one dimensionless parameter remains.
Note $\lambda^{-1} = \frac{rS_0}{\alpha}$ is reproductive rate of the infection (p. 3).

$$r_0 = \frac{S_0}{\lambda}$$

Also $\sqrt{1-\lambda}$ must be real and >0 . Thus $\lambda < 1$.



singularity in dispersion relation

Conditions for existence of travelling wave

$$c \geq 2\sqrt{1-\lambda}$$

$$\lambda < 1$$

Go back to dimensional variables:

$$\lambda = \frac{\alpha}{rS_0} = \frac{\beta}{S_0}$$

So $\lambda < 1$ corresponds to $S_0 > \beta$ which is the condition for an epidemic found on p. 3.

Traveling wave of infections?

Ausatz (\rightarrow p. 158)

$$I(x, t) = I(\bar{z})$$

$$S(x, t) = S(\bar{z})$$

with $\bar{z} = x - ct$
wave speed

Substituting into (*)

$$\frac{d^2 I}{d\bar{z}^2} + c \frac{dI}{d\bar{z}} + I(S - \lambda) = 0$$

$$\frac{d^2 S}{d\bar{z}^2} + c \frac{dS}{d\bar{z}} - IS = 0$$

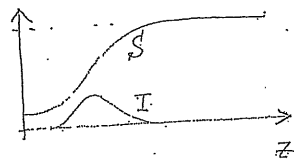
Boundary conditions

$$I(-\infty) = I(\infty) = 0,$$

$$0 \leq S(-\infty) < S(\infty) = 1,$$

constraint

$$I(\bar{z}) \geq 0, \quad S(\bar{z}) \geq 0.$$



Do not use approach from section 4.8 here because phase space is four-dimensional here (two second-order equations)
Instead linearise equations near leading edge of wave ($S=1, I=0$):

$$\frac{d^2 I}{d\bar{z}^2} + c \frac{dI}{d\bar{z}} + (1-\lambda) I = 0$$

Ausatz: $I(\bar{z}) = I_0 e^{-\gamma \bar{z}}$. Find:

$$\gamma^2 - c\gamma + (1-\lambda) = 0$$

$$\gamma^2 - c\gamma + \frac{c^2}{4} = \frac{c^2}{4} - (1-\lambda)$$

$$\gamma = \frac{c + \sqrt{c^2 - 4(1-\lambda)}}{2}$$

So

$$I(\bar{z}) = I_0 \exp\left(\frac{c + \sqrt{c^2 - 4(1-\lambda)}}{2} \bar{z}\right)$$

Take $\lambda < 1$.

Must have $c > 2\sqrt{1-\lambda}$ otherwise $I(\bar{z}) < 0$ for some \bar{z} (because $I(\bar{z})$ would be oscillatory).

Minimum wave speed

$$V = \sqrt{rS_0 D} c = 2 \sqrt{rS_0 D \left(1 - \frac{\alpha}{rS_0}\right)}$$

$$\frac{\alpha}{rS_0} < 1$$

The preceding analysis is valid near leading edge of wave.

The figure on p. 14 shows that $I(z)$ has in fact a maximum.

$S(z)$ cannot have a local maximum. At a maximum would have $\frac{dS}{dz} = 0$ and at that point

$$\frac{d^2 S}{dz^2} = IS > 0$$

which is the condition for a minimum, in contradiction with the assumption.

$S(z)$ is a monotonically increasing function of z . linearise

$$\frac{d^2 S}{dz^2} + c \frac{dS}{dz} - IS = 0$$

by putting $S = 1 - \delta$: $c \ll 1$

$$\frac{d^2 \delta}{dz^2} + c \frac{d\delta}{dz} - I = 0$$

\uparrow
small

Together with (*) find $\delta(z) = 0 (e^{-\beta z})$ with $\beta > 0$, so $S(z)$ approaches unity exponentially as $z \rightarrow \infty$.

Discussion:

epidemic

$$\boxed{\frac{rS_0}{\alpha} \equiv \frac{S_0}{\beta} > 1}$$

- ① minimum critical population density,

$$S_c = \frac{\alpha}{\beta} \equiv \gamma$$

for travelling wave to occur.

- ② for a given population S_0 minimum critical transmission coefficient (for disease to spread)

$$r_c = \frac{\alpha}{S_0}$$

- ③ given r and S_0 obtain threshold mortality rate

$$\kappa_c = r S_0$$

Control strategies: reduce S_0 by vaccination, reduce r by isolation. Discuss possible implications of sudden influx of susceptibles in near-threshold population.

6.3 Dynamics of diseases in large but finite populations

1. SIS model (infinite population; $N \rightarrow \infty$)

S Susceptibles

I Infectives

$$S \xrightarrow{\frac{\beta SI}{N}} I \xrightarrow{\gamma I} S$$

Infectives can recover (at rate γ) and become susceptible again.

$$\frac{dI}{dt} = \frac{\beta SI}{N} - \gamma I$$

$$\frac{dS}{dt} = -\frac{\beta SI}{N} + \gamma I$$

Find $S + I = \text{constant}$. Write $S + I = N$ where N is population size.

Eliminate S from first equation

$$\begin{aligned} \frac{dI}{dt} &= \frac{\beta}{N} (N-I)I - \gamma I \\ &= \beta (1 - \frac{I}{N})I - \gamma I \quad (*) \end{aligned}$$

the disease is called endemic if Eq. (*) can sustain a finite number of infectives, that is when Eq. (*) has a linearly stable steady state $I^* > 0$.

Find

$$I^* = N \left(1 - \frac{\gamma}{\beta} \right) = N \left(1 - \frac{1}{r_0} \right)$$

where

$$r_0 = \frac{\beta}{\gamma}$$

is the reproductive value (also referred to as reproductive ratio or reproductive rate, see p. 3).

Conclusion: the disease is endemic provided

$$r_0 > 1,$$

and the disease will disappear if

$$r_0 < 1.$$

Biological interpretation of reproductive value r_0 :

If a single infective individual introduced into a susceptible population produces more than one secondary infection before recovering, then $r_0 > 1$, the disease is endemic.

Show this by computing the expected number of secondary infections. To this end require the probability that an individual infective at $t=0$ is still infective at time t .

$$\begin{aligned} P_{\text{infective}}(t+\delta t) &= P_{\text{infective}}(t) (1 - \gamma \delta t) \\ \frac{dP_{\text{infective}}}{dt} &= -\gamma P_{\text{infective}} \end{aligned}$$

↑
recovery rate

Initial condition $P_{\text{infective}}(0) = 1$.

$$P_{\text{infective}}(t) = e^{-\gamma t}$$

Now compute expected number of secondary infections produced by one primary infective

$$\int_0^\infty P_{\text{infective}}(t) \frac{\beta}{N} S(t) dt$$

↑ ↑
prob. that expected number
primary of secondary infections
infective produced by single
still infectious infective in time dt

Assume that total number of secondary infections is small compared to N , $S(t) \approx N$.

$$\approx \beta \int_0^\infty dt P_{\text{infective}} = r_0$$

Note: dimensionless variables

$$\begin{aligned} I' &= \frac{I}{N} & r_0 &= \frac{\beta}{\gamma} \\ t' &= t\gamma \end{aligned}$$

Drop primes:

$$\frac{dI}{dt} = r_0 I (1 - I) \rightarrow I$$

2. Stochastic dynamics in large but finite population

Write a gain-loss equation for the probability $g_n(t)$

to observe n infectives at time t .

		rate
infection	$n-1 \rightarrow n$	$\lambda_{n-1} = \beta(1 - \frac{n-1}{N})(n-1)$
recovery	$n+1 \rightarrow n$	$\mu_{n+1} = \gamma(n+1)$

branching process
non-renewing
processes
population size N

Change in g_n in small time interval δt due to infection

$$(\lambda_{n-1} g_{n-1} - \lambda_n g_n) \delta t$$

and due to recovery

$$(\mu_{n+1} g_{n+1} - \mu_n g_n) \delta t$$

Together

$$\frac{dg_n}{dt} = \lambda_{n-1} g_{n-1} + \mu_{n+1} g_{n+1} - (\mu_n + \lambda_n) g_n$$

This gain-loss equation is also referred to as a Marco equation (van Kampen, 1981).

Marco equations of the form (*), corresponding to one-dimensional, one-step birth-death processes can be solved exactly (van Kampen).

In several dimensions (e.g. SIR model, p. 241) no exact solution in general. Must resort to approximate methods.

Plan: describe approximate method for solving (*) despite the fact that (*) is exactly soluble. The approximate method generalises to multi-species models.

Questions

Convenient representation of Marco equation in terms of step operators E^\pm (van Kampen, 1981). The operators are defined by their actions on functions of n :

$$E^\pm g_n = g_{n\pm 1}.$$

In terms of E^\pm , the Marco equation (*) takes the form

$$\frac{dg_n}{dt} = (E^- - 1) \lambda_n g_n + (E^+ - 1) \mu_n g_n.$$

3. Expansion of Master equation in N^{-1}

Consider large but finite values of N .
Introduce the variable

$$I = \frac{n}{N}$$

Compare I' on p. 24.

Define functions $\lambda(I)$ and $\mu(I)$ by.

$$\lambda_n = N\lambda(I) \quad \sim \quad \lambda(I) = \beta I(1-I)$$

$$\mu_n = N\mu(I) \quad \sim \quad \mu(I) = \gamma I$$

Expect that $g(I,t)$ is a smooth function of I in the limit of large values of N .
Represent action of E^\pm on smooth function $g(I)$ in terms of derivatives:

$$\begin{aligned} E^\pm g(I) &= g(I \pm \frac{1}{N}) \\ &= \sum_{k=0}^{\infty} \frac{(\pm \frac{1}{N})^k}{k!} \frac{d^k g}{dI^k} \\ &= e^{\pm \frac{1}{N} \frac{d}{dI}} g(I). \end{aligned}$$

Now expand Master equation to lowest order in N^{-1} .

$$\begin{aligned} \frac{\partial g}{\partial t} &= \left(e^{-\frac{1}{N} \frac{\partial}{\partial I}} - 1 \right) N\lambda(I)g(I) \\ &\quad + \left(e^{\frac{1}{N} \frac{\partial}{\partial I}} - 1 \right) N\mu(I)g(I) \\ &\approx \frac{\partial}{\partial I} (\mu(I) - \lambda(I)) g(I) \end{aligned}$$

This is a transport equation of the form

$$\frac{\partial p}{\partial t} + \frac{\partial}{\partial I} (v(I)p) = 0 \rightarrow p.$$

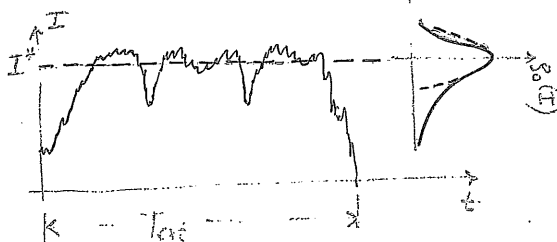
It corresponds to deterministic dynamics of the form

$$\begin{aligned} \frac{dI}{dt} &= v(I) = (\lambda(I) - \mu(I)) \\ &= \beta I(1-I) - \gamma I \end{aligned}$$

Up to a rescaling of I with a factor of N
this is the deterministic SIS model (#)
on p. 201 Disinfection variable, p. 24.

4. Quasi-steady state

Fundamental dichotomy:
epidemic must eventually become extinct due to fluctuations. But deterministic limit predicts it lasts ad infinitum.



Can show: $I_{\text{ext}} \sim e^{-N}$ for large N .

Quasi-steady state.

Expect long-lived quasi-steady state in the limit of large values of N .

Try to compute quasi-steady state distribution g_0 , given by

$$\frac{\partial g_0}{\partial t} \approx 0.$$

Ansatz

$$g_0(I) = e^{-N(S_0(I) - S_1(I) + \frac{1}{N} S_2(I))}$$

(compare WKB ansatz to describe quantum-mechanical tunneling: N^{-1} plays the role of \hbar).

Insert into

$$\begin{aligned} 0 &\approx \left(e^{-\frac{1}{N} \frac{\partial}{\partial I}} - 1 \right) N\lambda(I)g_0(I) \\ &\quad + \left(e^{\frac{1}{N} \frac{\partial}{\partial I}} + 1 \right) N\mu(I)g_0(I) \end{aligned}$$

and expand in N^{-1}

Write $S_0' = \frac{dS_0}{dI}$.

Now

$$\begin{aligned} & e^{\pm \frac{1}{N} \frac{\partial}{\partial I}} \left(e^{-NS_0(I)} - S_1(I) - \dots \right) \\ &= e^{-N(S_0 \pm \frac{S_0'}{N} + \dots)} - (S_1 \pm \frac{S_1'}{N} + \dots) \\ &\approx S_0(I) e^{\mp S_0'} \left(1 + \text{corrections in } N^{-1} \right) \end{aligned}$$

Insert into equation for $\rho_0(I)$ on p. 31

$$0 \approx S_0(I) \left[N\lambda(I)(e^{S_0'} - 1) + N\mu(I)(e^{-S_0'} - 1) \right]$$

Write this differential equation for $S_0(I)$ as

$$H(I, p) = 0 \quad \text{with } p = S_0' \text{ and}$$

$$H(I, p) = \lambda(I)(e^p - 1) + \mu(I)(e^{-p} - 1)$$

The condition $I_0 = 0$ implies

$$S_0'(I) = -\log \frac{\lambda(I)}{\mu(I)}$$

Now integrate to get $S_0(I)$.

Boundary conditions? Recall that the deterministic dynamics (p. 24)

$$\frac{dI}{dt} = \lambda(I) - \mu(I) = \beta I(1-I) - \gamma I$$

has two fixed points:

$$\left. \begin{aligned} I^* &= 0 && \text{unstable} \\ I^* &= 1 - \frac{\gamma}{\beta} = 1 - \frac{1}{r_0} && \text{stable} \end{aligned} \right\} \text{for } \frac{\gamma}{\beta} > 1$$

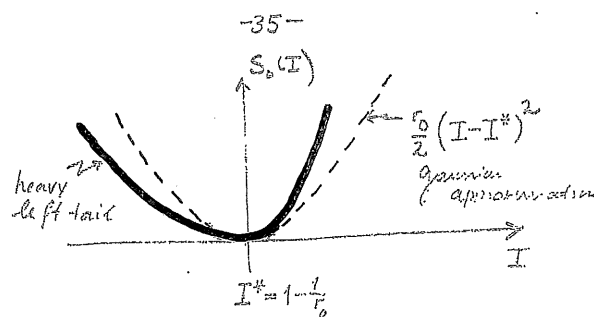
$$0 \rightarrow \dots \rightarrow I^* \leftarrow \dots \leftarrow 1 - \frac{1}{r_0} \rightarrow I$$

Expect $S_0(I)$ has maximum at $I^* = 1 - \frac{1}{r_0}$

so $S_0(I)$ has a minimum there.

Set $S_0(I^*) = 0$ (this defines normalization constant)

$$S_0(I) = \int_{I^*}^I dy S_0'(y) = \int_{1-\frac{1}{r_0}}^I dy \log [r_0(1-y)],$$



Distribution non-Gaussian.

Gaussian approximation

$$S_0(I) = \frac{r_0}{2} (I - I^*)^2 + \dots \quad \text{var}(I) \sim \frac{1}{r_0 N}$$

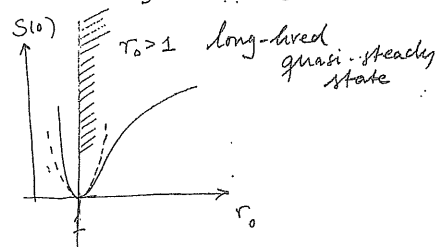
does not capture heavy tail for small I

Time to extinction of epidemic ($r_0 > 1$)
(this time and the possibility to affect it are of great interest)

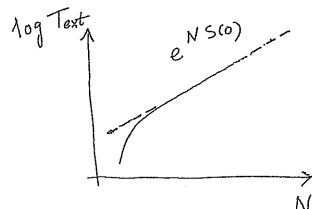
$$T_{ext} \sim e^{NS_0}$$

$$S_0(I) = - \int_{1-\frac{1}{r_0}}^I dy \log [r_0(1-y)]$$

$$= \log r_0 - (1 - \frac{1}{r_0})$$



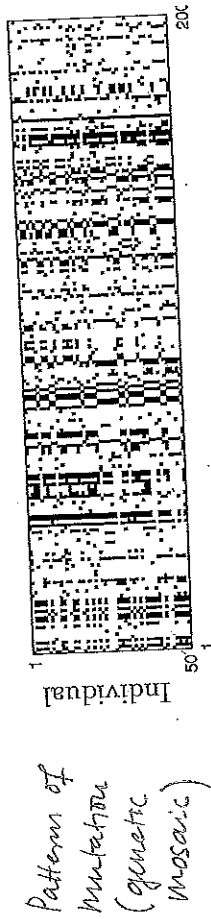
Extinction of disease in finite time



Population genetics

§ 1. Introduction

ancestral type
derived type



Empirically observed patterns of genetic variation

site index

ACTTTCGGAA ...
ACTTTCGCAA ...
ACTTTCGGAA ...
ACTTTCGCAA ...
site index (position along chromosome)

To infer ancestry from genetic mosaic
need a model for genealogies.

Which factors affect genetic evolution?

- ① inheritance
- ② mutations
- ③ Selection
- ④ recombination
- ⑤ demography (migration patterns, population size, ...)

Hypothesis of neutral evolution

Variation in large parts of genome
can be explained without involving
selection

How does genetic mosaic reflect the
the history of a population (its ancestry)?
Most recent common ancestor of Human
population ca. 200 000 years ago.

- If selection not important, which factors affect variation in a neutral region?
 - What difference does selection make where it matters?
 - How can we find genomic regions where it matters?
- Genes (regions expressed in protein sequences) are candidates. How to find genes?

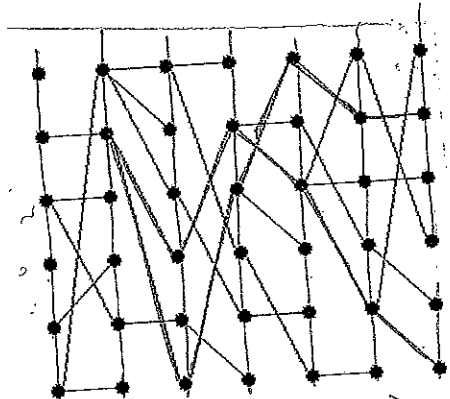
F. & W. Fisher-Wright model

$N=6$

Model for genealogy of selectively neutral loci

Assumptions

- (1) discrete non-overlapping generations $t = 1, 2, 3, \dots$
- (2) constant (haploid) population size N
- (3) freely mixing population
- (4) Mendelian inheritance.
(multinomial distribution of family sizes)



(3)+(4) \Rightarrow random Sampling with replacement

Number of generations to most common recent ancestor = 5 for sample of size $n=2$ illustrated in the plot above.

Random Sampling \Rightarrow fixation
with replacement

All genetic differences between individuals must eventually disappear (fixation).

However mutations cause differences to appear.

Different types of mutations.

- Single nucleotide polymorphism (SNP)
 - ACCTGTT $\xrightarrow{\text{G}}$ ACCCTT
- repeats in microsatellite loci (repetitive DNA sequence)
 - ATAG ATAG ATAG ... $\xrightarrow{\text{G}}$
 - ATAG ATAG ATAG ...
- inversion
- Alleles : Variants of sequences (genes) caused by mutation.

Neutral evolution mechanisms of

copy & paste (differences disappear) and mutations (causing differences to appear) balance to create a steady state.

Quantify by population homology going F_2

F_2 = prob. that two alleles sampled from population are identical.

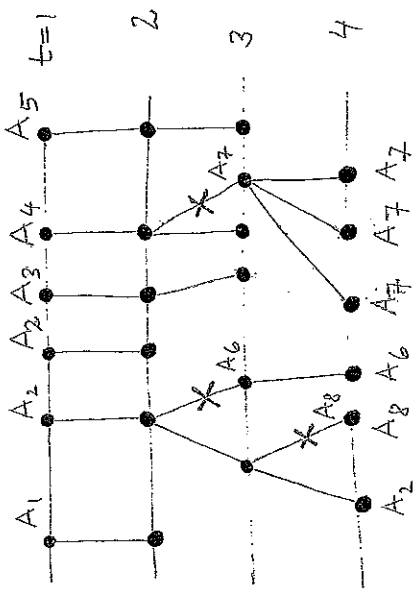
e.g. Mutations alleles occur

Alleles = variants of a certain locus on chromosome.

A sequence of 100 nucleotides can have up to

$$4^{100} \approx 10^{60}$$

different alleles. If a mutation strikes in this locus it is likely to create a new allele that did not exist in the population before.



In this model two identical alleles must share the same history:

Identity by state = identity by descent

Any given allele must eventually disappear from the population.

Classify genetic configuration of a population by allele frequencies (not types):

$$[\omega_1, \omega_2, \omega_3, \dots]$$

where ω_1 is the frequency of alleles of one type, ω_2 that of another type, and so forth. The list is usually size ordered

$$\omega_1 \geq \omega_2 \geq \omega_3 \dots$$

Mutations with rate μ per individual per generation.

Population homozygosity satisfies recursion

$$F_2^{(t+1)} = (1-\mu)^2 \left[\frac{1}{N} + \left(1 - \frac{1}{N}\right) F_2^{(t)} \right]$$

↑
Prob. to pick
two identical
alleles

Steady State

$$F_2^{(t+1)} = F_2^{(t)} \Rightarrow F_2 = \frac{(1-\mu)^2}{1 + 2N\mu - N\mu^2 + \mu^2 - 2\mu}$$

in the limit

$$N \rightarrow \infty \quad \mu \rightarrow 0 \quad \text{so that } \Theta = 2N\mu = \text{const.}$$

population mutation rate

find

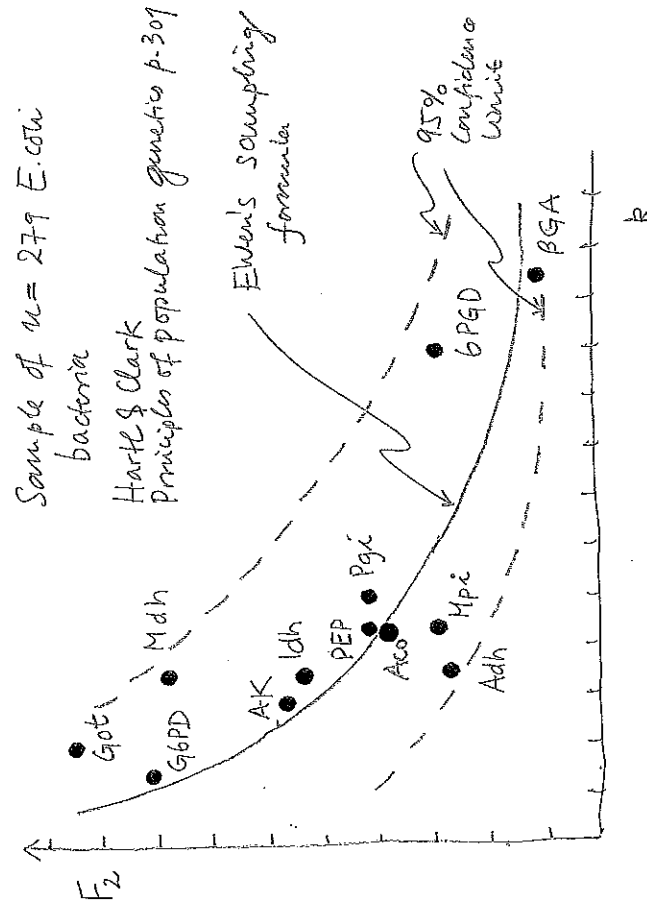
$$F_2 = \frac{1}{1+\Theta}$$

for a given Θ way

$$F_n = \frac{(n-1)!}{(\Theta+1)(\Theta+2)\dots(\Theta+n-1)}$$

Expected number of allelic types in
sample of size n from Ewens' Sampling
formula

$$\langle K \rangle = 1 + \frac{\Theta}{1+\Theta} + \frac{\Theta}{2+\Theta} + \dots + \frac{\Theta}{n-1+\Theta}$$



All loci fall into 95% confidence
limit \Rightarrow neutral evolution, no selection.

Q.4. Effective population size

In reality the population size is not constant

population expansions

bottlenecks

population-size fluctuations

Rapid population-size fluctuations \Rightarrow eff. pop. size N_{eff} .
Fisher-Wright model (no mutations) with constraint N

$$(1 - F_2^{(t+1)}) = \left(1 - \frac{1}{N}\right)^t (1 - F_2^{(t)})$$

Now if N depends on time

$$\begin{aligned} (1 - F_2^{(t+1)}) &= \left(1 - \frac{1}{N_t}\right) \left(1 - \frac{1}{N_{t-1}}\right) \cdots \left(1 - \frac{1}{N_1}\right) (1 - F_2^{(t)}) \\ &\equiv \left(1 - \frac{1}{N_{\text{eff}}}\right)^t (1 - F_2^{(t)}) \end{aligned}$$

This defines

$$t \log \left(1 - \frac{1}{N_{\text{eff}}}\right) = \sum_{j=1}^t \log \left(1 - \frac{1}{N_j}\right)$$

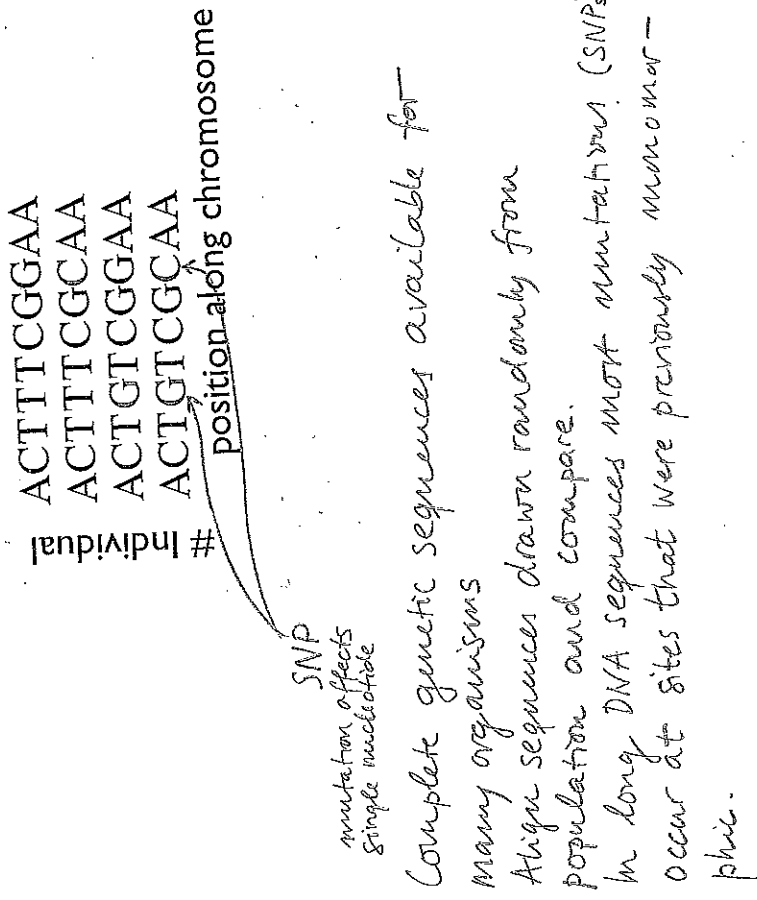
Large N

$$\frac{1}{N_{\text{eff}}} \approx \frac{1}{t} \sum_{j=1}^t \frac{1}{N_j}$$

When does this work?

geometric mean
 \Rightarrow small values of N_j matter

E.g. Single nucleotide polymorphisms (SNPs) (infinite sites model)



Infinite-sites model assumes that

every new single-site mutation occurs at a monomorphic site.

(closely related to infinite alleles model)

Distribution of number S_n of polymorphic sites
in sample of size n .

$$P(S_2=j) = \frac{1}{1+\theta} \left(\frac{\theta}{1+\theta} \right)^j$$

Compare p. 7: $P(S_2=0) = \frac{1}{1+\theta} = F_2$

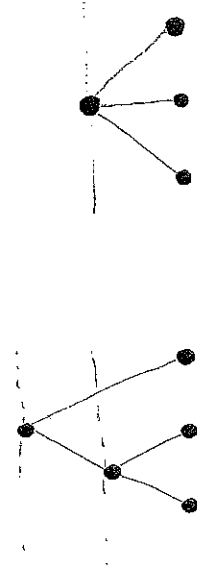
8.6. The coalescent process

Mathematical model for sample genealogy.
This is simplest form consistent with Fisher-Wright model.

Goal: Enumerating statistics of sample genealogies
under different models (mutation, selection,
recombination).

First consider basic genealogies.
Sample of size n from haploid population
of size N . Assume neutral model.

Two examples for genealogies from p. 5



Question: What is the prob. that the gene sequence of the sampled individuals are the same?

In neutral model the statistic of sample genealogies is entirely determined by the random sequence of copy & paste events — independent of mutations. Can therefore answer the above question as follows

- ① generate random sample genealogy with correct weight
- ② scatter mutations randomly with rate μ
- ③ ask: What is the probability that no mutations fell on sample genealogy?

Begin with step ①.

Idea: Create sample genealogies backwards in time.

Probability that two alleles have same ancestor in previous generation = N^{-1} in (haploid) population of size N .
Probability that the two alleles have different ancestors

$$P_2 = 1 - \frac{1}{N}.$$

Probability that all three alleles have different ancestors

$$P_3 = P_2 \underbrace{\frac{N-2}{N}}_{\text{prob. that 3rd allele has ancestor different from the other two}} = \left(1 - \frac{1}{N}\right) \left(1 - \frac{2}{N}\right)$$

Probability that n alleles have different ancestors in previous generation

$$\begin{aligned} P_n &= \left(1 - \frac{1}{N}\right) \left(1 - \frac{2}{N}\right) \cdots \left(1 - \frac{n-1}{N}\right) \\ &= \frac{n-1}{\prod_{j=1}^{n-1} \left(1 - \frac{j}{N}\right)} \approx \frac{1}{N} \sum_{j=1}^{n-1} \frac{1}{j} = 1 - \frac{\binom{n}{2}}{N} \end{aligned}$$

$$\text{where } \binom{n}{2} = \frac{n(n-1)}{2}.$$

Show this by considering logarithm

$$\log P_n = \sum_{j=1}^{n-1} \log \left(1 - \frac{j}{N}\right) \approx -\frac{1}{N} \sum_{j=1}^n j \quad \text{for } n \ll N$$

$$P_n = 1 - \frac{\binom{n}{2}}{N} \quad \text{when } n \ll N$$

What is the meaning of higher-order terms, N^{-2} for instance?

Higher-order collisions. The probability that three alleles have the same ancestor in the previous generation $\approx N^{-2} \ll N$ when N is large.

Conclusion. For $n \ll N$ the right genealogy on P is unlikely to occur.
So as you trace the genealogy back via time observe only binary coalescence of ancestral lines.

In other words: genealogies are binary trees.

Stochastic process generating these
genealogies \equiv coalescent process.

Probability that n alleles have distinct ancestors T generations back and that two alleles have the same ancestor in generation $T+1$

$$P_n^T (1 - P_n)$$

Equivalent interpretation: distribution of number of generations to first coalescence of ancestral lines.

When N is large, the distribution of T is approximately exponential

$$\log P_n^T = T \log P_n \approx -T \frac{\binom{n}{2}}{N}$$

$$P_n^T \approx e^{-T \frac{\binom{n}{2}}{N}}$$

$$\text{So } P_n^T (1 - P_n) \approx \frac{\binom{n}{2}}{N} e^{-T \frac{\binom{n}{2}}{N}}$$

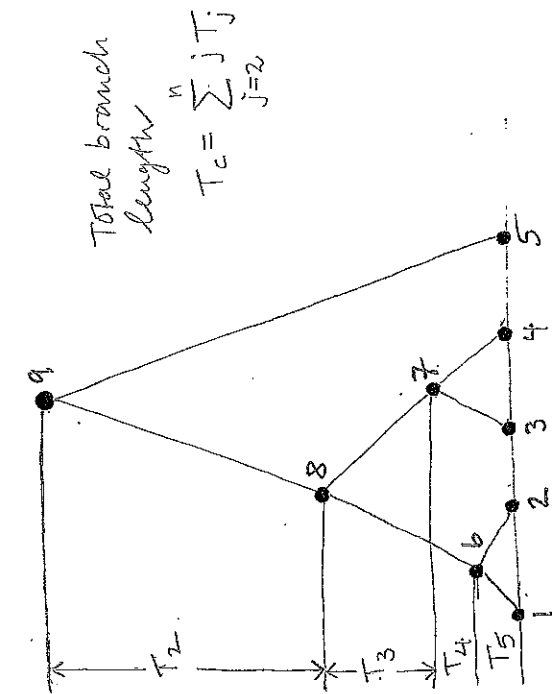
In other words: time T_j to first coalescent event backward in time,
Starting with j lines

- 17 -

$$\text{Prob}(\tau_j) = \lambda_j e^{-\lambda_j \tau_j} \text{ with } \lambda_j = \frac{\binom{j}{2}}{N}$$

Coalescence rate for j lines

$$\lambda_j = \frac{\binom{j}{2}}{N} \quad \leftarrow \text{number of possible pairs of lines}$$

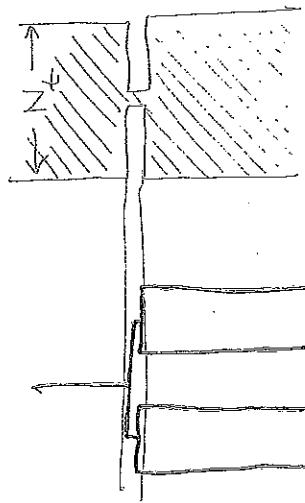


$$\langle \tau_j \rangle = \frac{N}{\binom{j}{2}}$$

- Two conclusions:
- (1) coalescent process is faster when there are more lines

- (2) coalescent process is slower when the population size is larger

Population bottleneck



Algorithm
Two arrays:

active lines

[1 2 3 4 5]	initially
[1 - 3 4 5]	after 1st coalescence
[1 - 3 - 5]	after 2nd coalescence

[1 2 3 4 5 6 7 8 9]

for each node store τ_j
index of ancestor
indices of descendants

nodes

5.7. Adding mutation to the genealogy

Neutral model: mutations accumulate randomly with constant rate μ .

So the number of mutations on a genealogy is Poisson-distributed with rate μT_c .

$$P(S=j) = \frac{(\mu T_c)^j}{j!} e^{-\mu T_c}$$

$$\text{where } T_c = \sum_{j=2}^n j \tau_j.$$

$$\langle j \rangle = \int_0^\infty \tau_c \text{Prob}(\tau_c) \sum_{j=0}^\infty j \frac{(\mu T_c)^j}{j!} e^{-\mu T_c} \text{d}\tau_c$$

change summation
order to $k = j - 1$

$$\langle j \rangle = \mu \langle \tau_c \rangle \quad \text{molecular clock}$$

In a sample of size $n=2$ $\langle \tau_c \rangle = 2 \langle \tau_2 \rangle$

Empirical data	$\langle j \rangle \sim 10^{-3}$	$\Rightarrow \langle \tau_2 \rangle \sim \frac{10^{-3} \cdot 10^8}{10} \sim 5 \cdot 10^{-8}$
Humans		$\sim 10,000$ years. $\sim 2,000,000$ years.

$$\text{Since } \langle \tau_c \rangle = \sum_{j=2}^n j \langle \tau_j \rangle = 2N \sum_{j=1}^{n-1} \frac{1}{j}$$

find $\langle j \rangle = \Theta \sum_{j=1}^{n-1} \frac{1}{j}$ weak dependence upon n

Example compute homozygosity F_2 with coalescent (p, θ)

$$\begin{aligned} P(S_2=0) &= \langle e^{-2\mu\tau_2} \rangle \\ &= \int_0^\infty \frac{1}{N} e^{-2\mu\tau_2 - \frac{\tau_2}{N}} = \int_0^\infty dt e^{-(1+\theta)t} \\ &= \frac{1}{1+\theta} \end{aligned}$$

$$\frac{P(S_n=0)}{P(S_2=0)} = \left(\frac{p}{1+\theta} \right)^{n-2}$$

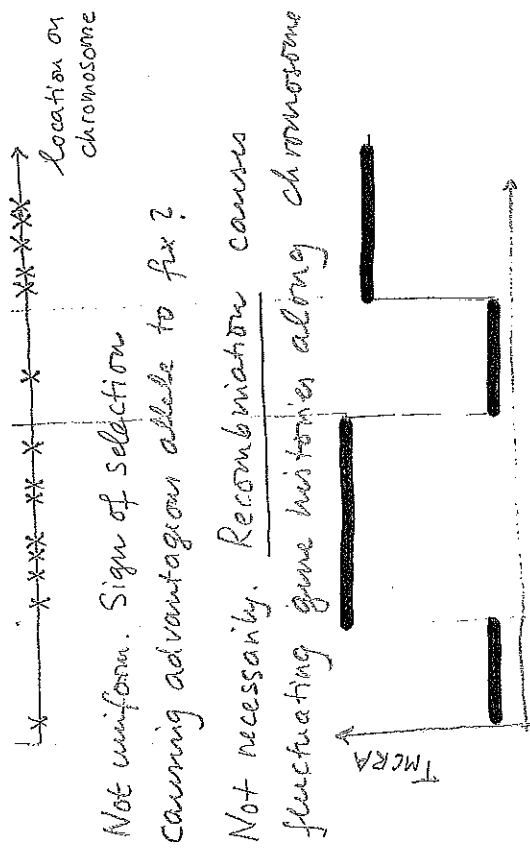
Exercise: Compute the distribution

of the number of SNPs in a sample of size $n=2$ in infinite-site model. Answer

$$P(S_2=j) = \frac{1}{1+\theta} \left(\frac{\theta}{1+\theta} \right)^j$$

§.5. Recombination

Locations of SNPs in sample of size $n=2$



Not necessarily. Recombination causes fluctuating gene histories along chromosome

MCA

Consequence: different parts of a chromosome have different histories.

Model (3) recombination events follow Poisson process in time, with rate τ (between two loci per individual, per generation)

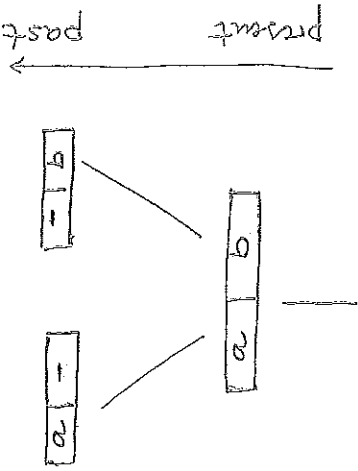
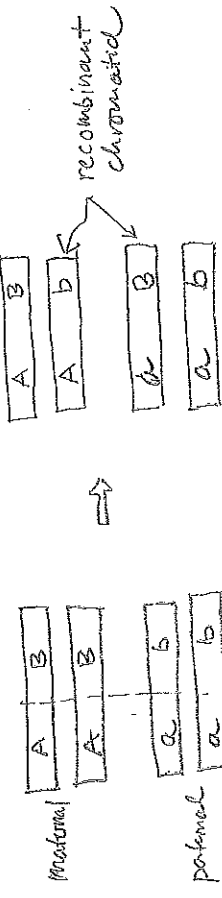
- (2) recombination gives uniformly distributed over chromosome

high probability to observe recombination between two loci that are far apart.

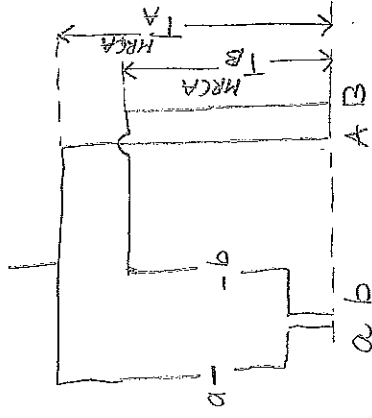
Linked loci: two closely loci that have identical gene histories

Linkage equilibrium: gene histories of two loci far apart from each other are independent.

Recombination: exchange of chromosome segments between paternal and maternal chromosomes during meiosis in eukaryotes (which normally carry two copies of each chromosome).



-23-



Coalescent with recombination.

For k ancestral lines, recombination occurs at rate $R \tau$.

Coalescences occur at rate $\binom{k}{2} \frac{\lambda_c}{2N}$.

Measuring time in units of $2N$ generations

$$\lambda_c = \binom{k}{2} \lambda_R = 2N k \lambda_R \equiv \frac{kR}{2}$$

Both processes are Poisson and independent.

If two times are independently exponentially distributed with rates λ_c and λ_R then the time to the first event

$$t_{\min} = \min \{ t_1, t_2 \}$$

An exponential distribution with rate $\lambda_c + \lambda_R$

-24-

$$\begin{aligned}
 P(t_{\min} > T) &= P(\min \{t_1, t_2\} > T) \\
 &= P(t_1 > T, t_2 > T) \\
 &= P(t_1 > T) P(t_2 > T) \\
 &= e^{-(\lambda_c + \lambda_R) T}
 \end{aligned}$$

Probability that coalescence occurs first is

$$\frac{\lambda_c}{\lambda_c + \lambda_R} = \frac{k-1}{k-1+R}$$

Probability that recombination occurs first

$$\frac{\lambda_R}{\lambda_c + \lambda_R} = \frac{R}{k-1+R}$$

Correlation of gene histories

$$\langle T_A^{\text{MRCA}} + T_B^{\text{MRCA}} \rangle - \langle T_A^{\text{MRCA}} \rangle - \langle T_B^{\text{MRCA}} \rangle$$

$$\sim R^{-1} \quad \text{for large } R_{AB}$$

-25-

§ 4. Selection

Consider one locus, two allelic types α (new mutation) and A (ancestral type)

Assume that α has higher fitness

$$W_\alpha = 1 + s \text{ with } s > 0 \quad W_A = 1$$

Model effect of selection as bias on Fisher-Wright model: initial frequencies:

$$X_\alpha^{(0)} \quad \text{and} \quad X_A^{(0)} \quad \text{in generation } t=0$$

Same as with $X_\alpha^{(0)}$ and $X_A^{(0)}$ but with bias

$$\frac{W_\alpha}{W_\alpha + W_A} X_\alpha^{(0)} \quad \text{and} \quad \frac{W_A}{W_\alpha + W_A} X_A^{(0)}$$

$$X_\alpha^{(1)} = \frac{W_\alpha X_\alpha^{(0)}}{W_\alpha X_\alpha^{(0)} + W_A X_A^{(0)}} = \frac{(1+s) X_\alpha^{(0)}}{(1+s) X_\alpha^{(0)} + (1-X_\alpha^{(0)})}$$

In the limit of infinite population size
 $t_S = \frac{1}{s} \int_{X_\alpha^{(0)}}^1 \frac{dx}{x(1-x)} = \left[\log \frac{x}{X_\alpha^{(0)}} \right]_{X_\alpha^{(0)}}^1 \approx \frac{1}{s} \log(N-1)$
 have set upper boundary to $1 - N^{-1}$ because
 the time to reach $X_\alpha = 1$ diverges in
 stochastic approximation

-26-

Change in allele frequency to next generation

$$X_\alpha^{(1)} - X_\alpha^{(0)} = \frac{(1+s) X_\alpha^{(0)} - X_\alpha^{(0)} [1 + s X_\alpha^{(0)}]}{1 + s X_\alpha^{(0)}} \\ \approx s X_\alpha^{(0)} (1 - X_\alpha^{(0)}) \quad \text{when } s \ll 1$$

When s is small and population size large
 then this change is small, so that

$$\frac{dX_\alpha}{dt} \approx s X_\alpha (1 - X_\alpha)$$

Logistic equation (p. 20) describes spreading of advantageous gene in population (Selective Sweep)

Duration of selective sweep

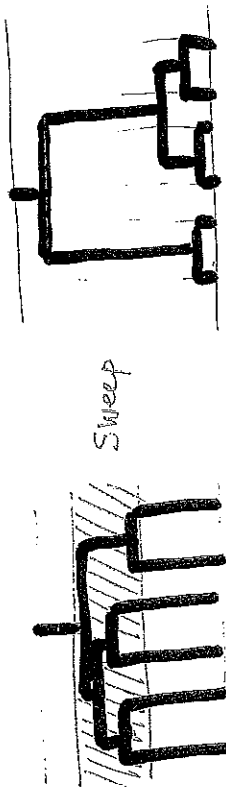
$$t_S = \frac{1}{s} \int_{X_\alpha^{(0)}}^{1-N^{-1}} \frac{dx}{x(1-x)} = \left[\log \frac{x}{X_\alpha^{(0)}} \right]_{X_\alpha^{(0)}}^{1-N^{-1}} \approx \frac{1}{s} \log(N-1)$$

300. Genetic bottleneck

Recombination shapes the effect of mechanisms such as selection (migration ...) How to detect selection from genetic mosaics?

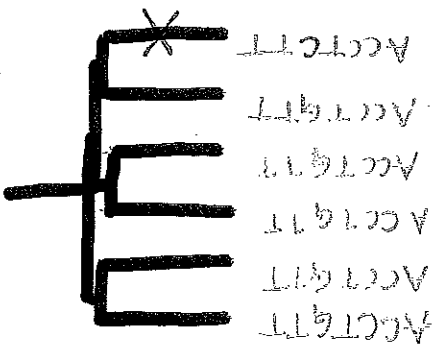
Signature of recent selective sweep on gene genealogy of neutral loci nearby?

Assume no recombination. Then genealogies of β looks like that of α

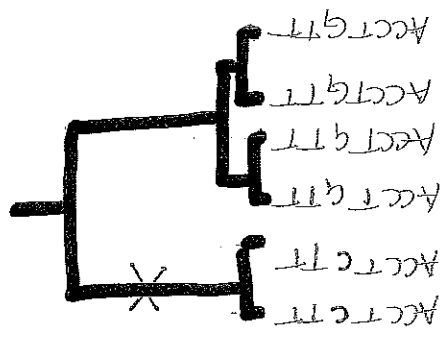


General
genealogy
locus B linked
to selected locus

Star-like topology: high prob. of evolutions



Whale tree by Standard Mining Co.
of Grinnell Point, Calif.



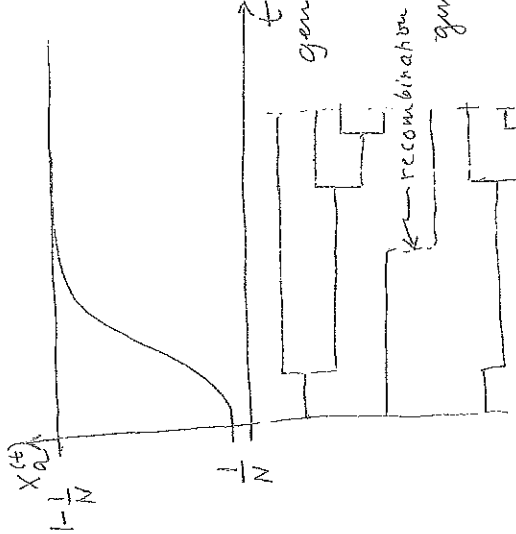
A hand-drawn diagram consisting of a large square with a smaller square cut out from its center, and a zigzag line extending from the top-right corner of the inner square.

Statistical tests to infer recent selective sweeps from singleton frequency.

Problems: ① Singletons can be due to sequencing error

- ② Bottlenecks (reduction of population size during short time in the past) result in star-shaped genealogies.

Distinguish bottlenecks from recent selective sweeps by analysing how genealogies vary with distance from selected locus.
Recombination allows lines of neutral loci to escape sweep (avoid genetic hitchhiking)



To quantify how the effect of selection decays on distance to selected locus increases compute prob. Q of a line at locus B to escape the sweep

$$Q = \int_0^{t_s} r e^{-rt} (1 - X_a^{(+)}) dt$$

prob. frequency of that recombination with singleton allele A at B in the past (recombination with a per sequence does not escape)

To compute Q , observe that $r = \frac{s}{N}$

$$X_a^{(t)} = \frac{1}{1 + e^{-st}} = \frac{1}{1 + e^{-s(t-t_s)}} = \frac{1}{1 + e^{-s(\frac{t}{2}-\frac{t_s}{2})}}$$

With $t_s = \frac{s}{2} \log(N-1)$

So

$$Q = \int_0^{t_s} r e^{-rt} \left[1 - \frac{1}{1 + e^{-s(\frac{t}{2}-\frac{t_s}{2})}} \right] dt$$

genealogy at B

-31-

Take limits

$N \rightarrow \infty$

$\frac{1}{N} \log N \rightarrow \text{constant}$

In this limit the first term in $[1-1]$ vanishes to infinity, so that

$$Q \approx 1 - \frac{\alpha_0 t^2 e^{-\alpha_0 t}}{1 + e^{-S(t-\frac{t^2}{2})}}$$

Main contribution to α_0 comes from $t < \frac{t^2}{2}$ where the constant value

$$\approx 1 - \frac{\alpha_0 t^2 e^{-\alpha_0 t}}{e^{-S(t-\frac{t^2}{2})}}$$

$$\approx 1 - e^{-\frac{1}{2} \log N}$$

Heterogeneity induced by initial state

$$\frac{H}{N} \approx 1 - e^{-\frac{1}{2} \log N}$$

Initial

~~Self-reinforcing
locus~~

~~Self-reinforcing
locus~~